DOKTORSAVHANDLINGAR VID CHALMERS TEKNISKA HÖGSKOLA
NR 11

PARALLELOGRAM PLATES

ANALYSED BY STRIP METHOD

BY

GUNNAR KÄRRHOLM

GÖTEBORG 1956

DOKTORSAVHANDLINGAR VID CHALMERS TEKNISKA HÖGSKOLA
NR 11

PARALLELOGRAM PLATES

ANALYSED BY STRIP METHOD

AV

GUNNAR KÄRRHOLM

AKADEMISK AVHANDLING

SOM MED TILLSTÅND AV CHALMERS TEKNISKA HÖGSKOLA FÖR TEKNOLOGIE DOKTORSGRADS VINNANDE TILL OFFENTLIG GRANSKNING FRAMLÄGGES Å FÖRELÄSNINGSSALEN FÖR FYSIK, GIBRALTARGATAN 5 B, GÖTEBORG, TORSDAGEN DEN 31 MAJ 1956 KL. 10

GÖTEBORG
1956

Errata

Page	Line from above				
22	11, 12	For	"$y_{r\pm 1/2\,t}$"	read	"$y_{r\pm 1/2}$"
25	14	„	"edge 2"	„	"$y = t$"
29	12	„	"middle plane"	„	"middle surface"
40	21	„	"(7)"	„	"(6)"
42	24	„	"$\begin{bmatrix} s_{0n} = \\ s_{1n} \end{bmatrix}$"	„	"$\begin{bmatrix} s_{0n} \\ s_{1n} \end{bmatrix} =$"
48	11	„	"$\lvert \Delta w_r \rvert \leqq$"	„	"$\lvert \Delta w_r \rvert <$"
49	8	„	"equations"	„	"equation"
50	7	„	"$\leqq .0043$"	„	"$< .0029$"
50	20	„	"$(a_{4,\,N+1} - 1$"	„	"$(a_{4,\,N+1} - 1)$"
51	3	„	"$(N+1)$"	„	"$(N+1)^3$"
54	7	„	"$\lvert \Delta w \leqq \lvert n^5 W_{rn\,max}$"	„	"$\lvert \Delta w_r \rvert \leqq \lvert n^5 W_{rn} \rvert_{max}$"
54	13	„	"$w_0 = \Big[\ldots$"	„	"$w_0 = \frac{1}{24} \Big[\ldots$"
64	19	„	"the deflection w_r of the"	„	"the"
70	20	„	"6"	„	"7"
75	34	„	".944"	„	".946"
76	8	„	".994"	„	".944"
76	14	„	".994"	„	".944"
76	14	„	".0345"	„	".0359"
76	19	„	"2.6 %"	„	"1.1 %"
77	12	„	"$\sin (m \pi x_0 / l)$"	„	"$\sin (n \pi x_0 / l)$"
78	9	„	"A^n"	„	"A_n"
80	11	„	"$\frac{d^2 w_2}{d x_r^2}$"	„	"$\frac{d^2 w_r}{d x_r^2}$"
98	18	„	"S^0_{ln}"	„	"S^0_{ln}"
101	16	„	"edges"	„	"corners"
102	3	„	"FAURE"	„	"FAVRE"
103	31	„	"$C_i w_i$"	„	"C_i"
105	1	„	"$\sin \frac{m \pi x_r}{l}$"	„	"$\sin \frac{m \pi a}{l}$"
105	10	„	"eq. (5)"	„	"$\frac{d^2 w_r}{d x_r^2} = -\frac{l}{D t} \Big[\Big(1 - \frac{a}{l} \Big) \frac{x_r}{l} - \frac{x_r'}{l} \Big] + \frac{2 l}{\pi^2 D t} \sum \Big[\frac{1}{n^2} \sin \frac{n \pi a}{l} - \frac{1}{n^4} \sum m^2 (w_{rm})_{rn} \sin \frac{m \pi a}{l} \Big] \sin \frac{n \pi x_r}{l}$"
107	10—14	For	Second column: "0, 0, — .012, — .001, — .015"	„	".040, .005, .012, .001, .015"

Page	Line from above				
107	20, 22	For	"$(M_{x0})_{l/2}$"	read	"$2\,(M_{x0})_{l/2}$"
108	1, 2	„	"$(M_{x0})_{l/2}$"	„	"$2\,(M_{x0})_{l/2}$"
108	4	„	"$x_0 = l/2$."	„	"$x_0 = l/2$. Ordinates for strips 1, 2, 3 are multiplied by 2."
108	7	„	"Fig. 235.1."	„	"Fig. 234.1."
110	20, 22	„	"$\dfrac{8\,l\ \mathrm{tg}\ \Theta}{t\,(1+\nu)}\,\delta$"	„	"$\dfrac{8\ \mathrm{tg}\ \Theta}{l\,t\,(1+\nu)}\,\delta$"
111	21	„	"$-\dfrac{4\,D}{l\,t}\,(1-\nu)$"	„	"$\dfrac{4\,D}{l\,t}\,(1-\nu)\,\delta$"
117	17	„	"r"	„	"r'"
118	9	„	"Line for 1 k in Table 241.1"	„	"$-\psi_2{}^1,\ -\psi_1{}^1,\ \psi_0{}^1,\ -\varphi_2{}^1,\ -\varphi_1{}^1,\ -\varphi_0{}^1$"
119	2	„	"$M_{si}\,\varphi_{rj}^{si}$"	„	"$M_{sj}\,\varphi_{rj}^{sj}$"
120	22	„	"$k\,\Delta\,M_{rj}^{\mathrm{I}} =$"	„	"$-\,k\,\Delta\,M_{rj}^{\mathrm{I}}$"
121	6	„	"24. Frames"	„	"25. Frames"
121	17	„	"242.1"	„	"25.1"
125	4	„	"236"	„	"235"
125	6	„	"236.1"	„	"235.1"
127	17	„	"eq. (1)"	„	"$E = 64\,\pi^2\,\gamma\,f_b{}^2\,l^4/1.875^4\,g\,d^2$"
129	4	„	"$\Delta\,\nu = .2\,d\,\dfrac{\partial\,\nu}{\partial\,d} = 8\,(1+\nu)\,\dfrac{d}{l}$"	„	"$\Delta\,\nu = .2\,d\,\dfrac{\partial\,\nu}{\partial\,l} = .8\,(1+\nu)\,\dfrac{d}{l}$"
135	22	„	"12.49"	„	"19.49"
136	19	„	"$\dfrac{2\,Q\,l}{D\,b\,h}$"	„	"$\dfrac{Q\,l\,h}{2\,D\,b}$"
136	19, 20	„	"$\Big)\,\pi\,n$"	„	"$\pi\,n\Big)$"
137	2	„	"$9\,(1-.09)$"	„	"$9^2\,(1-.09)$"
155	9	„	"Bihang 222"	„	"222, Bihang"
156	15	„	"alla avvikelser"	„	"avvikelserna i stort sett"
157	3	„	"w_r"	„	"w_0"
165	26	„	"$\lvert w_{rn}\rvert \leqq \dfrac{1}{m^4}\lvert m^4\,W_{rm}\rvert_{max}$"	„	"$\lvert w_{rn}\rvert \leqq \dfrac{1}{m^4}\lvert m^4 W_{rm}\rvert_{max}\ (1)$"
166	5	„	"(227.5)"	„	"(227.4)"
169	9	„	"228"	„	"224"
170	4, 7	„	"$(N+2)^2$"	„	"$(N+3)^2$"
173	1	„	"That is, the"	„	"The"
174	4, 5, 6, 10, 11	„	"δ"	„	"$\dfrac{1}{2}\,\delta$"
174	10	„	"q_1"	„	"q_0"
179	16	„	"Figs. 562.1, 2, 3, 4."	„	"Figs. 562.1, 2, 3, 4, 5."
180	1	„	"l/t"	„	"l/nt"

PARALLELOGRAM PLATES

Analysed by Strip Method

By

Gunnar Kärrholm

GÖTEBORG 1956

UPPSALA 1956
APPELBERGS BOKTRYCKERI AB

To Marianne

Preface

In 1946 the author worked out an approximate method of calculating the deformations of simply supported oblique plates carrying a uniformly distributed load. The problem was put to me by the late professor of Structural Theory at Chalmers University of Technology, SVEN HULTIN. He pointed out valuable aspects of the design of oblique plates during many interesting discussions. In addition, he made it possible for me to use the resources of his laboratory.

Encouraged by Professor Hultin I have now tried to genera lize the method. The results arrived at have been applied to numerical examples. Valuable help in the calculations was given by Mr ALF JOHANSSON. Expenses for assistance in this work and for performing experiments with model plates were defrayed by grants from the Chalmers Research Fund (Chalmerska Forskningsfonden). The tests were carried out with skill and interest by Mr SVEN KARLSSON.

Some mathematical problems were discussed with the Professor of Applied Mathematics at Chalmers University of Technology, HARALD BERGSTRÖM, who gave me appreciated advice and suggestions.

The statistical treatment of the experiments was developed with the valuable collaboration of fil. lic. MARTIN SANDELIUS, the statistician of the Swedish Institute for Textile Research. He has kindly worked out Appendices 581 and 583. Important suggestions regarding the experimental part of this paper have also been given by my wife, tekn. lic. MARIANNE KÄRRHOLM.

I am very much indebted to the Professor of Structural Theory at Chalmers University of Technology, S. O. ASPLUND, for his kind interest and expert advice. The discussions with him have led to greater distinctness of expression. I would also like to mention the great interest shown by the Professor of Structural Engineering technique at Chalmers University of Technology, HJALMAR GRANHOLM.

The figures of this paper have been drawn in cooperation with Mr Ingemar Dahl, who has also been of good help in performing some numerical calculations.

I wish to express my deep gratitude to all those who have contributed to and supported the fulfilment of this investigation.

Gothenburg, March

Gunnar Kärrholm

Contents

Notation

A_{rn}	Part of principal coefficient, W_{rn}
a_{rn}	Part of Fourier coefficient, w_{rn}
B	Constant of integration, general symbol for coefficient
b	Width of a plate measured perpendicularly to free edges
C	Constant of integration, general symbol for coefficient
c_{mn}	Factor in expression for correction of principal coefficient
D	Flexural rigidity of a plate
d_{mn}	Factor in expression for correction of principal coefficient
d	Index indicating results obtained by division into strips, diameter
E	Modulus of elasticity
e_{mn}	Factor in expression for correction of principal coefficient
e	Base of natural logarithms, index indicating exact value
F	Concentrated load
f_{mn}	Factor in expression for corrections of principal coefficient
f	Frequency
G	Modulus of shear
g_{mn}	Factor in expression for increment to principal coefficient
g	Gravitational acceleration
h_{mn}	Factor in expression for increment to principal coefficient
h	Thickness of a plate
I	Moment of inertia of a cross section with respect to x- or y-axis
I_p	Polar moment of inertia
j	Index indicating a particular support in order
K	Boundary curvature
k	Index indicating a particular support in order
L	Confidence limit
l	Length of a strip, length of a rod

l_1, l_2 Distance from load to supports

M_{rj} Boundary bending moment per unit length of section through the support j at strip r

M_x, M_y Bending moments per unit length of sections of a plate perpendicular to x- and y-axes respectively

M_{xy} Twisting moment per unit length of section of a plate perpendicular to x-axis

m, n Indices indicating order

N Maximum number in an order series

N_s, N_a Determinants

P Point

p Variable

Q Line load, reaction per unit length

q Intensity of load

r Index indicating a particular strip in order

S_{rn} Part of principal coefficient, W_{rn}

s_{rn} Part of Fourier coefficient, w_{rn}

T_x, T_y Shearing forces parallel to z-axis per unit length of sections of a plate perpendicular to x- and y-axes respectively

t Width of a strip

t_0 Width of loaded area perpendicular to y-axis

W_r Principal deflection of strip r

W_{rn} Principal coefficient

w_{rn} Fourier coefficient of strip deflection w_r

w_r Deflection of strip r

w Deflection of a point on a plate

x_r Distance of arbitrary point on strip r from one support of the strip

x, y, z Rectangular coordinates

z Function of x and y

α, β, γ Factors included in coefficients s_{rn} and a_{rn}

γ Mass per unit volume

δ Displacement

ε_x Unit elongation in x direction

ζ Factor in expression for maximum deflection of plate of infinite width

η Rectangular coordinate

Θ Angle between a supported edge and normal to free edge of an oblique plate

ϑ Angle

$\varkappa$ Factor in expression for maximum curvature of a plate of infinite width

λ_{Nn} Factor in expression for increment to principal coefficient

λ_m Factor in functional expression of w

$\mu l/\pi$ Distance in the x-direction between the supports of two adjacent strips

ν Poisson's ratio

ξ Rectangular coordinate

Φ_{rj}, Ψ_{rj} Slopes of strip r to the right and left, respectively, of the jth support

φ, ψ Slopes due to a unit boundary moment

X Angular deviation at a support

χ Angular deviation due to a unit boundary moment

In the enumeration of sections in this paper the first figure is the number of the part of the paper to which the section belongs. A second digit indicates order within the part. A third digit is used for subsections. Equations are assigned numbers containing the number of the section where the equation first occurs and the number of order within the section. Thus (211.1), for example, means the first equation of section 211. If in some section reference is made to an equation within the same section the number of the section is omitted. Figures and tables are numbered in the same way, but they are not bracketed.

References are made by quoting the author. A number indicating the year of printing is added if references are made to several papers by the same author. Such papers printed the same year are given a second number indicating the order in the list of references.

1. Introduction

Strip methods may be used for analysing parallelogram slabs with arbitrary edge conditions. The investigations in this paper are confined to slabs on two parallel edges. The difficulties involved in the calculation of such slabs vary widely with the kind of loading and the mode of support. In the case of a rectangular slab simply supported and with a uniformly distributed load the design is simple. On the other hand the treatment of oblique slabs subjected to concentrated loads forms one of the most difficult problems in the theory of plates.

The deformations and stresses of plates carrying live loads are determined according to the theory of elasticity. Small deflections of thin elastic plates satisfy a partial differential equation of the fourth order, eq. (211.6) in section 211, (see TIMOSHENKO 40, GIRKMANN). Its solution for a particular plate depends on the dimensions of the plate and the loads applied. In addition, the boundary conditions affect the result.

The boundary conditions for plates treated in this paper are of a relatively complicated form. This in general leads to involved expressions for the deflections. However, if no bending moments appear along the supports of a rectangular plate, results are obtained without much difficulty by methods given by Lévy (see, e. g. NADAI). The deflections then emerge as rapidly convergent series. The moments caused by concentrated loads appear as more slowly convergent or divergent series.

Deflections of plates subjected to different kinds of loading may be conveniently determined by combining characteristic functions (see ÖDMAN). Moments in the vicinity of concentrated loads are usually difficult to describe solely by series expressions. They may be found in the following way: a solution of (211.6) corresponding to the action of a concentrated load is obtained for a plate of infinite dimensions. This solution is combined with functions satisfying the homogeneous differential equation. The functions are chosen in forms suitable for the shape of the plate.

The magnitude of the ordinates is determined by the boundary conditions.

The solution of (211.6) for a concentrated load of arbitrary position forms the influence function for the deflection. It can be used for building up deflections and moments under arbitrary systems of loading (see PUCHER, OLSEN and REINITZHUBER). SCHULTZ-GRUNOW suggests a somewhat modified solution satisfying the boundary conditions at the corners of the plate exactly. Also KOEPCKE has introduced special functions to satisfy the boundary conditions at the corners of plates supported along four edges. The method might be suitable for the investigation of oblique plates with the boundary conditions treated in this paper.

The known methods for designing oblique plates are laborious. They are particularly unsuitable in cases where many kinds of loading are to be taken into consideration. Difficulties of design have restricted the use of oblique slabs. Thus in Sweden concrete slabs with acute angles less than 70° as a rule have not been permitted in road bridges.

Some authors have derived deflections and moments for oblique plates by combining exact solutions of (211.6) and solutions of the corresponding homogeneous differential equation. ANZELIUS computes the twisting moments in a plate resting on parallel supports and carrying a uniformly distributed load. LARDY represents the part of the deflection which is a solution of (211.6) as a double trigonometric series, the coefficients of which are determined by the external force. This is also done by KRETTNER, who has succeeded in transforming the double series to a simple one. FUCHSSTEINER represents the solution of the homogeneous differential equation in a general form as a sum of arbitrary harmonic and biharmonic functions. These are the solutions of homogeneous difference equations for particular boundary conditions. The solutions are then multiplied by constants determined by making the deviations from unutilized boundary conditions a minimum. This method of using minimum conditions has also been applied by ÖDMAN, RONGVED and GRAUDENZ. Graudenz writes influence functions for moments in oblique plates as the sum of the influence function for an infinite plate and a series of biharmonic polynomials. HERRMANN attempts to use Ritz's method for clamped plates, but the accuracy obtained is poor. Ritz's

method also has been applied to the problem of determining the resonance frequencies of oblique plates (see BEREUTER).

Exact solutions of (211.6) for oblique plates imply laborious and time-consuming calculations. Some authors have, therefore, determined the deflections of such plates by introducing finite differences. The elastic surface is described by a finite number of ordinates. The position of each ordinate is determined by points on the middle surface of the plate. These points are arranged in some sort of regular network. A rectangular network is suitable for rectangular plates. For treating oblique plates networks built up of parallelograms or hexagons may be convenient.

Parallelogrammatic networks have been used by FAVRE and NIELSEN. The former has applied this difference method to plates supported along four edges. The latter has examined the case of plates supported at two parallel edges. Tables have been drawn up for plates of different dimensions. In each case results are given for a uniformly distributed load. Deflections and moments are also computed for concentrated forces acting at the centre of the plate and at the centre of a free edge.

The use of hexagonal networks has been developed by MARCUS. It makes possible comparatively simple expressions for the boundary conditions along all the edges of oblique plates. VOGT, 39, has applied the method to plates resting on parallel supports. A comprehensive investigation of such plates has also been made by JENSEN. He uses both oblique hexagonal networks and rectangular ones. His paper also contains results obtained for slabs with curbs along the unsupported edges. An approximate method of correction for different magnitudes of the loaded area is also stated. Further calculations have been published by JENSEN and ALLEN.

Difference methods yield good approximations for the elastic surface of oblique plates if a large number of deflection ordinates are used in the calculations. These ordinates are evaluated as solutions of systems of linear equations. The solution involves considerable work for systems of many unknowns. However, difference methods do not easily lend themselves to general expressions for deflections and moments.

Results obtained from series solutions of (211.6) and difference methods have been used to establish rules for estimat-

ing moments in oblique plates (see VOGT 40, 55, RÜSCH, OLSEN and REINITZHUBER).

The effect of anisotropy seems to have been treated only for rectangular plates (see e. g. TIMOSHENKO 40, OLSEN and REINITZHUBER). The method described in this paper may be extended to anisotropic plates in principle without any difficulties.

Tests performed on oblique plates have been described by GOSSARD, SIESS, NEWMARK and GOODMAN, FAVRE and SCHUMANN. Oblique frames have been treated experimentally by VOGT 53, PLETTA and FREDERICK.

Plates treated in this paper transfer the loads to parallel supports. The variation of the deflections in the direction perpendicular to the supports is of essential significance for the moments Slopes and curvatures perpendicular to the free edges are often of secondary importance. The approximate solution described in 2 is evolved by considering this circumstance.

The fundamental principles and equations of the method are given in 21. Section 21 also contains the relations between deflections, moments, and shearing forces in thin elastic plates. The usual expressions must be modified in order to suit the method.

A case with especially simple boundary conditions is treated in 22. Approximate solutions of the fundamental equations are obtained in the form of sine series. A method of improving the convergence of the series is discussed. Errors originating from the neglect of terms in the series are estimated. The general formulas are then applied to rectangular plates. The results obtained show the effect of using finite differences. This effect is studied together with the influence of the distribution of load perpendicular to the free edges in the following section. Diagrams given there enable corrections to be made for both effects.

Simply supported oblique plates are treated in 23, starting from the approximate coefficients derived in 22. These are modified by increments accounting for the changed boundary conditions. The method is applied to the construction of influence functions.

The application of the method to continuous plates is outlined in 24. The design of simple frames is discussed in 25.

The method was applied to some model plates. These plates were also tested with respect to deflections and strains. The arrangement of the experiments is described in 3. This section

also contains tables and diagrams showing the experimental and theoretical results.

Some derivations of little primary interest are given in appendices. Diagrams and equations needed for practical computations are shown in Appendices 52, 54, 55, 56, 57.

2. Theoretical part. Description of the method

21. Fundamental principles and equations

211. Approximate description of the elastic surface

A thin rectangular plate is supported along two parallel edges as shown in Fig. 211.1. Points on the middle plane of the plate are referred to a rectangular coordinate system, $Oxyz$. The span of the plate is l, its width is b.

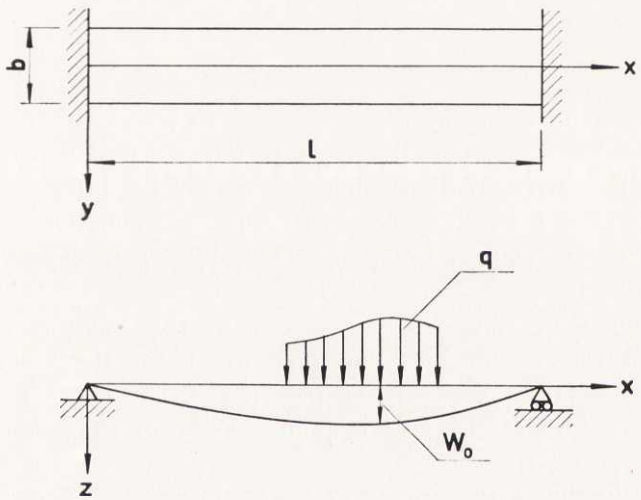

Fig. 211.1. Strip resting on two parallel supports.

The plate carries a transverse load of intensity $q = q(x; y)$. When loaded the plate is deformed; its deflections in the z-direction are $w = w(x; y)$ defining the middle surface of the plate.

The function w generally depends upon the two coordinates x and y. When the width b is small compared to the length l, the y variation is unimportant. The deflection is essentially described by its ordinates $W_0(x)$ along $y = 0$. This statement

can also be expressed in the following way: The plate functions as a beam of span l and flexural rigidity

$$EI = Eb\,h^3/12$$

where E is the modulus of elasticity and h the thickness of the plate. Applying the theory of bent beams (see TIMOSHENKO, 51.1), the deflection W_0 is obtained from the following equation:

$$\frac{d^4 W_0}{d x^4} = \frac{q_0 b}{EI} \tag{1}$$

The quantity

$$q_0 = \frac{1}{b} \int_{-\frac{1}{2}b}^{\frac{1}{2}b} q(x; y)\, d y$$

is the mean intensity of the load at each x coordinate.

When the deflection W_0 is determined, the moment can usually be derived with sufficient accuracy by integrating (1). The shearing forces are obtained from an equation of equilibrium for a plate element cut out by two adjacent planes perpendicular to the x-axis.

The moments and shearing forces in the vicinity of concentrated loads cannot be determined by this method. However, this circumstance is of little practical interest when $b \ll l$, since the width of the load is then usually of the same order of magnitude as b.

This simple method of regarding the plate as a beam is generally not applicable to square or nearly square plates. Neither is it suitable for treating plates wider than their spans. In more general cases with load intensities varying in the y direction the deflection cannot be described even roughly by a single function of x.

It is possible to take into consideration the variation of the deflection w with respect to y by cutting the plate into $R+1$ elemental strips, bounded by planes perpendicular to the y-axis. The width of the inside strips is assigned a constant value, t,

so small that variations of w within a strip can be neglected. Outside strips at the free boundaries of the plate are given the width $\frac{1}{2}t$. The reason why inside strips are made wider than the outer ones will appear from the derivation of the fundamental equations in 212.

In a simple case no shearing forces or twisting moments act on sections parallel to the xz-plane. An external load q is then transmitted to the edges directly by the loaded strip. As a matter of fact the distribution of stresses within the strip coincides with that of a beam. Denoting by W_r the deflection of the strip number r, the following expression can be established:

$$\frac{d^4 W_r}{d x^4} = \frac{q_r}{D} \tag{2}$$

where q_r is the load intensity. D is the flexural rigidity of the plate,

$$D = \frac{E h^3}{12 (1 - \nu^2)} \tag{3}$$

depending on the modulus of elasticity E, the thickness h of the plate, and Poisson's ratio ν. Equation (2) differs from the differential equation of a beam, (1), by the factor $1 - \nu^2$, indicating the effect of normal stresses in the y direction (see TIMOSHENKO 40).

The function W_r is the deflection caused by that portion of the load which acts directly on the strip r. It may be termed the "principal deflection".

The principal deflection for simply supported strips under various loads is obtained from (2). The equation contains only forces per unit area. Before inserting line loads F_r in the formula, they must be replaced by surface loads q_r of the appropriate intensity. For inside strips, Fig. 211. 2,

$$q_r = F_r / t$$

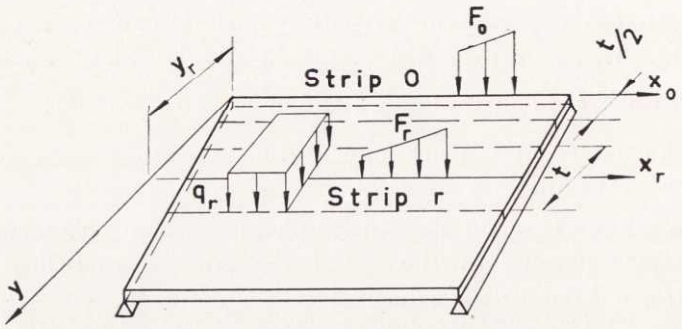

Fig. 211. 2. Loads on inside and outside strips.

Forces acting on the marginal strips are only distributed over the width $\frac{1}{2}t$. As a consequence, the load intensity on strip 0 is

$$q_0 = 2 F_0 / t$$

The plate in Fig. 211. 2 is assumed to be oblique (parallelogram-shaped). In this case, too, the W functions for simply supported strips are determined from (2).

In applying the method described in this paper the principal deflections should preferably be expressed as trigonometric series,

$$W_r = \sum_{n=1}^{\infty} W_{rn} \sin \frac{n \pi x_r}{l} \tag{4}$$

were x_r is the distance from the left support of strip r, Fig. 211. 2. An arbitrary Fourier coefficient W_{rn} is obtained by multiplying both sides of the equation by $\sin n \pi x_r / l$ and integrating from $x_r = 0$ to $x_r = l$ (see CHURCHILL 41):

$$W_{rn} = \frac{2}{l} \int_0^l W_r \sin \frac{n \pi x_r}{l} \, d x_r \tag{5}$$

Principal deflections for loadings of practical interest and general expressions for the corresponding Fourier coefficients, the "principal coefficients", are summarized in Appendix 55.

So far, only the direct effect of external loads on a strip has been treated. Generally the behaviour of a strip is also influenced by reactions from the adjacent strips. As long as the continuity of the plate is not destroyed, the deformations of adjacent strips must be compatible. When compatibility conditions are introduced, moments and shearing forces acting on the sides of each strip must be considered. Their influence is accounted for by applying the differential equation of elastic plates (see NADAI, TIMOSHENKO 40),

$$\frac{\partial^4 w}{\partial x^4} + 2\frac{\partial^4 w}{\partial x^2 \partial y^2} + \frac{\partial^4 w}{\partial y^4} = \frac{q}{D} \tag{6}$$

This equation can not be used in its original form for determining deflections of strips with finite widths. Necessary modifications can be made by introducing finite differences.

212. Differential equations for the deflections

The deflection w of a thin elastic plate subjected to a transverse load is determined by the partial differential equation (211. 6) together with the appropriate boundary conditions. It is accomplished by supposing the deflections to be small in relation to the thickness, h, of the plate. Deformations caused by shearing forces are neglected. Except in the vicinity of concentrated loads, this omission is permissible if h is small compared to the other dimensions of the plate.

In 211 the elastic surface was described by the deflections of the strips, that is, by a finite number of plane curves $w = w_r(x_r)$ situated at equal distances t from each other, Fig. 212. 1. The independent coordinate x_r of a w_r function is measured from the left support of the strip r. The horizontal distance of the curve formed by the centre line of strip r from the free edge of strip 0 is given by the coordinate $y = r \cdot t$: Fig. 212. 1

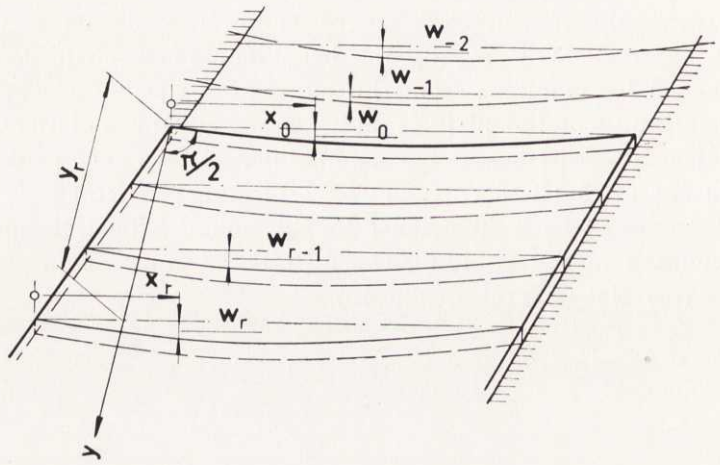

Fig. 212. 1. Notations used for strip deflections.

The transition from the elastic surface w to discrete curves does not alter the derivatives of w with respect to x along the r curves. For the curve r the partial derivative $\frac{\partial w}{\partial x}$ is equal to the derivative of w_r with respect to x_r. Partial derivatives with respect to y cannot be expressed exactly, however. They must be replaced by finite differences (see TIMOSHENKO 51, 2). The following approximation is obtained for the derivative of w with respect to y at $y = y_r$ (cf. Fig. 212. 2):

$$\left(\frac{\partial w}{\partial y}\right)_r \approx \frac{1}{2t}(w_{r+1} - w_{r-1}) \tag{1}$$

The difference between the derivatives $\frac{\partial w}{\partial y}$ at $y = y_{r+1/2}\,t$ and at $y = y_{r-1/2}\,t$, divided by t, is approximately the second derivative:

$$\left(\frac{\partial^2 w}{\partial y^2}\right)_r \approx \frac{1}{t^2}(w_{r+1} - 2\,w_r + w_{r-1}) \tag{2}$$

The third derivative can be interpreted as the first derivative of the second:

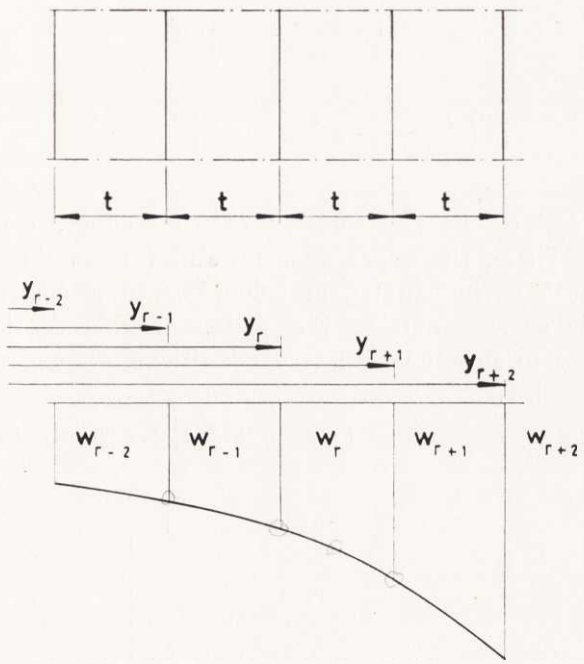

212. 2. Deflections used in difference expressions.

$$\left(\frac{\partial^3 w}{\partial y^3}\right)_r \approx \frac{1}{2t^3}(w_{r+2} - 2w_{r+1} + 2w_{r-1} - w_{r-2}) \tag{3}$$

If w_{r-1}, w_r and w_{r+1} in (2) are replaced by their second derivatives with respect to y at y_{r-1}, y_r, and y_{r+1}, the equation gives an approximation of the fourth derivative,

$$\left(\frac{\partial^4 w}{\partial y^4}\right)_r \approx \frac{1}{t^4}(w_{r+2} - 4w_{r+1} + 6w_r - 4w_{r-1} + w_{r-2}) \tag{4}$$

Along the centre line of strip r, $y = y_r$, Eq. (211. 6) assumes the form

$$\frac{d^4 w_r}{dx_r^4} + 2\frac{d^2}{dx_r^2}\left(\frac{\partial^2 w}{\partial y^2}\right)_r + \left(\frac{\partial^4 w}{\partial y^4}\right)_r = \frac{q_r}{D} \tag{5}$$

If (2) and (4) are inserted into this equation the general differential equation of the deflection w_r is obtained:

$$w_{r+2}+w_{r-2}+\left(2\,t^2\frac{d^2}{d\,x_r^{\,2}}-4\right)(w_{r+1}+w_{r-1})+$$

$$+\left(t^4\frac{d^4}{d\,x_r^{\,4}}-4\,t^2\frac{d^2}{d\,x_r^{\,2}}+6\right)w_r=\frac{q_r\,t^4}{D} \tag{6}$$

For deflections in the vicinity of free edges, (6) must be modified. There, the expressions (2) and (4) contain deflections which must be interpreted as belonging to a continuation of the elastic surface outside the plate. If this continuation is constructed to suit the boundary conditions, (2) and (4) can be directly applied.

Along the boundary $y=0$, Fig. 212. 1, Kirchhoff (see NADAI) obtains:

$$\left.\begin{aligned}\frac{\partial^2 w}{\partial y^2}+\nu\frac{\partial^2 w}{\partial x^2}&=0\\ \frac{\partial^3 w}{\partial y^3}+(2-\nu)\frac{\partial^3 w}{\partial x^2\,\partial y}&=\frac{F_0}{D}\end{aligned}\right\} \tag{7}$$

where F_0 is a line load applied along the free edge $y=0$. Here the derivatives with respect to y are replaced by (1), (2) and (3). Two equations then obtained contain functions w_{-1} and w_{-2}: Fig. 212. 1. These determine the continuation of the elastic surface for negative values of y:

$$\left.\begin{aligned}\frac{1}{t^2}(w_1-2\,w_0+w_{-1})+\nu\frac{d^2 w_0}{d\,x_0^{\,2}}&=0\\ \frac{1}{2\,t^3}(w_2-2\,w_1+2\,w_{-1}-w_{-2})+\frac{2-\nu}{2\,t}\,\frac{d^2}{d\,x_0^{\,2}}(w_1-w_{-1})&=\frac{F_0}{D}\end{aligned}\right\} \tag{8}$$

The deflections w_{-1} and w_{-2} are solved from this system and substituted in (6) for $r=0$ and $r=1$. This yields the following differential equations for the deflections of the strips 0 and 1:

$$\left[(1-\nu^2)t^4\frac{d^4}{d\,x_0^{\,4}}-4\,(1-\nu)\,t^2\frac{d^2}{d\,x_0^{\,2}}+2\right]w_0+$$

$$+\left[(4-2\nu)\,t^2\frac{d^2}{dx_0^2}-4\right]w_1+2\,w_2=\frac{q_0\,t^4}{D} \tag{9}$$

$$\left[(2-\nu)\,t^2\frac{d^2}{dx_1^2}-2\right]w_0+\left[t^4\frac{d^4}{dx_1^4}-4\,t^2\frac{d^2}{dx_1^2}+5\right]w_1+$$

$$+\left(2\,t^2\frac{d^2}{dx_1^2}-4\right)w_2+w_3=\frac{q_1\,t^4}{D} \tag{10}$$

The load intensity q_0 also includes possible line loads F_0:

$$q_0=q+2\,F_0/t \tag{11}$$

Where the number of strips is four or more a differential equation can only be influenced by the boundary conditions at one free border. This is not the case if a plate is divided into two elements, so that $R=1$. In forming the fourth derivative with respect to y for $y=0$ according to (4), not only w_{-1} and w_{-2} but also the function w_2 must be taken into account. This deflection refers to points outside a two-strip plate and is thus determined by the boundary conditions at ~~edge 2~~. $y=t$

The derivation of w_2 for a two-strip plate is given in Appendix 51 together with the corresponding transformation of (9). As a result the following system of equations is obtained for the deflections w_0 and w_1:

$$\left.\begin{aligned}\left[(1-\nu^2)\,t^4\frac{d^4}{dx_0^4}-4\,(1-\nu)\,t^2\frac{d^2}{dx_0^2}\right]w_0+4(1-\nu)\,t^2\frac{d^2w_1}{dx_0^2}&=\frac{q_0\,t^4}{D}\\ 4\,(1-\nu)\,t^2\frac{d^2w_0}{dx_1^2}+\left[(1-\nu^2)\,t^4\frac{d^4}{dx_1^4}-4\,(1-\nu)\,t^2\frac{d^2}{dx_1^2}\right]w_1&=\frac{q_1\,t^4}{D}\end{aligned}\right\} \tag{12}$$

The coordinates x_0 and x_1 are by definition measured from the left support of the plate, Fig. 212. 3

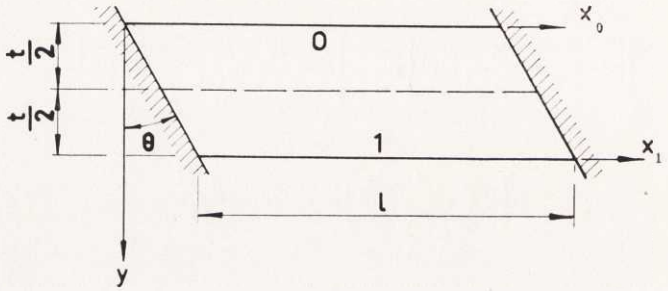

Fig. 212. 3. Plate divided into two strips.

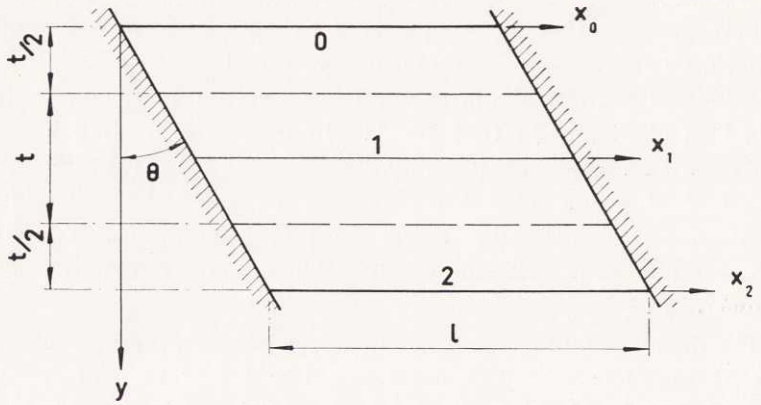

Fig. 212. 4. Plate divided into three strips.

If a plate is divided into three strips ($R = 2$), the differential equations for deflections at the free boundaries 0, 2 is formed by (9). The equation of the deflection of strip 1, Fig. 212. 4, is influenced by the edge conditions at $y = 0$ and at $y = 2\,t$. From Appendix 51 the following system is obtained for the three deflections:

$$
\left.
\begin{aligned}
&\left[(1-\nu^2)\,t^4\,\frac{d^4}{dx_0^4}-4\,(1-\nu)\,t^2\,\frac{d^2}{dx_0^2}+2\right]w_0+\\
&+\left[(4-2\nu)\,t^2\,\frac{d^2}{dx_0^2}-4\right]w_1+2\,w_2=\frac{q_0\,t^4}{D}\\
&\left[(2-\nu)\,t^2\,\frac{d^2}{dx_1^2}-2\right](w_0+w_2)+\\
&+\left(t^4\,\frac{d^4}{dx_1^4}-4\,t^2\,\frac{d^2}{dx_1^2}+4\right)w_1=\frac{q_1\,t^4}{D}\\
&2\,w_0+\left[(4-2\nu)\,t^2\,\frac{d^2}{dx_2^2}-4\right]w_1+\\
&+\left[(1-\nu^2)\,t^4\,\frac{d^4}{dx_2^4}-4\,(1-\nu)\,t^2\,\frac{d^2}{dx_2^2}+2\right]w_2=\frac{q_2\,t^4}{D}
\end{aligned}
\right\} \qquad (13)
$$

Irrespective of the mode of division of the plate, the functions w_r are determined by linear differential equations of the fourth order, with constant coefficients. Combined with the boundary conditions along the supports these equations yield single-valued expressions for the deflections.

The exact solution of the equations offers no theoretical difficulties. However, even for rectangular plates divided into more than two strips, results require considerable numerical work. Computations would be simplified by tables of function coefficients C_n in expressions $w_r = \sum C_n z_n(x_r)$ for various dimensions and loadings of plates. A great many coefficients would have to be computed, since the solutions contain different functions $z_n(x_r)$ depending on the number of strips, the type of loading and the boundary conditions. Furthermore, the functions z_n involved would be cumbersome to use. And the result of such complicated operations would be impaired by errors caused by the finite width of the strips.

Thus the exact solution of the equations is generally complicated, and can give but approximate expressions of the deflections. This paper aims at presenting a simpler solution in the form of trigonometric series. For comparison, the exact solution is given in 221 for a rectangular plate divided into two strips.

The use of trigonometric series for the deflection w is especially expedient for rectangular plates. For oblique plates deflections vanishing along the supports can also be represented in the same manner. The coordinates x_r now have their origins at different distances from the y-axis, Fig. 212. 4, the trigonometric functions are not in phase. This leads to complications, and suggests that some other coordinate system may be advantageous. Several authors have used oblique coordinates, (see FAVRE 43, 46), but the simplifications attained in formulating the boundary conditions along the supports are offset by complications in the differential equations. With orthogonal coordinates, derivatives of the second and fourth order will appear; with oblique coordinates the equations will contain derivatives of the first and third order also. These latter derivatives make the method described in 223 for improving the convergence of the trigonometric series cumbersome. Besides, the boundary conditions along the free edges are sometimes difficult to express with sufficient accuracy in oblique coordinates. Plates with large values of the angle of obliquity Θ and with Poisson's ratio $\nu \neq 0$ yield inapplicable values of some deflections, because the expressions for some coefficients in the series contain small denominators. Finally, an orthogonal system with one coordinate axis perpendicular to the free edges is useful for describing the effect of loadings of practical interest.

The application of rectangular coordinates causes some difficulties in expressing the boundary conditions along the supports. When the angle of obliquity Θ has a finite value between 0 and $\frac{1}{2}\pi$, the deflections w_r refer to a plate supported at separate points rather than along continuous edges. Errors arising from this discrepancy are usually small and limited to a region in the vicinity of the supports. The problem is discussed further in 232.

213. Moments and shearing forces as functions of the deflections

Some known formulas from the theory of plates may be useful in applying the method given in this paper. Fig. 213. 1 shows

moments and shearing forces acting on a small element cut out of a plate by two pairs of planes perpendicular to the x- and y-axes. The first subscript attributed to any notation indicates the direction of the normal of the corresponding surface.

The moments can be expressed as functions of the partial derivatives of w. For details of the derivation see, for instance, NADAI. If the distribution of strains is supposed to be a linear function of the distance from the middle plane of the plate the maximum strain is easily expressed by means of the deflection: In the x direction the maximum strain is

$$\varepsilon_{x,\,max} = \frac{h}{2\,r_x} \approx \frac{h}{2}\left|\frac{\partial^2 w}{\partial x^2}\right| \tag{1}$$

where $1/r_x$ is the curvature of the middle ~~plane~~ surface in a section perpendicular to the y-axis.

From (1) and a similar expression for $\varepsilon_{y,\,max}$ the normal stresses are obtained from Hooke's law and Poisson's ratio ν. As the stresses are also linear functions of the distance from the middle surface of the plate, the bending moments,

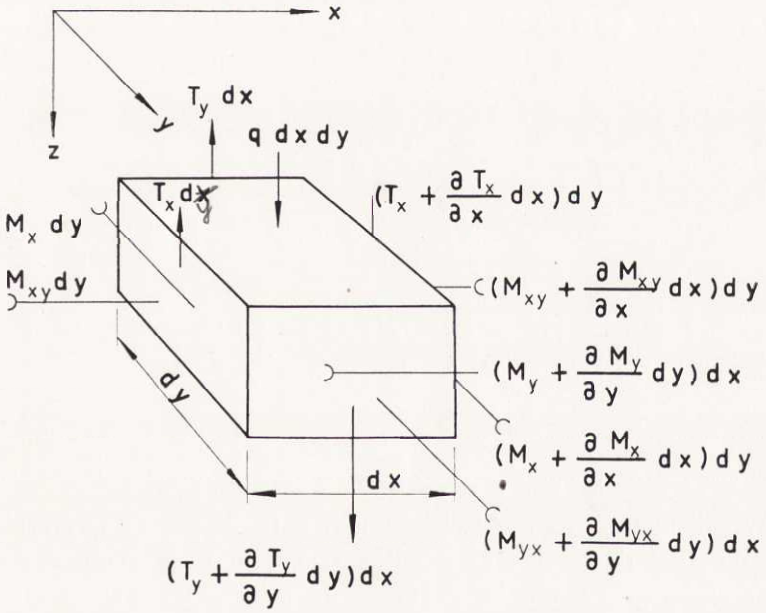

Fig. 213. 1. Moments and shearing forces acting on an element of a plate.

M_x, M_y, and twisting moments M_{xy} are obtained by simple integration,

$$M_x = -D\left(\frac{\partial^2 w}{\partial x^2} + \nu \frac{\partial^2 w}{\partial y^2}\right) \tag{2}$$

$$M_y = -D\left(\frac{\partial^2 w}{\partial y^2} + \nu \frac{\partial^2 w}{\partial x^2}\right) \tag{3}$$

$$M_{xy} = -M_{yx} = D(1-\nu)\frac{\partial^2 w}{\partial x\, \partial y} \tag{4}$$

or, in difference form, after substitution of (212. 1) and (212. 2):

$$M_{xr} = -D\left[\frac{\nu}{t^2}(w_{r+1} + w_{r-1}) + \left(\frac{d^2}{d x_r^2} - \frac{2\nu}{t^2}\right)w_r\right] \tag{5}$$

$$M_{yr} = -D\left[\frac{1}{t^2}(w_{r+1} + w_{r-1}) + \left(\nu \frac{d^2}{d x_r^2} - \frac{2}{t^2}\right)w_r\right] \tag{6}$$

$$M_{xyr} = \frac{D}{2t}\frac{d}{d x_r}(w_{r+1} - w_{r-1}) \tag{7}$$

The bending moment M_y vanishes along a free edge. There, according to (3)

$$\frac{\partial^2 w}{\partial y^2} + \nu \frac{\partial^2 w}{\partial x^2} = 0 \tag{8}$$

From (2) and (8) the moment M_x along $y = 0$ is obtained as a function of only one derivative,

$$M_{x0} = -D(1-\nu^2)\frac{d^2 w_0}{d x_0^2} \tag{9}$$

When computing the twisting moments M_{xyr}, an expression for the first derivative of w with respect to y is required. A general form is given by (212. 1). However, for points along the unsupported borders of the plate, this equation contains deflections referring to points outside the plate. At $y = 0$, Fig.

212.1, the approximation for $\frac{\partial w}{\partial y}$ is a function of w_{-1} which can be obtained from (212.8). Substituting the result in (212.1), the partial derivative with respect to y is obtained in the form

$$\left(\frac{\partial w}{\partial y}\right)_0 \approx \frac{1}{2t}(w_1 - w_{-1}) = \frac{1}{t}(w_1 - w_0) + \frac{1}{2}\nu t \frac{d^2 w_0}{d x_0^2} \tag{10}$$

Substitution in (7) gives an expression for M_{xy0}. Contrary to what might be expected, the value obtained for the twisting moment is not generally zero. The disagreement with the actual conditions along the free edges depends not only upon the approximate character of the finite differences but also upon simplifications made in the derivation of (211.6).

Generally, the maximum bending moment acts on a plane at an angle ϑ to the y-axis. This appears from the equilibrium of an element of the plate, Fig. 213.2. The planes AC, AB and BC cut out a triangular element with sides perpendicular

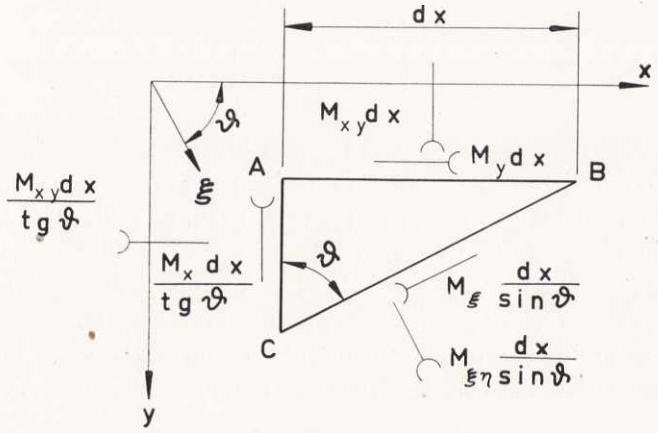

Fig. 213.2. Moments acting on different planes perpendicular to the $x\,y$ plane.

to the x, y and ξ directions, where ξ is an arbitrary oblique direction forming an angle ϑ with the x direction. The resultant of the moment vectors acting on this element vanishes:

$$\left.\begin{aligned} M_\xi &= M_x \cos^2\vartheta + M_y \sin^2\vartheta - 2 M_{xy} \sin\vartheta \cos\vartheta \\ -M_{\xi\eta} &= (M_y - M_x) \sin\vartheta \cos\vartheta - M_{xy}(\cos^2\vartheta - \sin^2\vartheta) \end{aligned}\right\} \tag{11}$$

For maximum M_ξ the angle ϑ will be ϑ_0:

$$\operatorname{tg} 2\,\vartheta_0 = \frac{2\,M_{xy}}{M_y - M_x} \tag{12}$$

Inserting $\sin \vartheta_0$ and $\cos \vartheta_0$ in the first equation of (11), the extreme values of the bending moments become

$$M_{1,\,2} = \frac{1}{2}(M_x + M_y) \pm \sqrt{\left[\frac{1}{2}\,(M_x - M_y)\right]^2 + M^2{}_{x\,y}} \tag{13}$$

The shearing forces T_x and T_y determine shearing stresses perpendicular to the middle plane of the plate. The shears are associated with the moments by equations of equilibrium. For the element shown in Fig. 213. 1 the equilibrium equations, combined with (2) — (4), give

$$\left.\begin{aligned} T_x &= -D\left(\frac{\partial^3 w}{\partial x^3} + \frac{\partial\, w^3}{\partial x\, \partial y^2}\right) \\ T_y &= -D\left(\frac{\partial^3 w}{\partial y^3} + \frac{\partial^3 w}{\partial x^2\, \partial y}\right) \end{aligned}\right\} \tag{14}$$

When this is applied to a plate divided into strips, the derivatives with respect to y must be replaced by the approximately equivalent differences (212. 1), (212. 2) and (212. 3). For strips in the vicinity of free edges this transformation involves the deflection of points outside the plate. These deflections can be determined by solving (212. 8) for $r = 0,\ R$.

For a strip along an unsupported border $y = 0,\ R\,t$, the operations here described give a particularly simple result

$$(T_x)_0 = -D\,(1 - \nu)\,\frac{d^3 w_0}{d\,x_0{}^3} \tag{15}$$

For a plane whose normal is at an angle ϑ to the x-axis, the shearing force T_ξ is obtained from an equation of equilibrium for the element shown in Fig. 213. 2. The force $T_y\,d\,x$ on the surface AB acts in the opposite direction of the z-axis, Fig. 213. 1. The force $T_x\,d\,y$ on AC also acts upwards. The surface

BC is subject to a force $T_\xi dy$ sec ϑ directed downwards. If there is no concentrated vertical load on the element, equilibrium demands that

$$T_\xi = T_x \cos \vartheta + T_y \sin \vartheta$$

The reactions Q along the supports have been derived by Kirchhoff. Introducing coordinates ξ and η, perpendicular and parallel to the support, Fig. 213.3, Kirchhoff's expression is

$$Q = -D\left[\frac{\partial^3 w}{\partial \xi^3} + (2-\nu)\frac{\partial^3 w}{\partial \xi \partial \eta^2}\right] \tag{16}$$

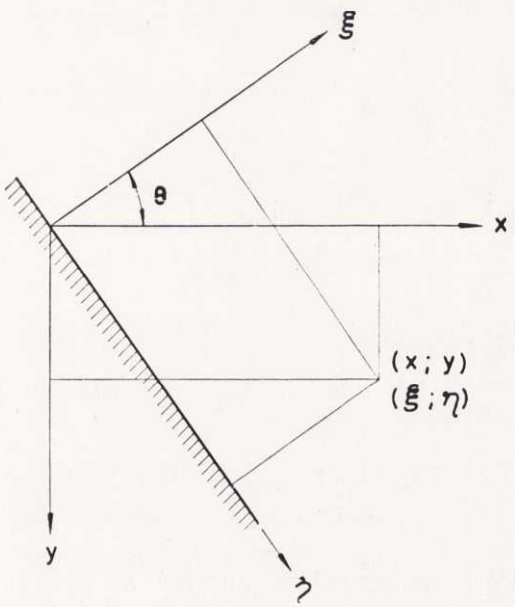

Fig. 213.3. Alternative rectangular coordinates for describing the position of a point.

The derivatives with respect to ξ and η in this equation can be written as functions of x and y. Fig. 213.3 shows that

$$x = \xi \cos \Theta + \eta \sin \Theta$$

$$y = -\xi \sin \Theta + \eta \cos \Theta$$

Hence, by the "chain rule" for partial derivatives,

$$\frac{\partial^3 w}{\partial \xi^3} = \frac{\partial^3 w}{\partial x^3} \cos^3 \Theta - 3 \frac{\partial^3 w}{\partial x^2 \partial y} \sin \Theta \cos^2 \Theta +$$

$$+ 3 \frac{\partial^3 w}{\partial x \partial y^2} \sin^2 \Theta \cos \Theta - \frac{\partial^3 w}{\partial y^3} \sin^3 \Theta$$

$$\frac{\partial^3 w}{\partial \xi \partial \eta^2} = \frac{\partial^3 w}{\partial x^3} \sin^2 \Theta \cos \Theta + \frac{\partial^3 w}{\partial x^2 \partial y} \sin \Theta (2 \cos^2 \Theta - \sin^2 \Theta) +$$

$$+ \frac{\partial^3 w}{\partial x \partial y^2} (\cos^2 \Theta - 2 \sin^2 \Theta) \cos \Theta - \frac{\partial^3 w}{\partial y^3} \sin \Theta \cos^2 \Theta$$

Here the derivatives with respect to x and y can be expressed by the deflections w_r.

22. Plates with simply supported strips

221. Exact solution of the differential equations in some special cases

A parallelogram plate is supported at the opposite edges $y = x \cot \Theta$ and $y = (x - l) \cot \Theta$ as shown in Fig. 221. 1. The width b of the plate is assumed to be small compared to the length l of the free edges $y = \pm \frac{1}{2} b$. In such a case the division of the plate into only two strips can yield a good approximation of the deflections along the free edges. Both strips are outside strips of width $\frac{1}{2} t$.

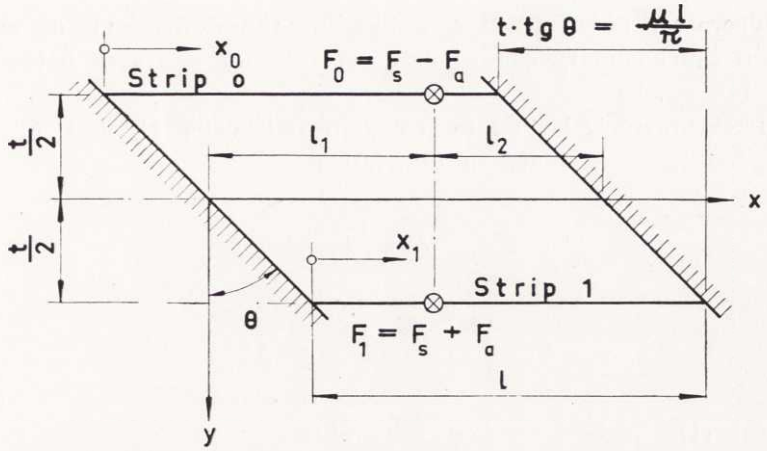

Fig. 221.1. Plate divided into two strips and carrying concentrated loads F_r.

The deflections w_0 for $y=-\frac{1}{2}t$ and w_1 for $y=+\frac{1}{2}t$ can be looked upon as composed of two parts:

$$w_0 = w_s - w_a$$

$$w_1 = w_s + w_a$$

The load intensities, q_0 and q_1, can also be rewritten:

$$q_0 = q_s - q_a$$

$$q_1 = q_s + q_a$$

Substituting the quantities w_s, w_a, q_s and q_a in (212.12), expressions are obtained which, added and subtracted, give

$$\frac{d^4 w_s}{dx^4} = \frac{q_s}{D(1-\nu^2)} \tag{1}$$

$$\left[\frac{d^4}{dx^4} - \frac{8}{t^2(1+\nu)}\frac{d^2}{dx^2}\right] w_a = \frac{q_a}{D(1-\nu^2)} \tag{2}$$

There are independent solutions for the deflections w_s and w_a if the boundary conditions do not imply relations between w_s and w_a.

If the plate is loaded by concentrated loads F_0 and F_1 at the points $x = l_1$ shown in Fig. 221. 1

$$F_0 = F_s - F_a = \frac{1}{2}(q_s - q_a)\, t$$

$$F_1 = F_s + F_a = \frac{1}{2}(q_s + q_a)\, t$$

Eq. (1) is solved by four integrations

$$w_s = \frac{F_s l^3}{D\, t\, (1 - \nu^2)} \left[\frac{1}{3} \left(\frac{x'}{l} \right)^3 + B_{1s} + B_{2s} \frac{x}{l} + B_{3s} \left(\frac{x}{l} \right)^2 + B_{4s} \left(\frac{x}{l} \right)^3 \right] \qquad (3)$$

where

$$x' = \begin{cases} 0 \text{ for } x < l_1 \\ x - l_1 \text{ for } x > l_1 \end{cases}$$

B_{is} are constants of integration.

Eq. (2) is solved by introducing the Laplace transform (see, for instance, CHURCHILL 44)

$$\overline{w}(p) = \int_0^\infty w_a(x)\, e^{-px}\, dx$$

and integrating. For a concentrated load F_a a linear equation for $\overline{w}$ emerges:

$$p^4 \overline{w} - \frac{k^2}{l^2} p^2 \overline{w} - \left(p^3 - \frac{k^2}{l^2} p \right) w_a(0) - \left(p^2 - \frac{k^2}{l^2} \right) w_a'(0) - p\, w_a''(0) -$$

$$- w_a'''(0) = \frac{2 F_a}{t D (1 - \nu^2)} e^{-pl}$$

Here $w_a(0)$, $w_a'(0)$, $w_a''(0)$ and $w_a'''(0)$ are fixed values at $x = 0$ of the function w_a and its first three derivatives and

$$k = \frac{2\,l}{t}\sqrt{\frac{2}{1+\nu}} \tag{4}$$

The transform $\overline{w}$ is obtained by solving the above equation Finally w_a can be calculated as the inverse transform of $\overline{w}$:

$$w_a = \frac{F_a\,l^3}{D\,t\,(1-\nu^2)}\left(\frac{2}{k^3}\sin\mathrm{h}\frac{k\,x'}{l} - \frac{2\,x'}{k^2\,l} + B_{1a} + B_{2a}\frac{x}{l} + \right.$$

$$\left. + B_{3a}\sin\mathrm{h}\frac{k\,x}{l} + B_{4a}\cos\mathrm{h}\frac{k\,x}{l}\right) \tag{5}$$

B_{ia} are constants of integration.

The eight constants B_{is} and B_{ia} are determined by the boundary conditions at the points of support,

$$x = \pm\frac{1}{2}\,t\,\mathrm{tg}\,\Theta$$

and

$$x = l \pm \frac{1}{2}\,t\,\mathrm{tg}\,\Theta$$

When $\Theta \neq 0$, even in the simple case of $w = \frac{\partial^2 w}{\partial x^2} = 0$ at the supports, the computations become laborious and result in involved expressions. For simply supported plates the equations for the deflections become still more complicated.

Only for rectangular plates is the solution easy. The boundary conditions for a simply supported rectangular plate are

$$x = 0,\ l\ ;\ w_s = w_a = \frac{d^2 w_s}{d\,x^2} = \frac{d^2 w_a}{d\,x^2} = 0 \tag{6}$$

The constants of integration can be determined from these conditions, and inserted in (3) and (5). Where only one concentrated load $F_0 = F$ is applied to the plate, the deflections become

$$w_s = \frac{F l^3}{2 D t (1-\nu^2)} \left[\frac{1}{3} \left(\frac{x'}{l} \right)^3 + \frac{l_1 l_2}{3 l^2} \left(1 + \frac{l_2}{l} \right) \frac{x}{l} - \frac{l_2}{3 l} \left(\frac{x}{l} \right)^3 \right] \tag{7}$$

$$w_a = \frac{-F l^3}{D t (1-\nu^2) k^3} \left[\sin \mathrm{h} \frac{k x'}{l} - \frac{\sin \mathrm{h} (k l_2 / l)}{\sin \mathrm{h} k} \sin \mathrm{h} \frac{k x}{l} + \right.$$

$$\left. + k \left(\frac{l_2 x}{l^2} - \frac{x'}{l} \right) \right] \tag{8}$$

where

$$l_2 = l - l_1$$

There are also easy solutions for rectangular plates carrying uniformly distributed loads. Suppose that strip 0 deflects w_0 when subjected to a load of intensity q. Then

$$q_s = \frac{1}{2} q, \quad q_a = -\frac{1}{2} q$$

Solving (1) and (2) by elementary methods the deflections are found to be

$$w_s = \frac{q l^4}{48 D (1-\nu^2)} \left[\frac{x}{l} - 2 \left(\frac{x}{l} \right)^3 + \left(\frac{x}{l} \right)^4 \right]$$

$$w_a = \frac{q l^4}{2 D (1-\nu^2)} \left[\frac{1}{k^2} - \frac{1}{2} \frac{x}{l} + \frac{1}{2} \left(\frac{x}{l} \right)^2 + \right.$$

$$\left. + \frac{1}{k^2} \operatorname{tg} \mathrm{h} \frac{k}{2} \sin \mathrm{h} \frac{k x}{l} - \frac{1}{k^2} \cos \mathrm{h} \frac{k x}{l} \right] \frac{1}{k^2}$$

In 225 Eqs. (7) and (8) will be applied to a special plate, and an exact value of the maximum moment compared with a value obtained by the following approximate method.

222. Approximate determination of the deflections

As mentioned in 212 the differential equations for the deflections can be approximately solved by using trigonometric series. This method is particularly expedient when the deflec-

tions and their second derivatives with respect to w vanish along the supports. For a plate divided into two strips the following deflections are assumed:

$$\left.\begin{aligned} w_0 &= \Sigma w_{0n} \sin (n\pi x_0/l) \\ w_1 &= \Sigma w_{1n} \sin (n\pi x_1/l) = \Sigma w_{1n} \cos n\mu \sin (n\pi x_0/l) - \\ &\quad - \Sigma w_{1n} \sin n\mu \cos (n\pi x_0/l) \end{aligned}\right\} \quad (1)$$

as

$$x_1 = x_0 - t \operatorname{tg} \Theta, \quad \mu = \frac{\pi t \operatorname{tg} \Theta}{l} \quad (2)$$

The coordinates x_0 and x_1 are measured from the left support of the strips 0 and 1 as shown in Fig. 212.3. Then w_0, w_1, $\frac{d^2 w_0}{d x_0^2}$ and $\frac{d^2 w_1}{d x_1^2}$, derived from (1), vanish at the supports.

The load intensities q_r are now replaced in Eq. (212.12) by their Fourier expansions

$$q_r = \Sigma q_{rn} \sin (n\pi x_r/l) \quad (3)$$

Here

$$q_{rn} = \frac{2}{l} \int_0^l q_r \sin \frac{n\pi x_r}{l} d x_r \quad (4)$$

is obtained as described in 211.

Substituting the series expressions for w_0, w_1, q_0 and q_1 in the first of Eqs. (212.12), the following equation is obtained

$$\sum \left\{ \left[(1-\nu^2) \left(\frac{n\pi t}{l}\right)^4 + 4(1-\nu) \left(\frac{n\pi t}{l}\right)^2 \right] w_{0n} - \right.$$

$$\left. - 4(1-\nu) \cos n\mu \left(\frac{n\pi t}{l}\right)^2 w_{1n} \right\} \sin \frac{n\pi x_0}{l} = \sum \frac{q_{0n} t^4}{D} \sin \frac{n\pi x_0}{l} -$$

$$- 4(1-\nu) \sum \sin n\mu \left(\frac{n\pi t}{l}\right)^2 w_{1n} \cos \frac{n\pi x_0}{l} \quad (5)$$

For any value of n the terms containing w_{1n} only differ from each other by the factors $\cos n\mu \sin (n\pi x_0/l)$ and $\sin n\mu \cos (n\pi x_0/l)$. Often the difference $\mu l/\pi$ between the zero points of w_0 and w_1 is small compared to the length of the strips. Hence $\sin n\mu$ can also be treated as a small quantity in relation to $\cos n\mu$ when only a few terms are included in the trigonometric series. Therefore, the cosine series are first neglected in (222.5). This equation then expresses the equality of two sine series. It should be satisfied for any value of x_0 between 0 and l. This condition yields

$$\left[(1-\nu^2)\left(\frac{n\pi t}{l}\right)^4 + 4(1-\nu)\left(\frac{n\pi t}{l}\right)^2\right] w_{0n} -$$

$$-4(1-\nu)\cos n\mu \left(\frac{n\pi t}{l}\right)^2 w_{1n} = \frac{q_{0n}t^4}{D}$$

or after division by $n^4\pi^4 t^4/l^4$,

$$\left[1-\nu^2+4(1-\nu)\left(\frac{l}{n\pi t}\right)^2\right] w_{0n} -$$

$$-4(1-\nu)\cos n\mu \left(\frac{l}{n\pi t}\right)^2 w_{1n} = W_{0n} \tag{6}$$

In this equation

$$W_{0n} = q_{0n}\, l^4/n^4\pi^4 D \tag{7}$$

is the general Fourier coefficient for the principal deflection W_0, see 211. Introducing the symbol

$$\beta_n = 4(1-\nu)\, l^2/n^2\pi^2 t^2 \tag{8}$$

(7) can be written

$$(1-\nu^2+\beta_n)\, w_{0n} - \beta_n \cos n\mu\, w_{1n} = W_{0n} \tag{9}$$

For the other strip, by interchange of subscripts,

$$-\beta_n \cos n\mu\, w_{0n} + (1-\nu^2+\beta_n)\, w_{1n} = W_{1n} \tag{10}$$

Thus for each n two equations are formed which determine the unknown Fourier coefficients w_{0n} and w_{1n}. The solution of (9) and (10) may be written (see, for instance, AITKEN)

$$\begin{bmatrix} w_{0n} \\ w_{1n} \end{bmatrix} = \frac{1}{(1-\nu^2+\beta_n)^2-\beta_n^2 \cos^2 n\mu} \begin{bmatrix} 1-\nu^2+\beta_n & \beta_n \cos n\mu \\ \beta_n \cos n\mu & 1-\nu^2+\beta_n \end{bmatrix} \begin{bmatrix} W_{0n} \\ W_{1n} \end{bmatrix} \quad (11)$$

If other coefficients are introduced,

$$\left.\begin{aligned} w_{0n} &= s_n - a_n \\ w_{1n} &= s_n + a_n \end{aligned}\right\} \quad (12)$$

$$\left.\begin{aligned} W_{0n} &= S_n - A_n \\ W_{1n} &= S_n + A_n \end{aligned}\right\} \quad (13)$$

simpler expressions emerge by adding and subtracting (11):

$$s_n = \frac{S_n}{1-\nu^2+\beta_n(1-\cos n\mu)} \quad (14)$$

$$a_n = \frac{A_n}{1-\nu^2+\beta_n(1+\cos n\mu)} \quad (15)$$

For a plate divided into three strips, the system (212. 13) determines all deflections. The deflections w_0, w_1 and w_2 of the three strips 0, 1 and 2 shown in Fig. 212. 4, may be expressed as trigonometric series:

$$\left.\begin{aligned} w_0 &= \Sigma w_{0n} \sin (n\pi x_0/l) \\ w_1 &= \Sigma w_{1n} \sin (n\pi x_1/l) \\ w_2 &= \Sigma w_{2n} \sin (n\pi x_2/l) \end{aligned}\right\} \quad (16)$$

Here

$$x_1 = x_0 - t \operatorname{tg} \Theta$$

$$x_2 = x_0 - 2\, t \operatorname{tg} \Theta$$

Substituting the series for w_0, w_1 and w_2 and the series for the principal deflections W_0, W_1 and W_2 in (212. 13), three

equations containing sine and cosine series are obtained. Neglecting the latter, as was done for plates divided into two strips, three equations result:

$$\left.\begin{aligned} \alpha_{1n}\, w_{0n} - 2\,\beta_{1n}\, w_{1n} + 2\,\gamma_n\, w_{2n} &= W_{0n} \\ -\beta_{1n}\, w_{0n} + \alpha_{2n}\, w_{1n} - \beta_{1n}\, w_{2n} &= W_{1n} \\ 2\,\gamma_n\, w_{0n} - 2\,\beta_{1n}\, w_{1n} + \alpha_{1n}\, w_{2n} &= W_{2n} \end{aligned}\right\} \qquad (17)$$

These determine the unknown coefficients. The new symbols introduced are

$$\alpha_{1n} = 1 - \nu^2 + 4\,(1-\nu)\,(l/n\pi t)^2 + 2\,(l/n\pi t)^4 \qquad (18)$$

$$\alpha_{2n} = 1 + 4\,(l/n\pi t)^2 + 4\,(l/n\pi t)^4 \qquad (19)$$

$$\beta_{1n} = [(2-\nu)\,(l/n\pi t)^2 + 2\,(l/n\pi t)^4]\,\cos\, n\mu \qquad (20)$$

$$\gamma_n = (l/n\pi t)^4\,\cos\, 2n\mu \qquad (21)$$

The derivation of (17) is given in extenso in Appendix 52.

The solution of (17) can be simplified by introducing other coefficients,

$$\left.\begin{aligned} w_{0n} &= s_{0n} - a_{0n} \\ w_{1n} &= s_{1n} \\ w_{2n} &= s_{0n} + a_{0n} \end{aligned}\right\} \qquad (22)$$

$$\left.\begin{aligned} W_{0n} &= S_{0n} - A_{0n} \\ W_{1n} &= S_{1n} \\ W_{2n} &= S_{0n} + A_{0n} \end{aligned}\right\} \qquad (23)$$

which yield three equations. From two of these the coefficients s_{0n} and s_{1n} can be solved,

$$\begin{bmatrix} s_{0n} \\ s_{1n} \end{bmatrix} = \frac{1}{(\alpha_{1n} + 2\,\gamma_n)\,\alpha_{2n} - 4\,\beta^2{}_{1n}} \begin{bmatrix} \alpha_{2n} & 2\,\beta_{1n} \\ 2\,\beta_{1n} & \alpha_{1n} + 2\,\gamma_n \end{bmatrix} \begin{bmatrix} S_{0n} \\ S_{1n} \end{bmatrix} \qquad (24)$$

From the third equation a_{0n} is obtained directly:

$$a_{0n} = \frac{A_{0n}}{a_{1n} - 2\gamma_n} \tag{25}$$

The derivation of the coefficients for a plate divided into five strips is given in Appendix 52.

When Poisson's ratio $\nu = 0$ the coefficients s_{rn} and a_{rn} can be evaluated from Appendix 56 giving diagrams for the coefficients B_{rsn} and C_{rsn} in the general equations

$$s_{rn} = \Sigma B_{rsn} S_{sn}$$

$$a_{rn} = \Sigma C_{rsn} A_{sn}$$

B_{rsn} and C_{rsn} are given as functions of $n\mu$ for different values of the fraction l/nt. These graphs are valid for plates divided into two, three and five strips. For practical computations the width ratio l/t should be chosen between 2 and 4: see 226. Narrow plates may thus be divided into two strips only. Plates with $1 \leqq l/b \leqq 2$ are conveniently treated by using three strips. Still wider plates make the introduction of five strips desirable. When $l/b < \frac{1}{2}$ the curves for $l/b = \frac{1}{2}$ can generally be used with sufficient accuracy.

Assuming $l/t = 2$ as a minimum value for practical computations and taking into account series terms of the first, second and third orders, the fraction l/nt can assume a minimum value of 2/3. The diagrams mentioned contain curves for several values of l/nt between 0.6 and 4.

223. A method of improving the convergence of the trigonometric series

When the quantities s_{rn} and a_{rn} are determined as described in 222, the Fourier coefficients w_{rn} can be computed from equations such as (222.22). The deflections w_r are then obtained

as trigonometric series by application of (222.16). However, such an expression is of practical value only when its convergence is rapid. It is therefore desirable to investigate how the Fourier coefficients for the deflections decrease with n.

Examination of the Fourier coefficients s_{rn} and a_{rn} expressed in (222.24) and (222.25) reveals that the angle Θ, the ratio l/t, and the Fourier coefficients of the principal deflections all influence the convergence.

The first of these three factors usually has little significance. Among all plates with the same length l, width b, and load q, the rectangular plate has the greatest deflections. Thus an upper limit of the sums of the trigonometric series is obtained by putting $\Theta = 0$.

The second factor, the ratio l/t, has greater influence upon the convergence. With increasing n the coefficients s_{rn} and a_{rn} tend to S_{rn} and A_{rn}. The rapidity depends upon the relative width of the strips. For wide strips ($l/t < 0.5$), only small deviations from the corresponding principal coefficients appear even in the coefficients of the first order. For narrow strips such a conformity can only be found for coefficients of higher order. The structure of (222.24) shows that the first terms in the series decrease slower for larger values of l/t.

The third factor, the form of the "principal coefficients" S_{rn} and A_{rn}, is most important. If the principal deflections can be expanded in rapidly converging sine series this is generally true of the deflections also. When a plate is subjected to a uniformly distributed load, the coefficients of its principal deflections decrease with the fifth power of n, (55.2). Then deflections and moments are both usually given with sufficient accuracy by the first term in their expansions.

Concentrated loads give more slowly converging series for the principal deflections. Sometimes deflections can be described satisfactorily only if two or three terms in the expansions are included. Even more difficult is the representation of the moments.

When a plate is divided into strips with finite widths as described in 212, it becomes impossible to represent the moment

where a force acts at a single point. The slope of the plate in the direction perpendicular to its free edges may be regarded as a constant throughout the width of a strip. This restraint upon the elastic surface of the plate makes its deflections almost equivalent to the deformations under a line load distributed over some finite part of the strip.

The approximate method here described therefore does not give unlimited values of the curvature at points of application of concentrated loads. A correct solution of (211.6) would do that. The diagram of the second derivatives $\frac{d^2 w_r}{d x_r^2}$ under each concentrated load has an apex, which is not easily represented by a trigonometric series.

In order to obtain more rapidly converging series, strip deflections are expressed as the sum of the principal deflection W_r of the strip and of a trigonometric series. The deflections of a plate divided into three strips obeys the equations, cf. (222.16):

$$w_0 = \sum w_{0n} \sin \frac{n \pi x_0}{l} = \frac{W_0}{1 - \nu^2} + \sum \left(w_{0n} - \frac{W_{0n}}{1 - \nu^2} \right) \sin \frac{n \pi x_0}{l} \quad (1)$$

$$w_1 = \sum w_{1n} \sin \frac{n \pi x_1}{l} = W_1 + \sum (w_{1n} - W_{1n}) \sin \frac{n \pi x_1}{l} \quad (2)$$

$$w_2 = \sum w_{2n} \sin \frac{n \pi x_2}{l} = \frac{W_2}{1 - \nu^2} + \sum \left(w_{2n} - \frac{W_{2n}}{1 - \nu^2} \right) \sin \frac{n \pi x_2}{l} \quad (3)$$

When $\Theta = 0$, the coefficient w_{1n} for the deflection of the central strip from the second equation of (222.24) becomes

$$w_{1n} = s_{1n} = \frac{1}{N_s} [2 \beta_{1n} S_{0n} + (\alpha_{1n} + 2 \gamma_n) S_{1n}] \quad (4)$$

where

$$N_s = (\alpha_{1n} + 2 \gamma_n) \alpha_{2n} - 4 \beta_{1n}^2 = (1 - \nu^2) \left[1 + \frac{8 \left(1 + \frac{1}{2} \nu \right)}{1 + \nu} \left(\frac{l}{n \pi t} \right)^2 + \right.$$

$$\left. + 8 \left(\frac{l}{n \pi t} \right)^4 \right]$$

Substituting (4) in the first expression in (2), w_1 is obtained:

$$w_1 = \sum \frac{4}{N_s}\left(\frac{l}{n\pi t}\right)^2 \left\{\left[\frac{1-\nu^2}{4}\left(\frac{n\pi t}{l}\right)^2 + 1 - \nu + \left(\frac{l}{n\pi t}\right)^2\right] S_{1n} + \right.$$

$$\left. + \left[1 - \frac{1}{2}\nu + \left(\frac{l}{n\pi t}\right)^2\right] S_{0n}\right\} \sin \frac{n\pi x_1}{l} \qquad (5)$$

The second, more complicated expression for w_1 in (2) can be put into the form:

$$w_1 = W_1 + \sum \left[\left(\frac{\alpha_{1n} + 2\gamma_n}{N_s} - 1\right) S_{1n} + \frac{2\beta_{1n}}{N_s} S_{0n}\right] \sin \frac{n\pi x_1}{l}$$

Substitution in this equation of the values of α_{1n}, β_{1n}, and γ_n according to (222.18), (222.20) and (222.21) gives:

$$w_1 = W_1 - \sum \frac{4}{N_s}\left(\frac{l}{n\pi t}\right)^2 \left\{\left[1 - \nu^2 + (1 - 2\nu^2)\left(\frac{l}{n\pi t}\right)^2\right] S_{1n} - \right.$$

$$\left. - \left[1 - \frac{\nu}{2} + \left(\frac{l}{n\pi t}\right)^2\right] S_{0n}\right\} \sin \frac{n\pi x_1}{l} \qquad (6)$$

The two series (5) and (6) differ in the coefficient of S_{1n}. In (5) the bracketed expression before the principal coefficient of the central strip increases with the second power of n. The corresponding bracketed expression in (6) tends to the finite value $1 - \nu^2$ for large numbers n.

The bracketed expression before S_{0n} in both cases tends to the value $1 - \frac{1}{2}\nu$ with increasing n. Thus (6), derived from the second expression for w_1 in (2), gives more rapidly converging series than (5), which is based on the first expression in (2).

This is true for the central deflection w_1. Similar investigations for the outside deflections w_0 and w_2 give analogous results. The expressions where the principal deflection is removed from the series and represented exactly, as a special term contain series of more rapid convergence than the simpler

series expressions do. The results obtained for a plate divided into three strips are valid for an arbitrary division of the plate. They can also be applied to oblique plates. In the equations $L_r(w_{0n}, \ldots w_{rn}, \ldots) = q_{rn}/D$ the coefficient of w_{rn} is independent of the angle of obliquity Θ.

Thus the convergence of the series for the deflections w_r can generally be improved by substituting for the series

$$w_r = \Sigma w_{rn} \sin (n \pi x_r / l) \tag{7}$$

the sum

$$w_r = W_r + \Sigma (w_{rn} - W_{rn}) \sin (n \pi x_r / l) \tag{8}$$

for inside strips and

$$w_0 = \frac{W_0}{1 - \nu^2} + \sum \left(w_{0n} - \frac{W_{0n}}{1 - \nu^2} \right) \sin \frac{n \pi x_0}{l} \tag{9}$$

for outside strips.

224. Estimation of errors

If only a finite number of terms are included in the series for the principal deflections, inaccurate strip deflections will result. To find a general upper limit for practical cases, a loading is chosen for which the coefficients W_{rn} converge slowly. Appendix 55 reveals that concentrated loads should be considered. The slowest convergence is obtained for forces applied near the supports.

Consider a plate in which strip r carries a concentrated load. The other strips are not loaded. According to Appendix 55,

$$W_r = \sum W_{rn} \sin \frac{n \pi x_r}{l} \leqq | n^4 W_{rn} |_{max} \sum \left| \frac{1}{n^4} \sin \frac{n \pi x_r}{l} \right| \tag{1}$$

According to (223), the series for w_r converges more slowly than the series for the deflections of the other strips (223.7). So the attention may be concentrated on w_r. The deflection of strip r is usually less than the principal deflection W_r. The

adjacent strips are forced to participate in the deformation, and thereby take over some part of the load. The deflection w_0 of outside strips might exceed the principal deflection by a small amount. This possibility is disregarded, however. The neglect of terms containing values of n larger than N results in an error

$$|\Delta w_r| \leqq |n^4 W_{rn}|_{max} \sum_{N+1}^{\infty} \frac{1}{n^4} \tag{2}$$

The sum is approximated by an integral:

$$\sum_{N+1}^{\infty} \frac{1}{n^4} < \int_{N+\frac{1}{2}}^{\infty} \frac{dn}{n^4} = \frac{1}{3\left(N+\frac{1}{2}\right)^3}$$

yielding

$$|\Delta w_r| \leqq \frac{1}{3\left(N+\frac{1}{2}\right)^3} |n^4 W_{rn}|_{max} \tag{3}$$

When the first three terms are included in the series for the deflections, the error estimated by (3) will usually be admissible in practical work. However, for exceptionally narrow strips the errors can often not be reduced to admissible values if not many terms are included. In such cases the series should be transformed as in (223.8):

$$w_r = W_r + \Sigma (w_{rn} - W_{rn}) \sin (n \pi x_r / l) =$$

$$= W_r + \Sigma z_{rn} \sin (n \pi x_r / l) \tag{4}$$

The other deflections are expressed by (223.7):

$$w_s = \Sigma w_{sn} \sin (n \pi x_s / l) \tag{5}$$

These expressions are substituted in the differential equations of 212 corresponding to the appropriate division of the plate. If the simple form (223.7) had been used for the de-

flection w_r, the coefficients w_{rn} in (4) would have taken the place of z_{rn}. In (4) W_r can be expanded into a trigonometric series. The unknowns w_{0n}, ... $w_{r-1,n}$, z_{rn}, $w_{r+1,n}$, ... w_{Rn} are obtained by solving the systems of equations given in 222 and Appendix 52. Known quantities originating from W_r in (4) must be added to the principal coefficients W_{sn}. The resulting principal coefficients W'_{sn} decrease more rapidly with n than do W_{sn}. To begin with, only the differential equations for strip r contained known quantities. In the transformed system the coefficients W'_{sn} appear in the equations for $w_{r-2,n}$, $w_{r-1,n}$, z_{rn}, $w_{r+1,n}$, $w_{r+2,n}$. For any number of strips the magnitude of the coefficients W'_{sn} does not exceed

$$|W'_{sn}|_{max} = |(\alpha_{4n} - 1)\, W_{rn}|_{max} \tag{6}$$

This is apparent from 222 and Appendix 52 where

$$\alpha_{4n} = 1 + 4\,(l / n\,\pi\,t)^2 + 6\,(l / n\,\pi\,t)^4 \tag{7}$$

The coefficients W'_{sn} for consecutive strips will be alternately positive and negative. Results "on the safe side" are obtained by considering the effect of $|W'_{sn}|_{max}$ only. The error $|\Delta w_s|$ arising from the omission of terms of higher order than $n = N$ is less than

$$|\Delta w_s| \leqq |n^4 W_{rn}|_{max} \sum_{N+1}^{\infty} \left| \frac{\alpha_{4n} - 1}{n^4} \sin \frac{n\,\pi\,x_s}{l} \right|_{max} \leqq$$

$$\leqq (N+1)^2\,(\alpha_{4,\,N+1} - 1) \sum_{N+1}^{\infty} \frac{1}{n^6} |n^4 W_{rn}|_{max} \tag{8}$$

Replacing the sum by an integral

$$\int_{N+1/2}^{\infty} \frac{d\,n}{n^6} = \frac{1}{5\left(N + \frac{1}{2}\right)^5}$$

yields

$$|\Delta w_s| < \frac{(N+1)^2 (a_{4,\,N+1} - 1)}{5\left(N+\frac{1}{2}\right)^5} |n^4 W_{rn}|_{max} \tag{9}$$

If only the first three terms are included ($N=3$) the error becomes

$$|\Delta w_s| < .0061\,(a_{44} - 1)\,|n^4 W_{rn}|_{max} \tag{10}$$

In 222 $l/t = 4$ was considered as a maximum value for practical computations yielding

$$|\Delta w_s| \leqq .0029\,|n^4 W_{rn}|_{max} \tag{11}$$

If the maximum deflection is about a quarter of the principal coefficient W_{r1}, (cf. diagrams in 56), and a concentrated force acts at the mid-point of a strip (11) gives a maximum error of only 1.1 % in the maximum deflection.

The relative errors in the series expressions for the second derivatives are often considerably larger. This necessitates the use of (223.8) and (223.9) for computing the moments. The error caused by neglecting terms in the Fourier series for the principal deflections can be estimated by differentiating the series (8). The maximum error in the second derivative with respect to x_s is:

$$\left|\Delta \frac{d^2 w_s}{d x_s^2}\right| \leqq \frac{\pi^2}{l^2} (N+1)^2 (a_{4,\,N+1} - 1)\,|n^4 W_{rn}|_{max} \sum_{N+1}^{\infty} \left|\frac{1}{n^4} \sin \frac{n\pi x_s}{l}\right|_{max} <$$

$$< \frac{\pi^2}{3\,l^2} \cdot \frac{(N+1)^2 (a_{4,\,N+1} - 1)}{\left(N+\frac{1}{2}\right)^3} |n^4 W_{rn}|_{max} \tag{12}$$

For a concentrated load acting at the mid-point of a strip, the bounds of $\frac{d^2 w_s}{d x_s^2}$ can be further contracted. In the sum in (12) every other term vanishes. For odd values of N the inequality

$$\sum_{N+1}^{\infty} \frac{1}{n^4} \sin \frac{n\pi}{2} = \sum_{N+2}^{\infty} \frac{1}{n^4} \sin \frac{n\pi}{2} < \frac{1}{2} \int_{N+1}^{\infty} \frac{dn}{n^4} = \frac{1}{6(N+1)^3} \qquad (13)$$

is valid which reduces the estimated maximum of $\Delta \frac{d^2 w_s}{d x_s^2}$ to

$$\left| \Delta \frac{d^2 w_s}{d x_s^2} \right| < \frac{\pi^2 (a_{4,\,N+1} - 1)}{6 l^2 (N+1)^3} |W_{r1}|$$

If a load is uniformly distributed over a finite area the principal coefficients have an upper bound:

$$W_{rn} \leqq |n^5 W_{rn}|_{max} \qquad (14)$$

Hence

$$\left| \Delta \frac{d^2 w_s}{d x_s^2} \right| \leqq \frac{\pi^2}{l^2} (N+1)^2 (a_{4,\,N+1} - 1) \, |n^5 W_{rn}|_{max} \sum_{N+1}^{\infty} \left| \frac{1}{n^5} \sin \frac{n\pi x_s}{l} \right| <$$

$$< \frac{\pi^2 (N+1)^2}{4 l^2 \left(N + \frac{1}{2}\right)^4} (a_{4,\,N+1} - 1) \, |n^5 W_{rn}|_{max}$$

By differentiating (12) with respect to x_s the maximum error in the third derivatives of the deflections can be estimated. This estimate is useful in studying the accuracy of the shearing forces computed from (213.14).

225. Application to rectangular plates

The Fourier coefficients for the deflections of rectangular plates assume a particularly simple form. The origins of the abscissae, Fig. 212.4, in this case all are situated on a straight line perpendicular to the free boundaries. Thus $\cos n\mu = 1$ and $\sin n\mu = 0$. Substitution from (223.7) in the differential equations for the deflections yields only sine series. Hence the coefficients w_{rn} are given exactly by the expressions in 222. If strip deflections with vanishing curvatures at the supports are inserted in (213.2), it is found that the moments at the

supports of the plate vanish—that is, that the plate is simply supported.

The results obtained in 222 will be applied to a rectangular plate with $l/b=2$, Fig. 225.1. The plate is divided into only two strips of width $t/2=l/4$. The value $l/t=2$ is the lower limit for width-ratios in practical computations, as explained in 222. Poisson's ratio $\nu=0$.

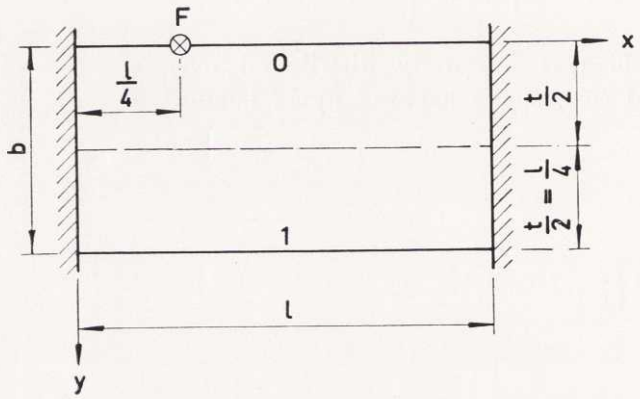

Fig. 225.1. Rectangular plate, concentrated load F at $x=l/4$.

To determine the Fourier coefficients for the deflections of strips 0 and 1, β_n is computed from (222.8):

$$\beta_n = 4 \cdot 2^2 / n^2 \pi^2 = 1.621 / n^2$$

Substituting β_n in (222.11) yields

$$\left.\begin{aligned} w_{01} &= \frac{1+1.621}{1+2\,(1.621)}\,W_{01} + \frac{1.621}{1+2\,(1.621)}\,W_{11} = .618\,W_{01} + .382\,W_{11} \\ w_{11} &= .382\,W_{01} + .618\,W_{11} \\ w_{02} &= \frac{1+1.621/4}{1+1.621/2}\,W_{02} + \frac{1.621/4}{1+1.621/2}\,W_{12} = \\ &= .776\,W_{02} + .224\,W_{12} \\ w_{12} &= .224\,W_{02} + .776\,W_{12} \end{aligned}\right\} \qquad (1)$$

This result could also be obtained by (222.14), (222.15) and (222.12). The latter method is advantageous when $\nu = 0$. Then $s_n = S_n$, and $a_n = C_n A_n$ where C_n can be taken from. Fig. 561.1 in Appendix 561.

Only coefficients of the first and second order have been determined. The error originating from neglecting coefficients of higher order can be estimated by means of (224.3). A plate loaded at $x = l/4$ has $|n^4 W_{rn}|_{max} = W_{r1} \cdot \sqrt{2}$. The maximum error of the deflection is

$$|\Delta w_r| < \frac{\sqrt{2}}{3\ (2.5)^3} W_{r1} = .030\ W_{r1}$$

When only strip 0 is loaded the maximum deflection becomes

$$w_{0\,max} \approx .618\ W_{01}$$

The relative error is

$$|\Delta w_r| / w_{0\,max} < .030 / 0.618 = .049$$

A concentrated load acting at the mid-point of strip 0 yields, by (224.2),

$$|\Delta w_r| / w_{0\,max} < .030 / 0.618 \sqrt{2} = .034$$

Deflections for arbitrary types of loading can be constructed from (1).

Assuming that strip 0 is subjected to a uniformly distributed load of intensity q, and that strip 1 is unloaded, the principal coefficients W_{0n} may be obtained from (55.2) in Appendix 55:

$$W_{01} = 4\, q\, l^4 / \pi^5 D;\ W_{02} = 0$$

The Fourier coefficients for the deflections are

$$w_{01} = .618 \cdot 4\, q\, l^4 / \pi^5 D = .00808\, q\, l^4 / D$$

$$w_{11} = .382 \cdot 4\, q\, l^4 / \pi^5 D = .00499\, q\, l^4 / D$$

$$w_{02} = w_{12} = 0$$

The corresponding trigonometric expressions,

$$\left.\begin{aligned} w_0 &= .00808 \sin \frac{\pi x}{l} \frac{q\,l^4}{D} \\ w_1 &= .00499 \sin \frac{\pi x}{l} \frac{q\,l^4}{D} \end{aligned}\right\} \qquad (2)$$

describe the deflections of each strip with sufficient accuracy. Using (224.14) in estimating $|\Delta w_r|$, the following inequalities are obtained for odd N:

$$|\Delta w_r| \leqq |n^5 W_{rn}|_{max} \sum_{N+2}^{\infty} 1/n^5 < \frac{1}{2} W_{r1} \int_{N+1}^{\infty} dn/n^5 =$$

$$= W_{r1}/8(N+1)^4, \quad |\Delta w_r|/w_{0\,max} < 1/8\,(0.618)\,2^4 = .013$$

Therefore the first Eq. (2) ought to give almost the same result as the more complicated expression (223.9). Substituting W_0 and W_{01} of (55.1) and (55.2) in (223.9), w_0 is obtained in the form

$$w_0 = \frac{1}{24}\left[\frac{x}{l} - 2\left(\frac{x}{l}\right)^3 + \left(\frac{x}{l}\right)^4\right]\frac{q\,l^4}{D} + \left(.00808 - \frac{4}{\pi^5}\right)\sin\frac{\pi x}{l}\frac{q\,l^4}{D} =$$

$$= \left[\frac{x}{l} - 2\left(\frac{x}{l}\right)^3 + \left(\frac{x}{l}\right)^4 - .120 \sin\frac{\pi x}{l}\right]\frac{q\,l^4}{24\,D} \qquad (3)$$

The maximum deflection occurs at $x = \frac{1}{2}l$:

$$w_{0\,max} = .00803\; q\,l^4/D$$

which differs from the maximum deflection according to the first Eq. (2) by .6 %.

The moments are found from (213.7) and (213.9). Denoting by M_{x0} the bending moment in strip 0, and using the simpler expression for w_0, (213.9) yields for $\nu = 0$:

$$M_{x0} = -D\frac{d^2 w_0}{dx^2} = .0797 \sin\frac{\pi x}{l} q\,l^2 \qquad (4)$$

The second derivative of w_0 also can be computed from (3), yielding the bending moment

$$M_{x0} = \left[\frac{1}{2}\,\frac{x}{l} - \frac{1}{2}\left(\frac{x}{l}\right)^2 - .0493 \sin \frac{\pi x}{l}\right] q\, l^2 \tag{5}$$

The maximum values obtained from (4) and (5) differ by 5.3 %. Thus the simpler expression (222.1) for w_0 can also be useful in determining the moments.

A load F applied on strip 0 at $x = l/4$, Fig. 225.1, yields according to (55.4) the following principal coefficients

$$\left.\begin{aligned} W_{01} &= 2\,\frac{2\,F\,l^3}{\pi^4\,t\,D} \sin \frac{\pi}{4} = .0581\,\frac{F\,l^2}{D} \\ W_{02} &= \frac{F\,l^3}{4\,\pi^4\,t\,D} \sin \frac{\pi}{2} = .00513\,\frac{F\,l^2}{D} \\ W_{11} &= W_{12} = 0 \end{aligned}\right\}$$

The width-ratio l/t here is replaced by $2l/t$ because an outside strip is loaded.

Substituting this in (1) yields the following series coefficients in the expressions for w_0 and w_1:

$$\left.\begin{aligned} w_0 &= [\,.359 \sin (\pi\,x/l) + .0398 \sin (2\,\pi\,x/l)]\,F\,l^2/10\,D \\ w_1 &= [\,.222 \sin (\pi\,x/l) + .0115 \sin (2\,\pi\,x/l)]\,F\,l^2/10\,D \end{aligned}\right\} \tag{6}$$

The first of these functions is unsuited for determining the moments in the loaded strip. By substituting in (223.9) the finite expression for W given in (55.3) and differentiating twice, the curvature is obtained:

$$\frac{d^2\,w_0}{d\,x^2} = \frac{d^2\,W_0}{d\,x^2} - \frac{\pi^2}{l^2} \sum n^2\,(w_{0n} - W_{0n}) \sin \frac{n\,\pi\,x}{l} =$$

$$= -\left(3\,\frac{x}{l} - 4\,\frac{x'}{l} - .219 \sin \frac{\pi x}{l} - .045 \sin \frac{2\,\pi\,x}{l}\right)\frac{F}{D} \tag{7}$$

Here $x' = 0$ for $0 \leqq x \leqq l/4$ and $x' = x - l/4$ for $l/4 \leqq x \leqq l$. Multiplication of (7) by $-D$ yields the bending moment M_{x0}. Its distribution along the x axis and a curve for the bending moment M_{x1} of strip 1 are shown in Fig. 225.2. The series for the unloaded strip converges better than the one for the loaded strip. Hence the moment M_{x1} can be derived from the second Eq. (6) by differentiation and multiplication by $-D$:

$$M_{x1} = F\left(.219 \sin \frac{\pi x}{l} + .045 \sin \frac{2\pi x}{l} \right)$$

The maximum value of M_{x0} occurs at $x = l/4$:

$$M_{x0\,max} = F\left(\frac{3}{4} - \frac{.219}{\sqrt{2}} - .045 \right) = .550\, F \tag{8}$$

The maximum value of M_{x1} is

$$M_{x1\,max} = .234\, F$$

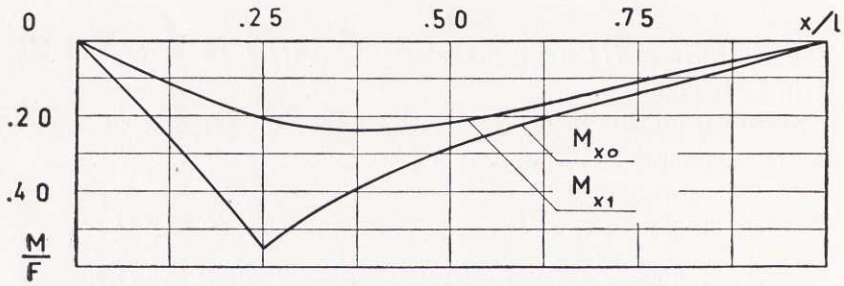

Fig. 225.2. Rectangular plate, concentrated load F at $x = l/4$. Moments M_{x0} and M_{x1} for a division into two strips.

This simple division of the plate into two strips does not yield a workable expression for the bending moments M_y, but these are small and of little practical interest.

The maximum error in the expression (7) for the curvature of strip 0 can be estimated by (224.12). With $N = 2$, (224.7) yields $a_{43} = 1.193$ and the maximum error

$$\left| \Delta \frac{\partial^2 w}{\partial x^2} \right| < \frac{3\pi^2 \sqrt{2}}{2.5^3 l^2} (a_{43} - 1) W_{r1} = .514 \frac{W_{r1}}{l^2}$$

The relative maximum error becomes

$$\left| \Delta \frac{\partial^2 w}{\partial x^2} \right| / \left| \frac{\partial^2 w}{\partial x^2} \right|_{max} < \frac{.514}{.550} 0.0581 = .054$$

The equations for w_r are solved exactly in 221. For a concentrated load F acting on strip 0, M_{x0} is obtained by subtracting (221.8) from (221.7), differentiating twice with respect to x, and multiplying by $-D$:

$$M_{x0} = \frac{F\,l}{t}\left[\frac{l_2\,x}{l^2} - \frac{x'}{l} + \frac{(\sin \mathrm{h}\, k\,x/l)\,\sin \mathrm{h}\, k\,l_2/l}{k\,\sin \mathrm{h}\, k} - \frac{\sin \mathrm{h}\; k\,x'/l}{k}\right]$$

$$l_1 = \frac{l}{4}, \quad l_2 = \frac{3\,l}{4}, \quad k = \frac{2\,l}{t}\sqrt{\frac{2}{1+\nu}} = 4\sqrt{2}$$

The maximum bending moment appears under the concentrated load at $x = l/4$,

$$M_{x0} = \frac{F\,l}{t}\left[\frac{l_1\,l_2}{l^2} + \frac{(\sin \mathrm{h}\; k\,l_1/l)\,\sin \mathrm{h}\, k\,l_2/l}{k\,\sin \mathrm{h}\; k}\right] =$$

$$= 2\,F\left(\frac{3}{16} + \frac{\sin \mathrm{h}\,\sqrt{2}\,\sin \mathrm{h}\; 3\sqrt{2}}{4\sqrt{2}\,\sin \mathrm{h}\; 4\sqrt{2}}\right) = .542\,F$$

This value differs from that given in (8) by only 1.5 %.

A more detailed description of the elastic surface requires a finer division. The deflection coefficients for a plate divided into three strips can be computed according to (222.24) and (222.25), or by using values of s_{rn} and a_{rn} from the diagrams in Appendix 562. The width of the inside strip is $b/2$, which signifies a width-ratio of $l/t = 4$. The series coefficients s_{rn} and a_{rn}, $n = 1, 2, 3$ become:

$$
\left.
\begin{aligned}
s_{01} &= .514\, S_{01} + .486\, S_{11} \\
s_{11} &= .486\, S_{01} + .514\, S_{11} \\
a_{01} &= .134\, A_{01} \\
s_{02} &= .590\, S_{02} + .410\, S_{12} \\
s_{12} &= .410\, S_{02} + .590\, S_{12} \\
a_{02} &= .382\, A_{02} \\
s_{03} &= .685\, S_{03} + .315\, S_{13} \\
s_{13} &= .315\, S_{03} + .685\, S_{13} \\
a_{03} &= .581\, A_{03}
\end{aligned}
\right\} \qquad (9)
$$

These formulas can be applied to arbitrary cases of loading. The concentrated force F applied at $x = l/4$ on strip $r = 0$ yields the following principal coefficients:

$$
\left.
\begin{aligned}
S_{01} &= \frac{8\,F\,l^2}{\pi^4\,D} \sin\frac{\pi}{4} = .0581 \quad \frac{F\,l^2}{D} = -A_{01} \\
S_{02} &= \frac{F\,l^2}{2\,\pi^4\,D} \sin\frac{\pi}{2} = .00513 \quad \frac{F\,l^2}{D} = -A_{02} \\
S_{03} &= \frac{8\,F\,l^2}{81\,\pi^4\,D} \sin\frac{3\,\pi}{4} = .000717 \quad \frac{F\,l^2}{D} = -A_{03} \\
S_{11} &= S_{12} = S_{13} = 0
\end{aligned}
\right\}
$$

Inserting these values in (9), and applying (222.22) the coefficients for the deflections w_0, w_1 and w_2 are obtained. The simple series expressions (223.7) can be employed for the deflections w_1 and w_2. However, in determining the bending moments, the deflections of strip 0 should be described by (223.9):

$$w_0 = \left[\frac{7x}{16l} - \left(\frac{x}{l}\right)^3 + \frac{4}{3}\left(\frac{x'}{l}\right)^3 - .0785 \sin\frac{\pi x}{l} - .00528 \sin\frac{2\pi x}{l} - \right.$$

$$\left. - .000526 \sin\frac{3\pi x}{l}\right]\frac{F l^2}{D}$$

$$w_1 = \left(.282 \sin\frac{\pi x}{l} + .0211 \sin\frac{2\pi x}{l} + .00226 \sin\frac{3\pi x}{l}\right)\frac{F l^2}{10 D} \qquad (10)$$

$$w_2 = \left(.221 \sin\frac{\pi x}{l} + .0107 \sin\frac{2\pi x}{l} + .00003 \sin\frac{3\pi x}{l}\right)\frac{F l^2}{10 D}$$

Here x' is zero for $0 < x \leqq l/4$, and equal to $x - l/4$ for $l/4 \leqq x < l$.

The deflections of strips 0 and 2 computed from (10) differ slightly from those obtained for strips 0 and 1 from (6). The difference between the mid-point deflections determined for the plate when divided into two and three strips is only 1.9 %.

The distribution of the moments M_{xr} along the three strips is shown in Fig. 225.3. M_{x0} is a maximum under the load and is $M_{x0\,max} = .711\ F$. The maximum value for strip 2 is $M_{x2\,max} = .232\ F$.

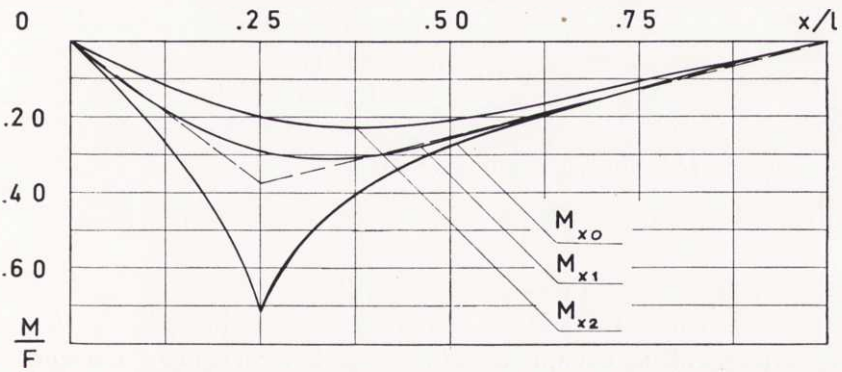

225.3. Rectangular plate, concentrated load F at $x_0 = l/4$. Moments M_{x0}, M_{x1} and M_{x2} for a division into three strips.

The dashed curve in Fig. 225.3 represents the moment caused by two forces $F/4$ upon the outside strips at $x = l/4$

and by one force $F/2$ acting on the central strip at $x = l/4$. The plate then behaves as a beam. This can be seen from (9) after inserting the coefficients

$$S_{0n} = S_{1n} = \frac{8 F l^2}{\pi^4 n^4 D} \sin \frac{n \pi}{4}$$

$$A_{0n} = 0$$

At some distance from the load this dashed line approaches the moment curves for a concentrated load on strip 0.

The moment M_y in strip 1 is determined from (213.6):

$$M_{y1} = -\frac{D}{l^2}(w_0 - 2 w_1 + w_2)$$

This expression contains differences between deflections of the same order of magnitude. Crudely approximate expressions for the deflections would yield unreliable results. Instead, w_0 ought to be estimated more accurately by means of (10). The bending moment then becomes

$$M_y = \left[-7 \frac{x}{l} + 16 \left(\frac{x}{l}\right)^3 - \frac{64}{3}\left(\frac{x'}{l}\right)^3 + 1.805 \sin \frac{\pi x}{l} + .135 \sin \frac{2 \pi x}{l} + \right.$$

$$\left. + .015 \sin \frac{3 \pi x}{l}\right] F$$

For $x = l/4$ this equation gives the moment

$$M_{y1} = -.078 F$$

which is 11 % of the maximum of M_{x0}.

The computations for a plate divided into three strips are accomplished with the three first terms in the trigonometric series. When the plate is divided into two strips, all except two series terms are neglected. Eq. (224.10) shows that the maximum error increases in direct proportion to the principal coefficient W_{rn}. This quantity increases for concentrated loads with the width-ratio l/t. The deflections change

only slightly for varying widths of the strips. Therefore, the errors will be relatively larger for narrow strips than for wider ones. The only way of reducing the relative errors is to include more terms of the series.

Results obtained for a wide plate are given in 226. Errors originating from the finite width of the strips are also discussed there.

226. The effect of the width of the strips upon the results

Deflections obtained as described in 222 and 223 involve errors due to the omission of principal coefficients of higher order. There is also another source of error in that the derivatives with respect to y were replaced by finite differences between values for positions one strip-width apart, $\Delta y = t$. Thus, in the example treated in 225 by division into 2 strips ($l/t = 2$), the following Fourier coefficients used in (225. 6) were obtained for the deflections:

$$\left.\begin{aligned} w_{01} &= .0359\frac{Fl^2}{D} & w_{02} &= .00398\frac{Fl^2}{D} \\ w_{11} &= .0222\frac{Fl^2}{D} & w_{12} &= .00115\frac{Fl^2}{D} \end{aligned}\right\} \quad (1)$$

For the same type of loading and a division into three strips ($l/t = 4$), the coefficients for the deflections of the outside strips 0 and 2 become

$$\left.\begin{aligned} w_{01} &= .0377\frac{Fl^2}{D} & w_{02} &= .00498\frac{Fl^2}{D} \\ w_{21} &= .0221\frac{Fl^2}{D} & w_{22} &= .00107\frac{Fl^2}{D} \end{aligned}\right\} \quad (2)$$

It will be seen from (1) and (2) that the differences between corresponding coefficients for $n = 2$ are relatively larger than for $n = 1$. This could be expected for the following reason.

The computation of a coefficient w_{rn} for a plate of width b is formally the same as the determination of the coefficient w_{r1} for a plate of width bn which is divided into the same number of strips as the first plate. The approximation by finite differences becomes cruder for coarser division. Hence larger errors are obtained as the order n of the Fourier coefficient increases.

The effect of the width of the strips must be specially considered when $b \geqq l$. The strips are then made wide in order to shorten the computations. Take, for instance, a plate with the proportions shown in Fig. 226.1. The coefficients w_{rn}, $n = 1$ and 2, are computed for two types of loading.

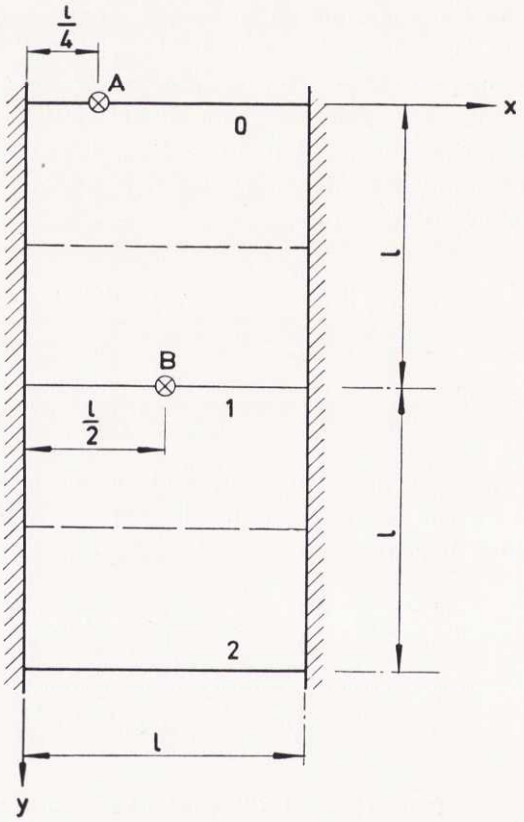

Fig. 226.1. Rectangular plate, concentrated load F at $x_0 = l/4$ and $x_1 = l/2$.

A concentrated load F is applied first at point A on a free edge, and subsequently at the mid-point B of the plate.

The calculations are performed for the first loading by dividing the plate into 3, 4, 5, and 6 strips, and for the second loading by a division into 3 and 5 strips. The results are presented in Table 226.1. The same conclusions can be drawn as for the plate treated in 225. The relative differences between corresponding coefficients computed for different modes of division increase with decreasing values of l/t and with increasing order n. Their absolute values are generally small.

If not multiplied by the multipliers in the last row, the values given in Table 226.1 are the Fourier coefficients for the moments M_x with $F = 1$. These coefficients differ but slightly for the same order number when the width-ratio $l/t \geqq 2$. This explains why in 222 $l/t = 2$ was proposed as a lower bound for practical computations.

Table 226.1

Rectangular plate, simply supported and subjected to a concentrated load F. Fourier coefficients for the deflections w_0, w_1 and w_2 along the lines indicated in Fig. 226.1

Number of strips	$\frac{l}{t}$	Load at A						Load at B	
		Line 0		Line 1		Line 2		Line 0(2)	Line 1
		w_{01}	w_{02}	w_{11}	w_{12}	w_{21}	w_{22}	w_{01}	w_{11}
3	1	.212	.092	.036	.004	.006	.000	.048	.155
4	1.5	.251	.126	—	—	.006	.000	—	—
5	2	.269	.149	.034	.003	.007	.000	.048	.180
6	2.5	.277	.166	—	—	.009	.000	—	—
Multiplier		$Fl^2/\pi^2 D$	$Fl^2/4\pi^2 D$	$Fl^2/\pi^2 D$	$Fl^2/4\pi^2 D$	$Fl^2/\pi^2 D$	$Fl^2/4\pi^2 D$	$Fl^2/\pi^2 D$	$Fl^2/\pi^2 D$

From the results given in (1) and (2) it is possible to trace another tendency which limits the validity of the conclusions stated above. The coefficients w_{rn} for the unloaded strips are practically independent of the mode of division. For the strip with the concentrated load the dependence on the width-ratio is more obvious. In fact, the differences between the w_{rn}

obtained for different widths of a loaded strip, r, can be considerable for higher values of n, also when $l/t>2$. Errors in the expressions for the partial derivatives of w with respect to y are of secondary importance. The large deviations are chiefly due to the change of the distribution of load by altering the width-ratio (see 223).

An accurate determination of the errors originating from the introduction of finite differences is often not possible, but the errors can be reduced by suitable corrections. To improve the results obtained by network methods some authors have proposed various methods applicable to plates subjected to concentrated loads (HERRMANN, MARCUS, JENSEN), but here a method of correction will be given for improving the results of strip methods.

It may be asked what quantities are so small that they may be neglected. The deflections w_s of the unloaded strips were only slightly affected by variations of l/t. Hence, according to Maxwell's reciprocal theorem (TIMOSHENKO 51, 2 p. 239), the supporting action of the more remote parts of the plate upon the deflection w_r of the loaded strip is in the main independent of the mode of division.

The angle Θ and the width of the plate affect the differential equation for w_r only through changes in the deflections w_s of adjacent strips. The influence of the angle Θ and the ratio l/b will therefore be supposed to be unaffected by the choice of width-ratio l/t. Results obtained for an infinitely wide, rectangular plate can be applied to plates with finite dimensions and moderate obliquity.

Assume, therefore, that an infinitely wide plate is subjected to a load,

$$q_r t = q t \sin \frac{n \pi x}{l}$$

acting on a central strip of width t.

Deflections at equal distances on either side of the loaded strip, r, are equal: $w_{r-s} = w_{r+s}$. Eq. (212.6) yields an infinite system of differential equations:

$$\left.\begin{aligned}
&\left(t^4\frac{d^4}{dx^4}-4t^2\frac{d^2}{dx^2}+6\right)w_r+\left(4t^2\frac{d^2}{dx^2}-8\right)w_{r+1}+2w_{r+2} &&= \frac{q_r t^4}{D}\\
&\left(2t^2\frac{d^2}{dx^2}-4\right)(w_r+w_{r+2})+\left(t^4\frac{d^4}{dx^4}-4t^2\frac{d^2}{dx^2}+7\right)w_{r+1}+w_{r+3} &&= 0\\
&w_r+w_{r+4}+\left(2t^2\frac{d^2}{dx^2}-4\right)(w_{r+1}+w_{r+3})+ &&\\
&+\left(t^4\frac{d^4}{dx^4}-4t^2\frac{d^2}{dx^2}+6\right)w_{r+2} &&= 0\\
&\cdot &&\cdot\\
&\cdot &&\cdot\\
&\cdot &&\cdot
\end{aligned}\right\} \quad (3)$$

This system is satisfied by a set of trigonometric functions

$$w_r = w_{rn}\sin\frac{n\pi x}{l},\quad w_{r+1} = w_{r+1,n}\sin\frac{n\pi x}{l},\quad \ldots$$

Introducing the notation

$$a_{5n} = 1+4\,(l/n\pi t)^2+7\,(l/n\pi t)^4 \qquad (4)$$

and the notations given in (222.21), (224.7) together with (52.10) in Appendix 52, the system of equations for the coefficients w_{rn}, $w_{r+1,n}$, ... assumes the form:

$$\left.\begin{aligned}
&a_{4n}w_{rn}-2\beta_{2n}w_{r+1,n}+2\gamma_n w_{r+2,n} &&= W_{rn}\\
&-\beta_{2n}w_{rn}+a_{5n}w_{r+1,n}-\beta_{2n}w_{r+2,n}+\gamma_n w_{r+3,n} &&= 0\\
&\gamma_n w_{rn}-\beta_{2n}w_{r+1,n}+a_{4n}w_{r+2,n}-\beta_{2n}w_{r+3,n}+ &&\\
&+\gamma_n w_{r+4,n} &&= 0\\
&\cdot &&\cdot\\
&\cdot &&\cdot\\
&\cdot &&\cdot
\end{aligned}\right\} \quad (5)$$

An exact solution is possible. However, for values of l/nt within the region of practical interest ($l/nt \leqq 4$), the unknowns w_{rn} are found more rapidly by successive approximation.

The coefficient w_{rn} is written in the form

$$w_{rn} = \zeta_{id} \frac{nt}{l} W_{rn} \tag{6}$$

The factor ζ_{id} tends to a finite limit for large values of l/nt corresponding to a sinusoidal line-load distributed in the x direction only. For small values of l/nt the coefficient w_{rn} approaches W_{rn}. Hence, $\zeta_{id} \cdot nt/l$ tends to unity, and ζ_{id} to zero. The relation between l/nt and ζ_{id} is shown graphically in Fig. 226. 2

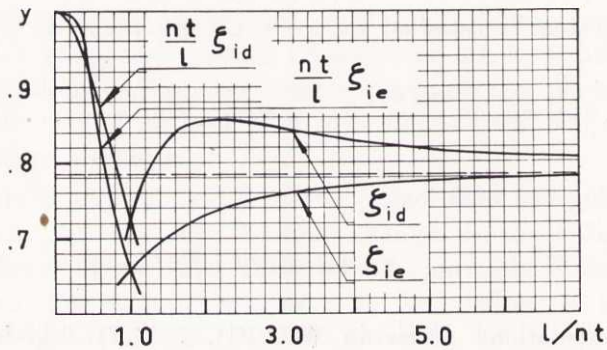

Fig. 226. 2. Factors ζ_{id}, ζ_{ie}, $\zeta_{id}\, nt/l$ and $\zeta_{ie}\, nt/l$ as functions y of l/nt. Dashed line indicates value for $l/nt = \infty$.

The solution of the system (5) can also be used for computing differences of the second order with respect to y along strip r:

$$\left(\frac{\partial^2 w}{\partial y^2}\right)_r \approx \frac{2}{t^2}(w_{r+1,n} - w_{rn}) \sin \frac{n\pi x}{l} = -\varkappa_d \frac{n^3 t}{l^3} W_{rn} \sin \frac{n\pi x}{l} \tag{7}$$

The factor $\varkappa_d$, which depends on l/nt, is represented graphically in Fig. 226. 3. It is zero for $l/nt = 0$, and increases asymptotically to a finite maximum as l/nt tends to infinity.

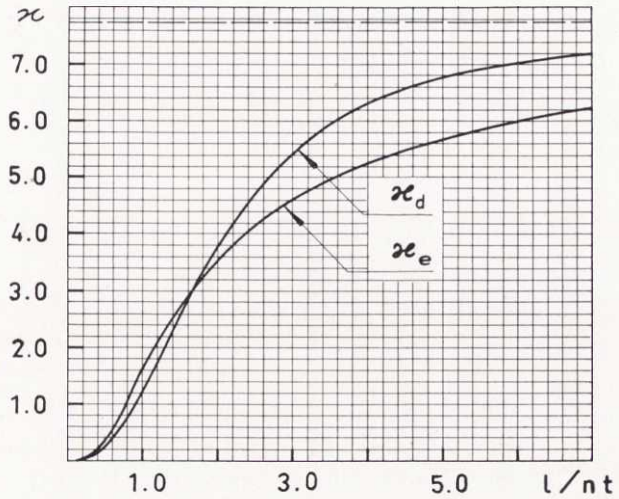

Fig. 226.3. Factors $\varkappa_d$ and $\varkappa_e$ as functions of l/nt. Dashed line indicates value for $l/nt = \infty$.

From the curves in Figs. 226.2 and 226.3 the deflections and curvatures of strip r can also be obtained for load distributions corresponding to sine functions with various wave-lengths $2l/n$.

The deflections for the case treated here will now be determined by an exact solution of (211.6). In the coordinate system shown in Fig. 226.4 the solution for positive values of y is:

$$w = (B_1 + B_2 y)\, e^{-\frac{\pi y}{l}} \sin \frac{\pi x}{l}$$

B_1 and B_2 are constants to be determined by the boundary conditions. Terms containing positive powers of e have been omitted, since the deflections vanish when y tends to infinity.

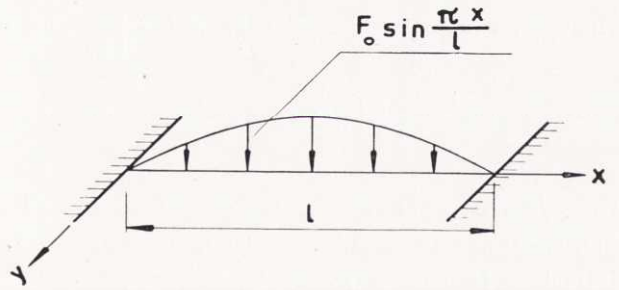

Fig. 226.4. Plate of infinite width, sinusoidal load along a line perpendicular to the supports.

The slope in the direction of the y-axis is zero along the x-axis. B_2 can be eliminated by this condition:

$$w = B_1 \left(1 + \frac{\pi y}{l}\right) e^{-\frac{\pi y}{l}} \sin \frac{\pi x}{l} \tag{8}$$

The remaining constant B_1 expresses the effect of the line load

$$F = F_0 \sin \frac{\pi x}{l}$$

acting along the x-axis, and shown in Fig. 226.4. It is obvious from symmetry that half the load is transferred to either side of the x-axis. Thus, using the last expression in (213.14), the following relation between F and the shearing force along the plane $y = +0$ is obtained:

$$\frac{1}{2} \int_0^l F_0 \sin \frac{\pi x}{l} \, dx = D \int_0^l \left(\frac{\partial^3 w}{\partial y^3} + \frac{\partial^3 w}{\partial x^2 \, \partial y} \right)_{y=+0} dx \tag{9}$$

The partial derivatives in this equation can be obtained from (8). On substituting in (9) the constant B_1 may be obtained. The deflection becomes

$$w = \frac{F_0 \, l^3}{4 \pi^3 D} \left(1 + \frac{\pi y}{l}\right) e^{-\frac{\pi y}{l}} \sin \frac{\pi x}{l} \tag{10}$$

Introducing the principal coefficient W_{r1} for a strip of width t and a load F, the maximum of $w \left(\text{at } \frac{1}{2} l, \, 0\right)$ becomes

$$w_{max} = \frac{\pi t}{4 l} W_{r1} \approx .785 \, \frac{t}{l} W_{r1}$$

The factor $\pi/4$ corresponds to ζ_{id}, defined in (6). Fig. 226.2 shows that ζ_{id} tends to about .8 with increasing $l/n\,t$.

The deflection (10) corresponds to a line load. Section 223 indicated that a loading q_r as in Fig. 226.5 might yield a de-

flection in better conformity with the strip deflection w_r. This load is distributed over a rectangular surface $l \cdot t_0$. The intensity of the load is constant in the y direction but varies in the x direction as a sine function:

$$q = q_0 \sin \frac{\pi x}{l}$$

The deflection w_r at $y = 0$ can be integrated from Δw_r, the effects of load elements acting between the planes $y = \eta$ and $y = \eta + \Delta\eta$, Fig. 226.5. The differences Δw_r are expressed by (10) after substitution of $q_0 \Delta\eta$ for F_0:

$$\Delta w_r = \frac{q_0 l^3}{4\pi^3 D}\left(1 + \frac{\pi\eta}{l}\right) e^{-\frac{\pi\eta}{l}} \sin \frac{\pi x}{l} \Delta\eta \tag{11}$$

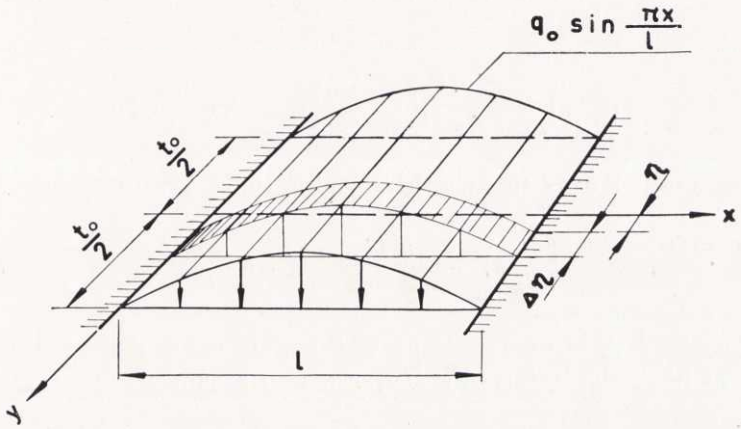

226.5. Plate of infinite width, sinusoidal load distributed over rectangular surface $l t_0$.

Integrating between the limits $\eta = 0$ and $\eta = t_0/2$, the deflection w_r assumes the form

$$w_r = 2 \int_0^{1/2 t_0} \frac{q_0 l^3}{4\pi^3 D}\left(1 + \frac{\pi\eta}{l}\right) e^{-\frac{\pi\eta}{l}} \sin \frac{\pi x}{l} d\eta =$$

$$= \frac{q_0 l^4}{\pi^4 D}\left[1 - \left(1 + \frac{\pi t_0}{4l}\right) e^{-\frac{\pi t_0}{2l}}\right] \sin \frac{\pi x}{l} \tag{12}$$

Substitution of the maximum value W_{r1} of the principal delection for the intensity q_r yields

$$w_r = W_{r1}\left[1-\left(1+\frac{\pi t_0}{4l}\right)e^{-\frac{\pi t_0}{2l}}\right]\sin\frac{\pi x}{l} = \zeta_{ie}\frac{t_0}{l}W_{r1}\sin\frac{\pi x}{l} \qquad (13)$$

The factor ζ_{ie}, computed for different values of $l/n\,t_0$, is represented graphically in Fig. 226.2. The difference between ζ_{id} and ζ_{ie} for $l/n\,t = l/n\,t_0$ expresses the error in the maximum deflection caused by using strips of finite width. When $l/n\,t$ exceeds 2, ζ_{id} and ζ_{ie} differ from $\pi/4$ by less than 9 %. Thus the width of the strips and the extension of load in the y direction has little influence upon the coefficients W_{r1} and the deflection w_r.

The second derivative of w with respect to y can be written for $y = 0$, cf. (11):

$$\Delta\left(\frac{\partial^2 w}{\partial y^2}\right)_0 = -\frac{q_0 l}{4\pi D}\left(1-\frac{\pi\eta}{l}\right)e^{-\frac{\pi\eta}{l}}\sin\frac{\pi x}{l}\Delta\eta$$

Integration over the width t_0 yields the curvature

$$\left(\frac{\partial^2 w}{\partial y^2}\right)_0 = -\frac{q_0 l\,t_0}{4\pi D}e^{-\frac{\pi t_0}{2l}}\sin\frac{\pi x}{l} \qquad (14)$$

The load q_0 is expressed as a function of a principal coefficient W_{rn}. Replacing l by l/n, Eq. (14) assumes the form

$$\left(\frac{\partial^2 w}{\partial y^2}\right)_0 = -\frac{n^3\pi^3 t_0}{4l^3}W_{rn}\,e^{-\frac{n\pi t_0}{2l}}\sin\frac{n\pi x}{l} = -\varkappa_e\frac{n^3 t_0}{l^3}W_{rn} \qquad (15)$$

For arbitrary values of $l/n\,t_0 \leqq 6$ the factor $\varkappa_e$ can be read from Fig. 226.3. When $l/n\,t_0$ tends to infinity, $\varkappa_e$ approaches the value $\pi^3/4$.

These results can be applied in correcting series coefficients for loaded inside strips, but not for outside strips. To improve coefficients for outside strips, consider a semi-infinite rectangular plate subjected to a sinusoidal load along the free edge. Numbering the loaded strip 0, applying (212.9), (212.10), and (212.6), and inserting

$$w_0 = w_{0n} \sin \frac{n\pi x}{l}, \quad w_1 = w_{1n} \sin \frac{n\pi x}{l}, \quad \ldots$$

$$q_0 = q \sin \frac{n\pi x}{l}, \quad q_1 = q_2 = \ldots = 0$$

an infinite number of linear equations is obtained:

$$\left.\begin{aligned}
&\alpha_{1n} w_{0n} - 2\beta_{1n} w_{1n} + 2\gamma_n w_{2n} && = W_{0n} \\
&-\beta_{1n} w_{0n} + \alpha_{3n} w_{1n} - \beta_{2n} w_{2n} + \gamma_n w_{3n} && = 0 \\
&\gamma_n w_{0n} - \beta_{2n} w_{1n} + \alpha_{4n} w_{2n} - \beta_{2n} w_{3n} + \gamma_n w_{4n} && = 0 \\
&\qquad\qquad . && . \\
&\qquad\qquad . && . \\
&\qquad\qquad . && .
\end{aligned}\right\}$$

The constants α_{mn}, β_{mn} and γ_n are defined in (222.18), (222.20), (222.21), (224.7), (52.9), and (52.10).

Applying the same method as mentioned for solving the system (5), the coefficient w_{0n} is obtained:

$$w_{0n} = \zeta_{0d} \frac{n\,t}{l} W_{0n} \tag{16}$$

In Fig. 226.6 the factor ζ_{0d} is represented graphically as a function of $l/n\,t$. It is dependent on Poisson's ratio ν. Curves are given for $\nu = 0$ and $\nu = 1/3$.

The deflection w_0 along the free edge can be exactly expressed by adding to the function w_r in (13) a solution w of the homogeneous, partial differential equation

$$\frac{\partial^4 w}{\partial x^4} + 2\,\frac{\partial^4 w}{\partial x^2\,\partial y^2} + \frac{\partial^4 w}{\partial y^4} = 0$$

As w must vanish for $y = \infty$ it can be represented in the form

$$\mathrm{w} = \left(C_1 + C_2 \frac{\pi y}{l}\right) e^{-\frac{\pi y}{l}} \sin \frac{\pi x}{l} \tag{17}$$

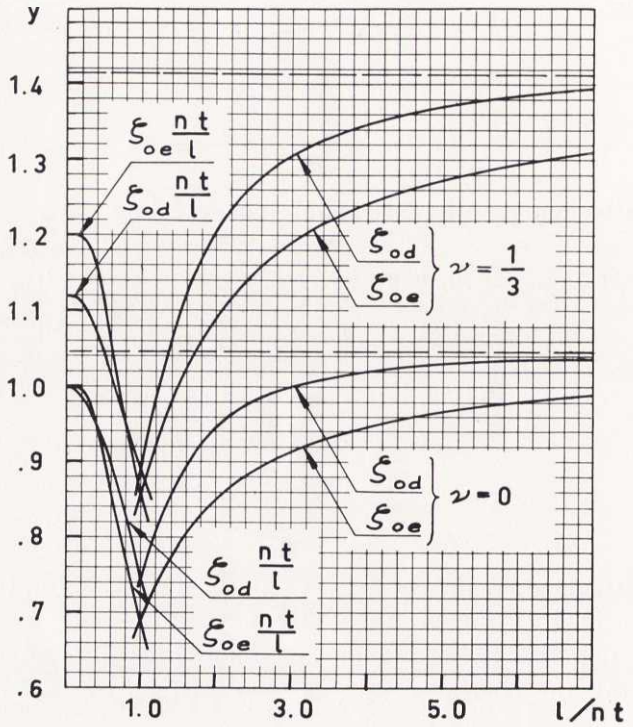

Fig. 226.6. Factors ζ_{0d}, ζ_{0e}, $\zeta_{0d}\, n\,t/l$ and $\zeta_{0e}\, n\,t/l$ as functions y of $l/n\,t$. Dashed lines indicate values for $l/n\,t = \infty$.

The boundary conditions at $y = 0$ require the partial derivatives of the second and third order. These may be determined from (13), (14) and (17).

Substituting the expressions for the derivatives in the boundary conditions (212.8), the constants of integration C_1 and C_2 in (17) may be computed, yielding

$$w = -\frac{1+\nu}{(1-\nu)(3+\nu)}\left[\frac{l^2}{\pi^2}\left(\frac{\partial^2 w}{\partial y^2}\right)_0 - \nu\, w_0\right]\left(1-\frac{1-\nu}{1+\nu}\,\frac{\pi y}{l}\right) e^{-\frac{\pi y}{l}}\,\sin\frac{\pi x}{l}$$

Combined with w this expression gives, for $y = 0$, the deflection

$$(w + \mathrm{w})_0 = \frac{1}{(1-\nu)\left(1+\frac{\nu}{3}\right)}\left[\zeta_{ie}\left(1-\frac{\nu}{3}\right)+\frac{\varkappa_e}{3\pi^2}(1+\nu)\right]\frac{t_0}{l}W_{01}\sin\frac{\pi x}{l} =$$

$$= \zeta_{oe}\frac{t_0}{l}W_{01}\sin\frac{\pi x}{l} \qquad (18)$$

The factor ζ_{oe} corresponding to the approximate factor ζ_{od} is a function of $l/n\,t_0$. For $\nu = 0$ and an infinitely small distribution of load in the y direction ζ_{oe} assumes the value

$$\zeta_{oe} = \zeta_{ie} + \varkappa_e/3\,\pi^2 = 1.047$$

Fig. 226.6 shows that ζ_{od} differs little from this quantity, even for small values of the fraction $l/n\,t$. Fig. 226.6 also shows the relation between the factors $l/n\,t_0$ and ζ_{oe} for $\nu = 0$ and $1/3$.

The diagrams of Figs. 226.2 and 226.6 can be used for correcting the series coefficients determined from the equations in 222.

The factors ζ_d and ζ_e corresponding to the value of $l/n\,t$ concerned are first determined. For an infinitely wide plate the correction is the difference between the values of w_{rn} obtained from (13) and from (6). Where this difference can be treated as independent of the dimensions of the plate, the correction is

$$\Delta\, w_{rn} = (\zeta_e - \zeta_d)\frac{n\,t}{l}W_{rn} \qquad (19)$$

Errors in w_{rn} arising from the use of finite differences occur mainly when the external load acts directly on strip r. Accordingly, among the factors determining the effects of the various principal coefficients W_{sm} upon a coefficient of deflection w_{rn}, only the one with $s = r$ and $m = n$ needs adjustment.

The finite differences of second order with respect to y can be corrected in a similar manner. The first approximation of $\left(\frac{\partial^2 w}{\partial y^2}\right)_r$ can be formed according to (212.2) from the uncorrected series coefficients w_{rn}:

$$\left(\frac{\partial^2 w}{\partial y^2}\right)_r \approx \frac{1}{t^2} \sum (w_{r+1,n} - 2\, w_{rn} + w_{r-1,n}) \sin \frac{n \pi x}{l}$$

Then a correction, $\Delta \left(\frac{\partial^2 w}{\partial y^2}\right)_r$, can be computed from (7) and (15) and added:

$$\Delta \left(\frac{\partial^2 w}{\partial y^2}\right)_r = - \sum (\varkappa_e - \varkappa_d) \frac{n^3 t}{l^3} W_{rn} \sin \frac{n \pi x}{l} \tag{20}$$

The diagrams in Figs. 226.2, 226.3 and 226.6 can also be used for changing the width of load in the y direction. Such an operation is often required. The width of the strips is determined by the dimensions of the plate and the degree of accuracy required. In general, the width of the strips does not coincide with the width of the loaded area.

Assume that the series coefficients of the deflections are determined for strips of width t. Actually the load is distributed over a rectangular area of width t_0. For an infinitely wide rectangular plate ($\Theta = 0$) loaded on strip r only, the coefficients w_{rn} are expressed by (6). Deflection coefficients for a loaded width t_0 can be exactly determined by means of (13). The difference between the exact and approximate coefficients is defined as the correction. On the same grounds as mentioned previously this correction is also used in treating oblique plates of finite dimensions.

Results obtained for a plate divided into strips of width t can thus be rendered valid for a load of width t_0 by adding a correction

$$\Delta w_{rn} = \zeta_e \frac{n t_0}{l} W^0_{rn} - \zeta_d \frac{n t}{l} W_{rn} = (\zeta_e - \zeta_d) \frac{n t}{l} W_{rn} \tag{21}$$

W_{rn} is the principal coefficient for strips of width t. W^0_{rn} is the principal coefficient for width t_0. Eq. (21) shows that (19) is applicable if the value of ζ_e for $l/n\,t_0$ is taken, and that of ζ_d for $l/n\,t$. These values may be read from Figs. 226.2 and 226.6.

The expressions for the second derivative of w_r with respect to y can also be modified so as to describe $\left(\frac{\partial^2 w}{\partial y^2}\right)_r$ for a load of width t_0. The quantity $\varkappa_e$ in (20) contained in the exact solution must then be calculated for the width t_0.

The diagrams in Appendix 56 are drawn for uncorrected series coefficients. There would be little point in giving the improved values, which hold only for a single width of load. Besides, the corrections appearing in the treatment of oblique plates can best be computed from the approximate coefficients.

When the loaded area is smaller than about .2 l in the x and y directions, difficulties arise in applying this correction method. Many terms must be included in the series in order to obtain usable approximations for the moments in the loaded strip. Another complication arises if the loaded area can be inscribed in a circle with a radius of the same order of magnitude as the thickness h of the plate. Then the fundamental partial differential equation (211. 6) is valid only at distances from the centre of the load that are larger than h. The large stresses in the loaded region perpendicular to the surface of the plate increase the deformations. If these are taken into account, larger compressive stresses and smaller tensile stresses are obtained than from (211. 6), (see NADAI, WOINOWSKY-KRIEGER), but in practice this can often be neglected. Swedish bridge specifications require that wheel loads be distributed over a width $t_0 = .6$ m. In such a case the ratio l/t_0 for a span of 3 m becomes five. A pavement on top of the slab will increase the width of the load upon the slab and will reduce the value 5 further.

The correction method will be applied to the plate treated in 225. A division of the plate into three strips yields the coefficients w_{rn} of (2). The width of the load is assumed to be $t_0 = t = l/4$. The factors ζ_{od} and ζ_{oe} apply, since an outside strip is loaded. The following values are obtained from Fig. 226. 6.

$$\left.\begin{aligned} l/n\,t = 4 \quad &: \zeta_{oe} = .944, \quad \zeta_{od} = 1.020 \\ l/n\,t = 2 \quad &: \zeta_{oe} = .850, \quad \zeta_{od} = .944 \\ l/n\,t = 4/3 \,&: \zeta_{oe} = .765, \quad \zeta_{od} = .835 \end{aligned}\right\} \tag{22}$$

The corrected coefficients w_{on} become, according to (19):

$$\left.\begin{aligned} w_{01} &= \left[.0377 + \frac{1}{4}(.946 - 1.020)\frac{16}{\pi^4\sqrt{2}}\right]\frac{Fl^2}{D} = .0355\ \frac{Fl^2}{D} \\ w_{02} &= \left[.00498 + \frac{1}{2}(.850 - .944)\frac{1}{\pi^4}\right]\frac{Fl^2}{D} = .00449\frac{Fl^2}{D} \\ w_{03} &= \left[.00091 + \frac{3}{4}(.765 - .835)\frac{16}{81\pi^4\sqrt{2}}\right]\frac{Fl^2}{D} = .00083\frac{Fl^2}{D} \end{aligned}\right\} \quad (23)$$

If the plate is divided into two strips, t and t_0 would not coincide. The factors ζ_{od} would in that case be computed for $l/n\,t_0 = 4/n$ and ζ_{oe} for $l/n\,t = 2/n$. Fig. 226.6 would give

$$l/n\,t = 2 \quad : \zeta_{od} = .994$$

$$l/n\,t = 1 \quad : \zeta_{od} = .738$$

$$l/n\,t = 2/3 : \zeta_{od} = .580$$

The values of ζ_{oe} would be the same as those given in (22). For $l/t = 2$, the corrected coefficients W_{rn} become, according to (19),

$$\left.\begin{aligned} w_{01} &= \left[.0359 + \frac{1}{2}(.946 - .994)\frac{8}{\pi^4\sqrt{2}}\right]\frac{Fl^2}{D} = .0345\frac{Fl^2}{D} \\ w_{02} &= \left[.00398 + (.850 - .738)\frac{1}{2\pi^4}\right]\frac{Fl^2}{D} = .00456\frac{Fl^2}{D} \\ w_{03} &= \left[.00062 + \frac{3}{2}(.765 - .580)\frac{8}{81\pi^4\sqrt{2}}\right]\frac{Fl^2}{D} = .00082\frac{Fl^2}{D} \end{aligned}\right\} \quad (24)$$

The differences between (23) and (24) are smaller than those between the original expressions (1) and (2). For $n = 1$ the difference has decreased from 4.9 % to 2.6 %. This reduction is obtained for the narrow plate in Fig. 225.1 in spite of the fact that the diagrams for ζ_{oe} and ζ_{od} were computed for plates of infinite width.

227. Consideration of cosine series before neglected

The sine series for the deflections of different strips are not in phase whenever $\Theta \neq 0$. Cosine functions then appear in the equations for the coefficients w_{rn}. In 222 these functions were neglected. When Θ is not small, the neglect of the cosine functions yields only rough values.

The significance of the cosine terms will now be evaluated. In (222.5) for strip 0 of a plate divided into two strips, q_0 increases by Δq_0^*,

$$\Delta q_0^* = \frac{D}{t^4}\frac{d^4}{d x_0^4}(\Delta W_0^*) = -\frac{4(1-\nu)}{t^4} D \sum \frac{m^2 \pi^2 t^2}{l^2} w_{1m} \sin m\mu \cos \frac{m \pi x_0}{l}$$

ΔW_0^* being the principal deflection corresponding to Δq_0^*. Multiplication by $\sin (m \pi x_0 / l)$, integration over the length of the strip, and multiplication by $l^4/n^4 \pi^4 t^4$, results in

$$\Delta W_{on}^* = \frac{2 l^3}{n^4 \pi^4 t^4} \int_0^l \frac{d^4}{d x^4}(\Delta W_0^*) \sin \frac{n \pi x_0}{l} d x_0 =$$

$$= \frac{4}{\pi} \sum_{m \neq n} \frac{m^4 \sin m\mu}{n^3 (m^2 - n^2)} \beta_m w_{1m} \sin^2 \frac{\pi}{2}(m+n)$$

as a correction of the principal coefficient W_{on}. Introducing the notation

$$c_{mn} = \frac{4}{\pi} \frac{m^4 \sin m\mu}{n^3 (m^2 - n^2)} \beta_m \sin^2 \frac{\pi}{2}(m+n) =$$

$$= \frac{16\, m^2 \sin m\mu}{\pi^3 n^3 (m^2 - n^2)} \frac{l^2 (1-\nu)}{t^2} \sin^2 \frac{\pi}{2}(m+n) \qquad (1)$$

for $m \neq n$ and $c_{mm} = 0$ for $m = n$

the correction can be expressed in the form:

$$\Delta W_{on}^* = \Sigma c_{mn} w_{1m}$$

The value of c_{mn} is given for different numbers m and n in Appendix 57.

The cosine terms in the equation for strip 1 can be treated in a similar manner as for strip 0. The correction, ΔW_{1n}^*, for W_{1n} becomes:

$$\Delta W_{1n}^* = -\Sigma c_{mn} w_{0m}$$

The corrections ΔW_{on}^* and ΔW_{1n}^* are replaced by quantities ΔS_n^* and ΔA_n^*, in the same way as W_n was replaced by S_n and A^n in 222 for the original principal coefficients:

$$\left.\begin{aligned} \Delta S_n^* &= \frac{1}{2}(\Delta W_{1n}^* + \Delta W_{on}^*) = \Sigma c_{mn} a_m \\ \Delta A_n^* &= \frac{1}{2}(\Delta W_{1n}^* - \Delta W_{on}^*) = -\Sigma c_{mn} s_m \end{aligned}\right\} \qquad (2)$$

For a plate divided into three strips, the effect of the cosine series is evaluated in Appendix 52, which leads to the following corrections

$$\left.\begin{aligned} \Delta S_{on}^* &= -\Sigma d_{mn} a_{om} \\ \Delta S_{1n}^* &= \Sigma e_{mn} a_{om} \\ \Delta A_{on}^* &= \Sigma (d_{mn} s_{om} - e_{mn} s_{1m}) \end{aligned}\right\} \qquad (3)$$

where

$$d_{mn} = \frac{8 \sin 2 m\mu}{\pi^5 n^3 (m^2 - n^2)} \frac{l^4}{t^4} \sin^2 \frac{\pi}{2}(m+n) \qquad (4)$$

for $m \neq n$ and $d_{mm} = 0$ for $m = n$

and

$$e_{mn} = \frac{16 m^2 \sin m\mu}{\pi^3 n^3 (m^2 - n^2)} \frac{l^2}{t^2}\left(1 - \frac{\nu}{2} + \frac{l^2}{m^2 \pi^2 t^2}\right) \sin^2 \frac{\pi}{2}(m+n) \qquad (5)$$

for $m \neq n$ and $e_{mm} = 0$ for $m = n$.

The factors d_{mn} and e_{mn} can be expressed as simple factors given in Appendix 57, times c_{mn}.

For a plate divided into five strips, Appendix 52 leads to the following expressions

$$\left.\begin{aligned}
\Delta S_{on}^{*} &= -\sum e_{mn}\, a_{1m} \\
\Delta S_{1n}^{*} &= \sum \frac{1}{2}(e_{mn}\, a_{om} - d_{mn}\, a_{1m}) \\
\Delta S_{2n}^{*} &= \sum (-d_{mn}\, a_{om} + f_{mn}\, a_{1m}) \\
\Delta A_{on}^{*} &= \sum (-e_{mn}\, s_{1m} + d_{mn}\, s_{2m}) \\
\Delta A_{1n}^{*} &= \sum \frac{1}{2}(e_{mn}\, s_{om} + d_{mn}\, s_{1m} - f_{mn}\, s_{2m})
\end{aligned}\right\} \qquad (6)$$

Here the factor f_{mn} appears, defined by the equation:

$$f_{mn} = \frac{16\, m^2 \sin m\mu}{\pi^3\, n^3\, (m^2 - n^2)} \frac{l^2}{t^2}\left(1 + \frac{2\, l^2}{m^2\, \pi^2\, t^2}\right) \sin^2 \frac{\pi}{2}(m+n) \qquad (7)$$

for $m \neq n$ and $f_{mm} = 0$ for $m = n$

also given in Appendix 57 as a function of c_{mn}.

Replacing S_{rn} by $S_{rn} + \Delta S_{rn}^{*}$, and A_{rn} by $A_{rn} + \Delta A_{rn}^{*}$, in (222.14) and (222.15), (222.24) and (222.25), or (52.21) and (52.22) approximations for the series coefficients s_{rn} and a_{rn} are obtained. The corrected values of s_{rn} and a_{rn} yield new corrections of the principal coefficients, and so on until the coefficients of major importance have assumed stationary values. When the number of series terms and strips is small the unknown coefficients are obtained directly from the system of equations combining s_{rn}, a_{rn} with the principal coefficients.

The expressions for the factors c_{mn}, d_{mn}, e_{mn} and f_{mn} indicate that odd coefficients appear only in corrections for even coefficients and conversely. Moreover, the coefficients s_{rn} occur only in the equations for the principal coefficients ΔA_{rn}^{*}, and vice versa. Thus the relations between s_{rn} and a_{rn} can be gathered into two mutually independent systems of equations.

An example of a computation of series coefficients where cosine corrections are taken into account is given in 233.

Errors arising from neglecting terms in the series for ΔW_{rn}^* are discussed in Appendix 531.

23. Simply supported plates

231. Boundary conditions

So far, equations for the series coefficients of the deflections have been derived for special boundary conditions. The deflections and the curvatures of the strips were assumed to be zero at the supports. For a rectangular plate this assumption means that the plate is simply supported.

The centre lines of the strips of an oblique plate are not perpendicular to the supports. If the second derivatives $\frac{d^2 w_2}{d x_r^2}$ vanish for $x_r = 0$ and $x_r = l$, the bending moments acting along the supported edges of the plate need not be zero. In Fig. 231.1 the η-axis of a rectangular coordinate system, $\xi\eta$, coincides with a supported edge. At a simple support, $\xi = 0$, the bending moment $M_\xi = 0$. Writing $\vartheta = -\Theta$ in the first equation of the system (213.11) and substituting for M_x, M_y and M_{xy} the expressions in Eqs. (213.2), (213.3), and (213.4), M_ξ is obtained:

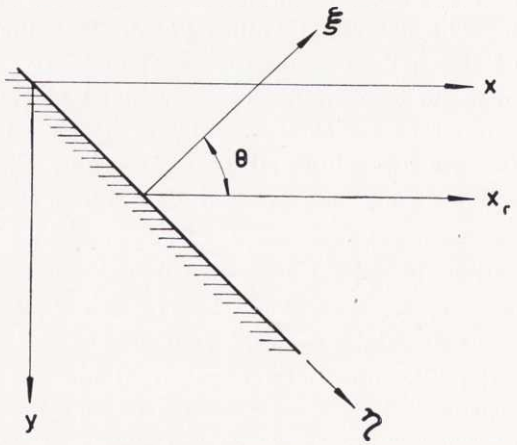

Fig. 231.1. Coordinates for expressing boundary conditions.

$$M_\xi = -D\left[(\nu \sin^2\Theta + \cos^2\Theta)\frac{\partial^2 w}{\partial x^2} - 2(1-\nu)\frac{\partial^2 w}{\partial x\,\partial y}\sin\Theta\cos\Theta + \right.$$

$$\left. + (\sin^2\Theta + \nu\cos^2\Theta)\frac{\partial^2 w}{\partial y^2}\right] \qquad (1)$$

The partial derivatives can be expressed by the deflections w_r. For strip r

$$\left(\frac{\partial^2 w}{\partial x\,\partial y}\right)_r \approx \frac{1}{2t}\frac{d}{dx}(w_{r+1} - w_{r-1}) =$$

$$= \frac{\pi}{2tl}\sum m\left[w_{r+1,m}\cos\frac{m\pi x_{r+1}}{l} - w_{r-1,m}\cos\frac{m\pi x_{r-1}}{l}\right] \qquad (2)$$

and

$$\left(\frac{\partial^2 w}{\partial y^2}\right)_r \approx \frac{1}{t^2}\sum\left[w_{r+1,m}\sin\frac{m\pi x_{r+1}}{l} - 2\,w_{rm}\sin\frac{m\pi x_r}{l} + \right.$$

$$\left. + w_{r-1,m}\sin\frac{m\pi x_{r-1}}{l}\right] \qquad (3)$$

The curvature of the strip for $x_r = 0$ is denoted by ΔK_{r0}:

$$\left(\frac{d^2 w_r}{d x_r^2}\right)_0 = \left(\frac{\partial^2 w}{\partial x^2}\right)_r = \Delta K_{r0}$$

Eqs. (2) and (3) yield, with $x_r = 0$:

$$\left(\frac{\partial^2 w}{\partial x^2}\right)_r = \Delta K_{r0}, \qquad \left(\frac{\partial^2 w}{\partial x\,\partial y}\right)_r \approx \frac{\pi}{2tl}\sum m\,(w_{r+1,m} - w_{r-1,m})\cos m\mu$$

$$\left(\frac{\partial^2 w}{\partial y^2}\right)_r \approx -\frac{1}{t^2}\sum (w_{r+1,m} - w_{r-1,m})\sin m\mu$$

The boundary condition $M_\xi = 0$ for $x_r = 0$ can now be written, (1),

$$\Delta K_{r0} =$$

$$= \frac{\pi(1-\nu)\operatorname{tg}\Theta}{(1+\nu\operatorname{tg}^2\Theta)tl}\sum m\left(\cos m\mu + \frac{\sin m\mu}{m\mu}\,\frac{\nu+\operatorname{tg}^2\Theta}{1-\nu}\right)(w_{r+1,m} - w_{r-1,m}) \qquad (4)$$

The boundary condition at $x_r = l$ can also be expressed by an equation containing the series coefficients w_{rn}. Denoting by ΔK_{rl} the curvature of the strip at $x_r = l$, and substituting for the other second derivatives in (1) according to (2) and (3), the following expression is formed:

$$\Delta K_{rl} = \frac{\pi (1-\nu) \operatorname{tg} \Theta}{(1+\nu \operatorname{tg}^2 \Theta)\, t\, l} \sum m \left(\cos m\mu + \frac{\sin m\mu}{m\mu} \frac{\nu + \operatorname{tg}^2 \Theta}{1-\nu} \right) (w_{r+1,m} -$$

$$- w_{r-1,m}) \cos m\pi \tag{5}$$

The boundary curvatures of an outside strip, 0, depend upon the conditions at the free edges. Therefore eqs. (4) and (5) cannot be applied without modifications. Eq. (213. 8) is valid along the free edges and yields a relation between two of the second derivatives

$$\frac{\partial^2 w}{\partial y^2} = -\nu \frac{\partial^2 w}{\partial x^2}$$

Substituting this relation for $\frac{\partial^2 w}{\partial y^2}$ in (1), the boundary condition becomes

$$\frac{\partial^2 w}{\partial x^2} - \frac{2 \operatorname{tg} \Theta}{1+\nu} \frac{\partial^2 w}{\partial x\, \partial y} = 0 \tag{6}$$

The second derivative $\frac{\partial^2 w}{\partial x\, \partial y}$ should be determined by differentiating $\left(\frac{\partial w}{\partial y}\right)_0$, (213. 10). The result will contain a third derivative of w_0 with respect to x_0. This function will retard the convergence of the deflection series. The slope of the elastic surface in the y direction at a distance $\frac{1}{2} t$ from the free edge is:

$$\left(\frac{\partial w}{\partial y}\right)_0 \approx \frac{1}{t} (w_1 - w_0) \tag{7}$$

Neglecting the small variation of the slope within the region $0 < y < \frac{1}{2} t$, Fig. 212. 4, the second derivative becomes

$$\left(\frac{\partial^2 w}{\partial x \, \partial y}\right)_0 \approx \frac{\pi}{t\,l} \sum m \left(w_{1m} \cos \frac{m \pi x_1}{l} - w_{0m} \cos \frac{m \pi x_0}{l} \right)$$

Substitution in (6) yields for the curvatures ΔK_{00} and ΔK_{0l} at the supports $x_0 = 0$ and $x_0 = l$:

$$\Delta K_{00} = \frac{2 \pi \operatorname{tg} \Theta}{(1+\nu)\, t\, l} \sum m \, (w_{1m} \cos m \mu - w_{0m}) \tag{8}$$

$$\Delta K_{0l} = \frac{2 \pi \operatorname{tg} \Theta}{(1+\nu)\, t\, l} \sum m \, (w_{1m} \cos m \mu - w_{0m}) \cos m \pi \tag{9}$$

Eqs. (4) and (5), (8) and (9) show that the curvatures ΔK_r are generally not zero for simply supported oblique plates. The second derivative with respect to x disappears only for special conditions of loading or at special points of support.

232. Construction of deflections satisfying the boundary conditions

Functions satisfying the boundary conditions

$$x = 0, \; l; \; w = \frac{\partial^2 w}{\partial x^2} = 0 \tag{1}$$

do not generally satisfy (231. 1) but describe the deflection of a plate loaded by bending moments along the supports, and must be combined with other functions which do not satisfy (1).

It is possible to construct solutions w_r yielding a definite curvature K_{r0} at one support $x_r = 0$ of a strip r while $K_{s0} = K_{sl} = 0$ for all other points of support $x_s = 0, \; l$. According to (55. 7) in Appendix 55, the principal deflection is

$$W_r = -\frac{K_{r0}\, l^2}{3}\left[\frac{x_r}{l} - \frac{3}{2}\left(\frac{x_r}{l}\right)^2 + \frac{1}{2}\left(\frac{x_r}{l}\right)^3\right] \tag{2}$$

The second derivative of this expression is K_{r0} at $x_r = 0$, and zero at $x_r = l$, as required. However, W_r does not satisfy the differential equations for the deflections. It has to be replaced by a suitable trigonometric series:

$$w_r = \sum w_{rn} \sin \frac{n\pi x_r}{l} = -\frac{K_{r0}\, l^2}{3}\left[\frac{x_r}{l} - \frac{3}{2}\left(\frac{x_r}{l}\right)^2 + \frac{1}{2}\left(\frac{x_r}{l}\right)^3\right] +$$

$$+ \sum (w_{rn} - W_{rn}) \sin \frac{n\pi x_r}{l} \tag{3}$$

This w_r has the curvature K_{r0} at $x_r = 0$. The principal coefficient W_{rn} is obtained from (55. 8):

$$W_{rn} = -2\, K_{r0}\, l^2/\pi^3\, n^3 \tag{4}$$

The other strips, where the second derivatives of the deflections w_s are zero at both supports, require only the simple expression

$$w_s = \Sigma\, w_{sn} \sin (n\pi x_s/l) \tag{224. 5}$$

The first and simpler of the two expressions for w_r given in (3) can generally be applied to the differential equations for w_r and w_s, except for the fourth derivative with respect to x_r that appears in the differential equation for strip r. The two formulas (3) then yield essentially different values. The first formula gives

$$\frac{d^4 w_r}{d\, x_r^4} = \frac{\pi^4}{l^4} \sum n^4\, w_{rn} \sin \frac{n\pi x_r}{l}$$

and the second

$$\frac{d^4 w_r}{d\, x_r^4} = \frac{\pi^4}{l^4} \sum n^4 (w_{rn} - W_{rn}) \sin \frac{n\pi x_r}{l} \tag{5}$$

The second term within brackets in (5) can be moved to the right hand side of the differential equation and treated as a known quantity. The system of equations formed by substituting (3) and (224. 5) in the differential equations of the strips is then treated in the same way as the system for transverse loads.

If the curvature is K_{rl} at $x_r = l$ and zero at $x_r = 0$, the principal deflection is, according to (55. 9) and (55. 10),

$$W_r = -\frac{K_{rl}\, l^2}{6}\left[\frac{x_r}{l} - \left(\frac{x_r}{l}\right)^3\right] = \frac{2\, K_{rl}\, l^2}{\pi^3}\sum \frac{\cos n\pi}{n^3} \sin \frac{n\pi\, x_r}{l} \qquad (6)$$

The corresponding Fourier coefficients of the deflections can be determined in the way described above.

Outside strips have principal deflections according to (2) or (6), and deflections

$$w_0 = \frac{W_0}{1-\nu^2} + \sum\left(w_{0n} - \frac{W_{0n}}{1-\nu^2}\right) \sin \frac{n\pi\, x_0}{l}$$

which yield $1/(1-\nu^2)$ times larger curvatures at the supports than the actual values K_{00} or K_{0l} (second derivative of w_0). In order to obtain correct values at the supports the principal Fourier coefficients must be written in the form:

$$W_{0n} = -2\, K_{00}\, l^2\,(1-\nu^2)/\pi^3\, n^3 \qquad (7)$$

This equation is valid when the curvature is K_{00} at $x_0 = 0$ and zero at $x_0 = l$. In the case when $\frac{d^2 w_0}{d\, x_0^2}$ is zero at $x_0 = 0$ and K_{0l} at $x_0 = l$, an expression for the principal coefficients of an outside strip is obtained from (6) after multiplication by $1-\nu^2$.

The general case with arbitrary boundary curvatures corresponds to principal coefficients which are linear combinations of the type (55. 8) and (55. 10). By adding deflections valid for finite boundary curvatures ΔK_{r0} and ΔK_{rl}, it is possible to describe the deflection of a plate loaded by bending moments distributed in any way along the edges. Such supplementary

deflections can be used in correcting w functions satisfying the conditions (1). From (4) and (6) the general principal coefficient for these supplements becomes

$$\Delta W_{rn}^{**} = -\frac{2\,l^2}{n^3\,\pi^3}(\Delta K_{r0} - \Delta K_{rl}\cos n\,\pi) \tag{8}$$

Substituting (231. 4) and (231. 5) for ΔK_{r0} and ΔK_{rl}, the supplementary coefficient ΔW_{rn}^{**} is obtained:

$$\Delta W_{rn}^{**} = -\frac{4\,(1-\nu)\,l^2}{\pi^3\,(1+\nu\ \mathrm{tg}^2\ \Theta)\,t^2\,n^3}\sum m\,\mu\left(\cos m\,\mu + \right.$$

$$\left. + \frac{\sin m\,\mu}{m\,\mu}\ \frac{\nu+\mathrm{tg}^2\,\Theta}{1-\nu}\right)(w_{r+1,m} - w_{r-1,m})\ \sin^2\frac{\pi}{2}(m+n) \tag{9}$$

For an outside strip the right hand side members of (8) must be multiplied by the factor $1-\nu^2$, in accordance with (7). Applying (231. 8) and (231. 9), the supplementary coefficient for strip 0 becomes

$$\Delta W_{0n}^{**} = -\frac{2\,l^2\,(1-\nu^2)}{n^3\,\pi^3}(\Delta K_{00} - \Delta K_{0l}\cos n\,\pi) =$$

$$= -\frac{8\,(1-\nu)\,l^2}{n^3\,t^2\,\pi^3}\sum m\,\mu\,(w_{1m}\cos m\,\mu - w_{0m})\sin^2\frac{\pi}{2}(m+n) \tag{10}$$

The supplementary coefficients are built up in such a way that the coefficients w_{rn} can be modified for simple supports at the same time as for the cosine terms according to 227. The coefficients w_{rn} are approximately determined by the equations in 222. The sums $\Delta W_{rn}^{*} + \Delta W_{rn}^{**}$ are determined from the approximate values of w_{0n}, $w_{1n}\ldots$, and added to the principal coefficients W_{rn}. Improved values of the deflections are determined from the new principal coefficients, and the procedure is repeated until a satisfactory result is obtained.

The series for the supplementary increments ΔW_{rn}^{**} do not converge as rapidly as the approximate series coefficients for the deflections. To avoid this disadvantage, the moments at the

supports of the strips will be replaced by another type of loading. Fig. 232. 1 a shows the principal deflection of strip r, having a second derivative K_{rj} at the support $j\,(x_r = 0)$. The rest of the strip is unloaded. The same strip is now uniformly loaded, Fig. 232. 1 b, with the intensity q_{rj} over a length l_1 immediately to the right of the support j. In order to make the two cases

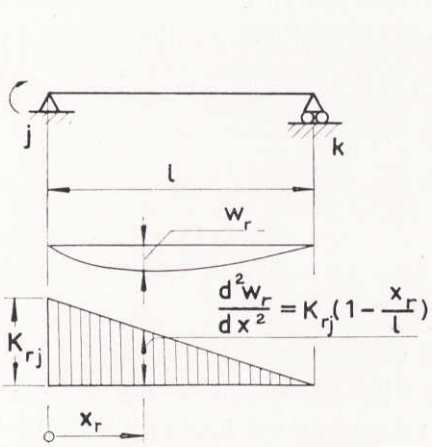

Fig. 232. 1 a. Strip deflection yielding a linear curvature.

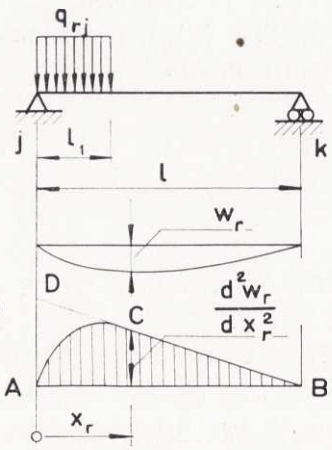

Fig. 232. 1 b. Strip deflection and curvature caused by a uniformly distributed load at the left-hand support.

of loading nearly equal, q_{rj} is chosen so large that the reaction at the support k, $x_r = l$, remains unaltered:

$$q_{rj} = -2\,D\,K_{rj}/l_1^2 \qquad (11)$$

The difference between the forces and moments formed by the two cases of loading in Fig. 232. 1 keeps the plate in equilibrium; it is distributed over a small region near $x_r = 0$. According to St. Venant's principle (see TIMOSHENKO 51, 2 p. 33), its effect (moments and shearing forces) is negligible at some distance from j. In the vicinity of this support j, the difference between the curvatures corresponding to the two cases in Fig. 232. 1 is considerable. However, this discrepancy can be

adjusted by reverting to the original state of loading with finite curvatures determined by (11). Only principal deflections need be taken into account.

MARCUS has pointed out that the curvatures derived from an exact solution of (211. 6) must be zero at the corners of an oblique plate. Moreover, the curvatures are small within a considerable region near unloaded corners with acute angles, because the plate forms stiff elements across the corner. Using coordinates as in Fig. 231. 1, the boundary conditions for the bending moments result in

$$\frac{\partial^2 w}{\partial x^2} = \frac{\partial^2 w}{\partial y^2} = \frac{\partial^2 w}{\partial \xi^2} = \frac{\partial^2 w}{\partial \eta^2} = 0$$

This means that the second derivatives of the solutions of (211. 6) all vanish at the corners. If the plate is divided into strips, the third and fourth members in this equation do not necessarily vanish. The free edge of the plate along the support is now replaced by a number of separate points. The continuation of the elastic surface outside the plate does not in general assume the value zero for $x_{-1} = 0$. When correcting for this discrepancy between the exact results and the values obtained by using finite differences, the latter values should be modified for the effect of reactions acting along the supported free edge. This correction may be calculated by means of an artifice similar to the transition from moments to distributed forces illustrated in Fig. 232.1. This is another reason why forces instead of moments should be used in making the deflection functions suitable for simply supported plates.

The curvature is also zero at an obtuse corner. However the effect of the continuous distribution of the point reactions of the strips, the "corner effect", is probably localized within a small region of the plate. This is also indicated by the experiments, Part. 3.

The load accounting for the effect of boundary curvatures corresponds to a principal deflection with Fourier coefficients determined by (211. 4) and (55. 12) in Appendix 55:

$$\Delta W_{rn}^{**} = -\frac{4\,l^2}{\pi^5\,n^5}\left(1-\cos\frac{n\,\pi\,l_1}{l}\right)\left(\frac{l}{l_1}\right)^2(\Delta K_{r0}-\Delta K_{rl}\cos n\,\pi) \quad (12)$$

This expression differs from the Fourier coefficient for a plate with finite curvatures at the supports, (8), by the factor

$$\lambda_{Nn} = \frac{2}{\pi^2\,n^2}\left(\frac{l}{l_1}\right)^2\left(1-\cos\frac{n\,\pi\,l_1}{l}\right) = \frac{2\,N^2}{\pi^2\,n^2}\left(1-\cos\frac{n\,\pi}{N}\right) \quad (13)$$

Here the length l_1 is chosen equal to half the wave-length for the sine-function of the highest order, N, included in the series.

After multiplication by the factor λ_{Nn}, the supplementary coefficients ΔW_{rn}^{**} in (10) and (9) become

$$\Delta W_{0n}^{**} = -\Sigma\, g_{mn}\,(w_{1m}\cos m\,\mu - w_{0m}) \quad (14)$$

and

$$\Delta W_{rn}^{**} = -\Sigma\, h_{mn}\,(w_{r+1,\,m} - w_{r-1,\,m}) \quad (15)$$

where

$$g_{mn} = \frac{16\,N^2\,(1-\nu)\,l^2}{\pi^5\,t^2\,n^5}\left(1-\cos\frac{n\,\pi}{N}\right) m\,\mu\,\sin^2\frac{\pi}{2}\,(m+n) \quad (16)$$

and

$$h_{mn} = \frac{g_{mn}}{2\,(1+\nu\,\mathrm{tg}^2\,\Theta)}\left(\cos m\,\mu + \frac{\sin m\,\mu}{m\,\mu}\;\frac{\nu+\mathrm{tg}^2\,\Theta}{1-\nu}\right) \quad (17)$$

The factor g_{mn} for $m, n = 1, 2, 3$ is represented in Appendix 57 as a function of μ, ν and l/t.

After determination of the coefficients w_{rn}, the curvatures ΔK_{r0} and ΔK_{rl} are obtained from (12). This equation yields, for $n = 1$ and $n = 2$,

$$\left.\begin{aligned}\Delta W_{r1}^{**} &= -\frac{2\,l^2\,\lambda_{N1}}{\pi^3}(\Delta K_{r0}+\Delta K_{rl})\\ \Delta W_{r2}^{**} &= -\frac{l^2\,\lambda_{N2}}{4\,\pi^3}(\Delta K_{r0}-\Delta K_{rl})\end{aligned}\right\}$$

The left-hand members of these equations are known. The curvatures ΔK_{r0} and ΔK_{rl} are found by solving the system:

$$\left.\begin{aligned} \Delta K_{r0} &= -\frac{\pi^3}{4\,l^2}\left(\frac{\Delta W_{r1}^{**}}{\lambda_{N1}} + 8\,\frac{\Delta W_{r2}^{**}}{\lambda_{N2}}\right) \\ \Delta K_{rl} &= -\frac{\pi^3}{4\,l^2}\left(\frac{\Delta W_{r1}^{**}}{\lambda_{N1}} - 8\,\frac{\Delta W_{r2}^{**}}{\lambda_{N1}}\right) \end{aligned}\right\} \qquad (18)$$

The factors λ_{N1} and λ_{N2} differ but slightly from 1 when $N > 3$. When applied to outside strips, (18) must be modified by dividing the right-hand members by the factor $1 - \nu^2$.

The computations may be simplified by exchanging the coefficients w_{rn} for the coefficients s_{rn} and a_{rn}. The expressions in (14) and (15) must then be replaced by sums containing s_{rn} and a_{rn}.

A plate subdivided into two strips has no inside strips. The supplementary coefficients of (14) become, for $r = 0,1$:

$$\left.\begin{aligned} \Delta W_{0n}^{**} &= -\Sigma\, g_{mn}\,(w_{1m}\cos m\,\mu - w_{0m}) \\ \Delta W_{1n}^{**} &= -\Sigma\, g_{mn}\,(w_{1m} - w_{0m}\cos m\,\mu) \end{aligned}\right\}$$

Equations (222. 13) yield the coefficients ΔS_n^{**} and ΔA_n^{**}:

$$\left.\begin{aligned} \Delta S_n^{**} &= \frac{1}{2}\,(\Delta W_{1n}^{**} + \Delta W_{0n}^{**}) = -\Sigma\, g_{mn}\,(1 + \cos m\,\mu)\,a_m \\ \Delta A_n^{**} &= \frac{1}{2}\,(\Delta W_{1n}^{**} - \Delta W_{0n}^{**}) = -\Sigma\, g_{mn}\,(1 - \cos m\,\mu)\,s_m \end{aligned}\right\} \qquad (19)$$

By adding these to the corrections (227. 2), the total increments of the original principal coefficients S_n and A_n are obtained.

The curvatures ΔK_{r0} and ΔK_{rl} are determined from (18) after dividing the right-hand members by $1 - \nu^2$. Often $N = 3$ in practical computations. Substituting this value in (13) and inserting the corresponding λ_{Nn} in (18) results in

$$\left.\begin{aligned} \Delta K_{r0} &= -\frac{\pi^5}{36\,(1-\nu^2)\,l^2}\left(\Delta W_{r1}^{**}+\frac{32}{3}\Delta W_{r2}^{**}\right) \\ \Delta K_{rl} &= -\frac{\pi^5}{36\,(1-\nu^2)\,l^2}\left(\Delta W_{r1}^{**}-\frac{32}{3}\Delta W_{r2}^{**}\right) \end{aligned}\right\} \qquad (20)$$

When a plate is divided into three strips, the supplementary coefficients for the outside strips 0 and 2 are determined by (14), and those for strip 1 by (15), introducing the coefficients, defined in (222. 12) and (222. 13),

$$\left.\begin{aligned} \Delta S_{0n}^{**} &= \frac{1}{2}\,(\Delta W_{2n}^{**}+\Delta W_{0n}^{**}) = -\Sigma\, g_{mn}\, a_{0m} \\ \Delta S_{1n}^{**} &= \Delta W_{1n}^{**} \qquad\qquad = -2\,\Sigma\, h_{mn}\, a_{0m} \\ \Delta A_{0n}^{**} &= \frac{1}{2}\,(\Delta W_{2n}^{**}-\Delta W_{0n}^{**}) = -\Sigma\, g_{mn}\,(s_{0m}-s_{1m}\cos m\,\mu) \end{aligned}\right\} \qquad (21)$$

With other subscripts, (20) can be used in determining the boundary curvatures of the outside strips, and of the inside strip, after omitting the factor $1-\nu^2$.

For a plate divided into five strips, (14) and (15) give:

$$\Delta W_{0n}^{**} = -\Sigma\, g_{mn}\,(w_{1m}\cos m\,\mu - w_{0m})$$

$$\Delta W_{1n}^{**} = -\Sigma\, h_{mn}\,(w_{2m}-w_{0m})$$

$$\Delta W_{2n}^{**} = -\Sigma\, h_{mn}\,(w_{3m}-w_{1m})$$

$$\Delta W_{3n}^{**} = -\Sigma\, h_{mn}\,(w_{4m}-w_{2m})$$

$$\Delta W_{4n}^{**} = -\Sigma\, g_{mn}\,(w_{4m}-w_{3m}\cos m\,\mu)$$

The coefficients ΔS_{rn}^{**} and ΔA_{rn}^{**} become:

$$
\left.
\begin{aligned}
\Delta S_{0n}^{**} &= \frac{1}{2}(\Delta W_{4n}^{**} + \Delta W_{0n}^{**}) = -\Sigma g_{mn}(a_{0m} - a_{1m}\cos m\mu) \\
\Delta S_{1n}^{**} &= \frac{1}{2}(\Delta W_{3n}^{**} + \Delta W_{1n}^{**}) = -\Sigma h_{mn} a_{0m} \\
\Delta S_{2n}^{**} &= \Delta W_{2n}^{**} \qquad\qquad = -2\Sigma h_{mn} a_{1m} \\
\Delta A_{0n}^{**} &= \frac{1}{2}(\Delta W_{4n}^{**} - \Delta W_{0n}^{**}) = -\Sigma g_{mn}(s_{0m} - s_{1m}\cos m\mu) \\
\Delta A_{1n}^{**} &= \frac{1}{2}(\Delta W_{3n}^{**} - \Delta W_{1n}^{**}) = -\Sigma h_{mn}(s_{0m} - s_{2m})
\end{aligned}
\right\} \qquad (22)
$$

The curvatures ΔK_{r0} and ΔK_{rl} can be computed as for a plate divided into three strips.

A survey of the total increments of S_{rn} and A_{rn} is given in Appendix 57. Some of the equations shown in this section are applied to the oblique plate treated in 233.

The deflections w_r are formed by applying (223. 7), or (223. 8) and (223. 9). When using the last two equations only the principal deflections of the real transverse loads need be excluded from the representation in trigonometric series. The effect of the fictitious loads q_{rj} indicated in Fig. 232. 1 are described with satisfactory accuracy by the simple series expressions. For the second derivatives of the strip deflections a correction yielding the real curvatures at the supports may be necessary. Then in the vicinity of the supports (but not at corners with acute angles) parabolic functions are added. In Fig. 232. 1 b such a function is illustrated by the area between the straight line DC and the curve AC. The parabolic increment for strip r at the support j has DC as tangent at C and the ordinate K_{rj} at $x_r = 0$. In general this modification of the curvatures need only be made in the vicinity of obtuse corners. A concentration of stresses occurs there. The finite curvatures at the supports may yield upper limits for normal stresses in the x_r direction.

Errors due to neglected terms in the series for ΔW_{rn}^{**} are discussed in Appendix 532. There also equations are given

for estimating the effect of using the simplified expressions (231.7) for the slope $\frac{\partial w}{\partial y}$.

233. Numerical application

The method described in 232 will be applied to a simply supported oblique plate, Fig. 233.1, with Poissons ratio $\nu = .336$. If the plate is divided into three strips the width ratio l/t becomes

$$l/t = 2 \cdot 33.68/30.38 = 2.217$$

This value falls within the range proposed for practical computations. Inserting the numerical value of the width ratio and $\operatorname{tg} \Theta = .575$ into (532.6) yields a margin of error which is only a few percent of the maximum principal coefficient. Hence three terms in the series for the deflections should suffice. The ratio l/t and

$$\mu = \frac{\pi t}{l} \operatorname{tg} \Theta = .815$$

determine the constants α_{rn}, β_{rn} and γ_n.

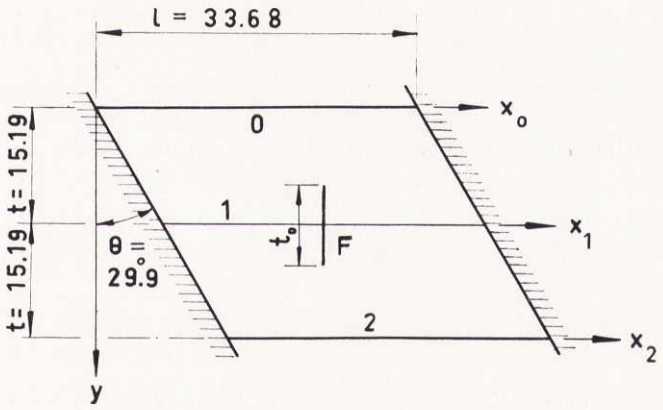

Fig. 233.1. Oblique plate, divided into three strips, line load F at $x_1 = \frac{1}{2}$.

Approximate values of the series coefficients $(s_{rn})_a$ and $(a_{rn})_a$ are obtained from (222.24) and (222.25) for $n = 1, 2, 3$:

$$\left.\begin{aligned}
(s_{01})_a &= .5413\, S_{01} + .2470\, S_{11} \\
(s_{11})_a &= .2470\, S_{01} + .3637\, S_{11} \\
(a_{01})_a &= .3656\, A_{01} \\
(s_{02})_a &= .8213\, S_{02} - .0146\, S_{12} \\
(s_{12})_a &= -.0146\, S_{02} + .6412\, S_{12} \\
(a_{02})_a &= .7815\, A_{02} \\
(s_{03})_a &= .9776\, S_{03} - .1193\, S_{13} \\
(s_{13})_a &= -.1193\, S_{03} + .8243\, S_{13} \\
(a_{03})_a &= .9623\, A_{03}
\end{aligned}\right\} \qquad (1)$$

The increments ΔS_{rn} and ΔA_{rn} due to the cosine series and the simple supporting depend upon the factors d_{mn}, e_{mn}, g_{mn}, h_{mn}. These factors are computed from formulas assembled in Appendix 57:

$$\left.\begin{aligned}
d_{12} &= -.0263 & d_{21} &= -.0245 & d_{23} &= .0005 & d_{32} &= -.0156 \\
e_{12} &= -.01023 & e_{21} &= 3.230 & e_{23} &= -.0718 & e_{32} &= .3255 \\
g_{12} &= .0586 & g_{21} &= 1.251 & g_{23} &= .0205 & g_{32} &= .1759 \\
h_{12} &= .0417 & h_{21} &= .3136 & h_{23} &= .0051 & h_{32} &= -.0397
\end{aligned}\right\} \qquad (2)$$

Substitution of these values in the equations in Appendix 57 yields:

$$\Delta S_{01} = \Delta S_{01}^{*} + \Delta S_{02}^{**} = -1.227\, a_{02}$$

$$\Delta S_{11} = \Delta S_{11}^{*} + \Delta S_{11}^{**} = 2.603\, a_{02}$$

$$\Delta A_{01} = \Delta A_{01}^{*} + \Delta A_{01}^{**} = -1.276\, s_{02} - 3.303\, s_{12}$$

$$\Delta S_{02} = -.0323\, a_{01} - .1603\, a_{03}$$

$$\Delta S_{12} = -.1857\, a_{01} + .4049\, a_{03}$$

$$\Delta A_{02} = -.0849\, s_{01} + .1425\, s_{11} - .1915\, s_{03} - .4602\, s_{13}$$

$$\Delta S_{03} = -.0210\, a_{02}$$

$$\Delta S_{13} = -.0820\, a_{02}$$

$$\Delta A_{03} = -.0200\, s_{02} + .0706\, s_{12}$$

These increments are added to S_{rn} and A_{rn} and introduced into (1). This may be done by applying matrix operations see AITKEN):

$$\begin{bmatrix} s_{01} \\ s_{11} \\ a_{02} \\ s_{03} \\ s_{13} \end{bmatrix} = \begin{bmatrix} .5413 & .2470 & & & \\ .2470 & .3637 & & & \\ & & .7815 & & \\ & & & .9776 & -.1193 \\ & & & -.1193 & .8243 \end{bmatrix} \begin{bmatrix} S_{01} + \Delta S_{01} \\ S_{11} + \Delta S_{11} \\ A_{02} + \Delta A_{02} \\ S_{03} + \Delta S_{03} \\ S_{13} + \Delta S_{13} \end{bmatrix} =$$

$$= \begin{bmatrix} (s_{01})_a \\ (s_{11})_a \\ (a_{02})_a \\ (s_{03})_a \\ (s_{13})_a \end{bmatrix} + \begin{bmatrix} .5413 & .2470 & & & \\ .2470 & .3637 & & & \\ & & .7815 & & \\ & & & .9776 & -.1193 \\ & & & -.1193 & .8243 \end{bmatrix}$$

$$\begin{bmatrix} & & -1.227 & & \\ & & 2.603 & & \\ -.0849 & .1425 & -.1915 & -.4602 & \\ & & -.0210 & & \\ & & -.0820 & & \end{bmatrix} \begin{bmatrix} s_{01} \\ s_{11} \\ a_{02} \\ s_{03} \\ s_{13} \end{bmatrix}$$

$$= \begin{bmatrix} (s_{01})_a \\ (s_{11})_a \\ (a_{02})_a \\ (s_{03})_a \\ (s_{13})_a \end{bmatrix} + \begin{bmatrix} & & -.021 & & \\ & & .644 & & \\ -.0663 & .1114 & -.1497 & -.3596 & \\ & & -.0107 & & \\ & & -.0651 & & \end{bmatrix} \begin{bmatrix} s_{01} \\ s_{11} \\ a_{02} \\ s_{03} \\ s_{13} \end{bmatrix} =$$

$$= \begin{bmatrix} (s)_a \\ (a)_a \end{bmatrix} + c_s \begin{bmatrix} s \\ a \end{bmatrix} \qquad (3)$$

Similar equations can be obtained for a_{01}, s_{02}, s_{12}, a_{03}. The unknowns, s_{rn} and a_{rn}, are solved from (3) directly or by successive approximations. The equations can also be written in the form (see ZURMÜHL)

$$\begin{bmatrix} s \\ a \end{bmatrix} = (1 + c + c^2 + \ldots) \begin{bmatrix} (s)_a \\ (a)_a \end{bmatrix} \tag{4}$$

Eq. (4) is applicable only if the matrix series is convergent. This condition is not satisfied when the width ratio l/t is large. It is then necessary to obtain exact expressions for some deflection coefficients of lower order as functions of the principal coefficients and the deflection coefficients of higher order. The latter coefficients may be determined by equations similar to (4).

For the plate in Fig. 233.1 the convergence of the matrix series is satisfactory. Application of multiplication rules to c_s in (3) yields the terms c_s^n of the series in (4)

$$c_s + c_s^2 = \begin{bmatrix} .0014 & -.0023 & -.021 & .003 & .008 \\ -.0427 & .0717 & .644 & -.096 & -.232 \\ -.0663 & .1114 & .098 & -.150 & -.360 \\ .0007 & -.0012 & -.011 & .002 & .004 \\ .0043 & -.0073 & -.065 & .010 & .023 \end{bmatrix}$$

$$c_s^3 (c_s + c_s^2) = c_s^3 + c_s^4 = \begin{bmatrix} .0001 & -.0002 & -.002 & .000 & .001 \\ -.0043 & .0070 & .063 & -.009 & -.023 \\ -.0034 & .0057 & .010 & -.008 & -.019 \\ .0001 & -.0001 & -.001 & .000 & .000 \\ .0003 & -.0007 & -.006 & .001 & .002 \end{bmatrix}$$

Insertion in (4) results in:

$$\begin{bmatrix} s_{01} \\ s_{11} \\ a_{02} \\ s_{03} \\ s_{13} \end{bmatrix} = \begin{bmatrix} 1.0015 & -.0025 & -.023 & .003 & .008 \\ -.0467 & 1.0794 & .704 & -.105 & -.253 \\ -.0700 & .1178 & .109 & -.158 & -.380 \\ .0008 & -.0013 & -.012 & 1.002 & .004 \\ .0046 & -.0081 & -.072 & .011 & 1.026 \end{bmatrix} \begin{bmatrix} (s_{01})_a \\ (s_{11})_a \\ (a_{02})_a \\ (s_{03})_a \\ (s_{13})_a \end{bmatrix} \quad (5)$$

A line load F is applied at the centre of the plate. From Appendix 55 the following principal coefficients are obtained:

$$S_{0n} = A_{0n} = 0$$

$$S_{1n} = \frac{2 F l^3}{D t \pi^4 n^4} \sin \frac{n\pi}{2} = .0455 \frac{F l^2}{D n^4} \sin \frac{n\pi}{2}$$

Substitution into (1) yields:

$$(s_{01})_a = .01124 \, F l^2/D$$

$$(s_{11})_a = .01656 \, F l^2/D$$

$$(s_{03})_a = .000067 \, F l^2/D$$

$$(s_{13})_a = -.000461 \, F l^2/D$$

The other coefficients are zero.

These values are substituted into (5):

$$\left.\begin{aligned} s_{01} &= .01121 \, F l^2/D \\ s_{11} &= .01744 \, F l^2/D \\ a_{02} &= .00133 \, F l^2/D \\ s_{03} &= .000052 \, F l^2/D \\ s_{13} &= -.000553 \, F l^2/D \end{aligned}\right\} \quad (6)$$

The improved coefficients for n = 1 differ but slightly from the approximate ones.

The coefficients s_{1n} may also be adjusted with respect to the width of load $t_0 = l/4$. The factors ζ_{id} and ζ_{ie} may be evaluated from Fig. 226. 2:

$$
\begin{aligned}
l/t &= 2.217: \quad \zeta_{id} = .855 \\
l/3\,t &= .739: \quad \zeta_{id}\, 3t/l = .835 \quad \zeta_{id} = .618 \\
l/t_0 &= 4: \quad \zeta_{ie} = .768 \\
l/3\,t_0 &= 4/3: \quad \zeta_{ie} = .682 \\
l/5\,t_0 &= 4/5: \quad \zeta_{ie}\, t_0/l = .722 \quad \zeta_{ie} = .578 \\
l/7\,t_0 &= 4/7: \quad \zeta_{ie}\, t_0/l = .841 \quad \zeta_{ie} = .480 \\
l/9\,t_0 &= 4/9: \quad \zeta_{ie}\, t_0/l = .917 \quad \zeta_{ie} = .407
\end{aligned}
$$

Applying (226. 21) the following improved coefficients are obtained:

$$
\left.
\begin{aligned}
s_{11} &= \left[.01744 + (.768 - .855) \frac{0.0455}{2.217} \right] \frac{F l^2}{D} = .01565 \frac{F l^2}{D} \\
s_{13} &= \left[-.000553 - (.682 - .618) \frac{0.0455}{27 \cdot 2.217} \right] \frac{F l^2}{D} = -.000600 \frac{F l^2}{D} \\
s_{15} &= .578 \cdot 5\, S_{15}/2.217 = .724\, S^0_{15} \\
s_{17} &= .480 \cdot 7\, S_{17}/2.217 = .841\, S^0_{17} \\
s_{19} &= .407 \cdot 9\, S_{19}/2.217 = .915\, S^0_{19}
\end{aligned}
\right\} \quad (7)
$$

The symbols S^0_{ln} with the superscript 0 indicate principal coefficients for $l/t = l/t_0 = 4$. The coefficients s_{1n} tend to S^0_{1n} with increasing n. Hence the contribution of terms of higher order becomes small when w_1 is expressed by (223. 8).

The function w_0 is determined by forming simple sine series with the coefficients given in (6):

$$
\begin{aligned}
w_0 = (&.1121 \sin \pi x_0/l - .0133 \sin 2\pi x_0/l + \\
&+ .00052 \sin 3\pi x_0/l)\, F l^2/10\, D
\end{aligned} \quad (8)
$$

For the deflection w_1 of the central strip the adjusted coefficients in (7) are used:

$$w_1 = (.1565 \sin \pi x_1/l - .0060 \sin 3\pi x_1/l + \\ + .00095 \sin 5\pi x_1/l) F l^2/10 D \qquad (9)$$

The deflection of strip 2 can be derived from (8) by changing the signs before terms with even n and substituting 2 for 0 as subscripts.

If the second derivatives of the deflections are also to be determined, the function w_1 should be expressed by (223. 8). According to (55. 3) in Appendix 55 the principal deflection W_1 for $l/t = 4$ is

$$W_1 = \left[\frac{3}{8}\frac{x_1}{l} - \frac{1}{2}\left(\frac{x_1}{l}\right)^3 + \left(\frac{x_1'}{l}\right)^3\right]\frac{F l^3}{6 t_0 D} = \left[\frac{1}{4}\frac{x_1}{l} - \frac{1}{3}\left(\frac{x_1}{l}\right)^3 + \right.$$

$$\left. + \frac{2}{3}\left(\frac{x_1'}{l}\right)^3\right]\frac{F l^2}{D}$$

where $x_1' = 0$ for $x_1 \leqq \frac{1}{2}$ and $x_1' = x_1 - \frac{1}{2} l$ for $x_1 > \frac{1}{2} l$. The corresponding principal coefficients are:

$$W_{11} = 2 F l^3/\pi^4 t_0 D = .08213 F l^2/D$$

$$W_{13} = -2 F l^3/81 \pi^4 t_0 D = -.00101 F l^2/D$$

$$W_{15} = +.000131 F l^2/D$$

$$W_{17} = -.000034 F l^2/D$$

Inserting these values in (223. 8) an expression is obtained for w_1:

$$w_1 = \left[\frac{1}{4}\frac{x_1}{l} - \frac{1}{3}\left(\frac{x_1}{l}\right)^3 + \frac{2}{3}\left(\frac{x_1'}{l}\right)^3 - .06648 \sin \frac{\pi x_1}{l} + \right.$$

$$+ .00041 \sin \frac{3\pi x_1}{l} - .000036 \sin \frac{5\pi x_1}{l} +$$

$$\left. + .000005 \sin \frac{7\pi x_1}{l}\right]\frac{F l^2}{D} \qquad (10)$$

The second derivative of this function is

$$\frac{d^2 w_1}{d x_1^2} = -\left[2\frac{x_1}{l} - 4\frac{x_1'}{l} - .656 \sin\frac{\pi x_1}{l} + .036 \sin\frac{3\pi x_1}{l} - \right.$$

$$\left. - .009 \sin\frac{5\pi x_1}{l} + .002 \sin\frac{7\pi x_1}{l}\right]\frac{F}{D} \qquad (11)$$

The second derivative with respect to y can be determined for $y = t$, Fig. 233.1, by applying (231.3). The result, modified for the actual width of loading, becomes:

$$\left(\frac{\partial^2 w}{\partial y^2}\right)_1 = \left(-.121 \sin\frac{\pi x_1}{l} - .013 \cos\frac{2\pi x_1}{l} + .017 \sin\frac{3\pi x_1}{l} - \right.$$

$$\left. - .003 \sin\frac{5\pi x_1}{l}\right)\frac{F}{D}$$

Combining this expression with (11) the moments M_{x1} and M_{y1} can be computed according to (213.2) and (213.3). Their distribution along the x-axis is shown in Fig. (233.2). Fig. (233.2) also shows the moment M_{x0} computed from (213.9).

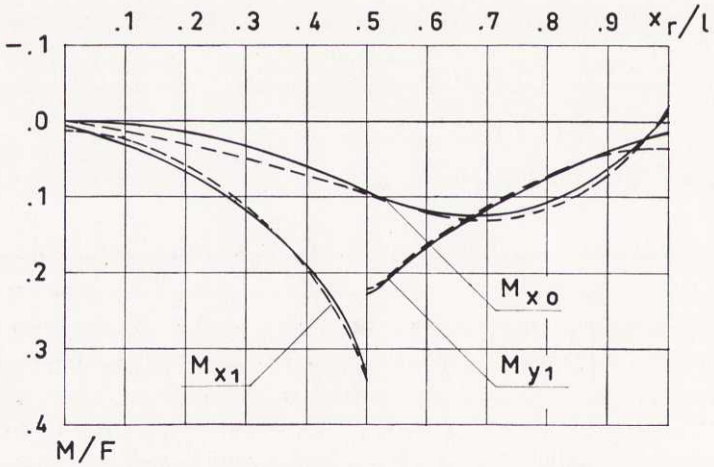

Fig. 233.2. Oblique plate, line load F at the centre, $\Theta = 29.9°$. Moments M_{x0}, M_{x1} and M_{y1} for a division into three strips, $l/t = 2.22$. The same moments obtained for a division into five strips are indicated by dashed curves

The curvatures at the supports are determined by the supplementary coefficients ΔS_{rn}^{**} and ΔA_{rn}^{**}. Substitution into (232.21) yields:

$$\Delta S_{01}^{**} = -g_{21}\, a_{02} = -.00166\, F l^2/D$$

$$\Delta S_{11}^{**} = -2\, h_{21}\, a_{02} = -.00083\, F l^2/D$$

$$\Delta A_{02}^{**} = -g_{12}\,(s_{01} - s_{11}\cos\mu) - g_{32}\,(s_{03} - s_{13}\cos 3\mu) = .000106\, F l^2/D$$

With these values the curvatures become, according to (232.20):

$$\left.\begin{aligned} \Delta K_{00} &= -\frac{\pi^5}{36\,(1-.336^2)}\left(-.00166 - \frac{32}{3}\,0.000106\right)\frac{F}{D} = .0267\,\frac{F}{D} \\ \Delta K_{0l} &= .0050\,\frac{F}{D} \\ \Delta K_{10} &= \Delta K_{1l} = \frac{\pi^5}{36}\,0.00083 = .0071\,\frac{F}{D} \end{aligned}\right\} \quad (12)$$

The curvature $\dfrac{d^2 w_1}{d x_1^2}$ is a maximum for $x_1 = \dfrac{1}{2} l$:

$$\left|\frac{d^2 w}{d x^2}\right|_{max} = .297\, F/D$$

The boundary curvatures given in (12) are small compared with this value. They are taken into account in Fig. (233.2) by drawing parabolic curves in the vicinity of the edges as proposed in 232. When the concentrated force acts on an outside strip the second derivative with respect to x can be large at the boundaries, especially at corners with obtuse angles. An example of this is shown in Fig. 333.3, part 3, where the curvatures illustrated are due to a concentrated load at the mid-point of strip 0.

The method has also been applied to a rhombic plate with

$\Theta = 45°$, $\nu = 0$ and a concentrated force acting at the centre. The moments M_1, M_2 according to (213.13) are in good agreement with experimental results published by FAURE—SCHUMANN.

234. Influence surfaces

Any effect of parallel loads of arbitrary positions upon a beam can be determined by an "influence line". This curve defines a diagram from which the effect of a unit load is taken as the ordinate at the point of loading. Such a diagram, illustrating a certain "influence function", can be used for an arbitrary system of loads, provided the action of one of the forces included in the system is independent of the other forces, and that the quantity measured is linearly dependent of the loads. The total effect is then obtained by measuring the ordinates for the different points of loading and adding the results after multiplication by the magnitude of the forces.

The requisite conditions for the use of influence functions are satisfied for elastic plates with small deflections. However, in this case the position of the loads cannot be fixed by a single coordinate. The effect of the load is not measured as the ordinate under a line but as the distance between the point of a surface, the "influence surface", and a zero plane. For loads uniformly distributed over a region A of the zero plane the effect is obtained by multiplying the intensity of load by the part of the volume under the influence surface that is bounded by the ordinates for the contour line of A.

Different ways of representing the influence surface can be applied. According to the methods used by PUCHER and BITTNER, the effect of transverse loads may be illustrated by a group of curves drawn within the contour of the plate. If a load moves along one of these curves the quantity determined by the influence surface remains constant. The curves indicate different levels of the influence surface. The constant quantities are chosen to be even multiples of a simple number. The effect of concentrated and uniformly distributed loads is then easy to obtain.

Ordinates for points of loading situated between the contour curves are computed by interpolation.

Another method better suited for the use of strips is to describe the influence surface by its curves of intersection with equidistant planes perpendicular to the zero-plane. Assume that these planes coincide with the free edges and the middle planes of the inside strips. Then, if the coefficients w_{rn} are computed, expressions can be formed for the deflections caused by a concentrated load $F = 1$ of arbitrary position. For a given point x_r of strip r the function w_r constructed in this way determines the influence surface for the deflection at the point mentioned. The distance $x_s = l_1$, Appendix 55, serves as independent variable.

Influence lines for moments and shearing forces are obtained by forming the corresponding differential expressions for the deflections.

The effect of loads applied on the centre lines of the strips are determined directly by measuring the ordinates under the curves at the points of loading. If the points of loading are situated between the centre lines, the influence ordinates are computed by interpolation.

If loads of different widths t_0 emerge, the "influence lines" can be drawn without considering the corrections treated in 226. These corrections are made afterwards.

The determination of influence surfaces by difference methods may be simplified by a method given by NEWMARK. The influence ordinates are sums of products of constants C_i and deflections w_i at certain points P_i. These deflections originate from a unit load applied at an arbitrary point P_0 and are equal to the deflection at P_0 caused by unit loads applied at the points P_i. Hence the influence surface coincides with the elastic surface for forces $C_i w_i$ acting at the points P_i.

The method can in some cases be applied to plates divided into strips. The influence lines of the deflection at a point P_i conforms to the deflections w_r for a unit load acting at P_i.

The determination of influence lines of moments is somewhat more complicated. The moment M_{xr} at $x_r = a$ is, according to (213. 5):

$$(M_{xr})_a = -D\left[\frac{d^2 w_r}{dx_r^2} + \frac{\nu}{t^2}(w_{r+1} - 2\,w_r + w_{r-1})\right]_a \qquad (1)$$

The deflections w_{r+1}, w_r and w_{r-1} in (1) are obtained as the deflections caused by unit loads at $x_{r+1} = a - t \operatorname{tg} \Theta$, $x_r = a$ and $x_{r-1} = a + t \operatorname{tg} \Theta$. The second derivative is the limit of the difference of second order of w_r with respect to x_r when Δx_r tends to zero. Applying NEWMARK'S method this difference, caused by a unit load at P_0, is substituted by the deflection at P_0 caused by three forces, $1/(\Delta x_r)^2$, $-2/(\Delta x_r)^2$, $1/(\Delta x_r)^2$. The first and third of these forces are applied at a distance Δx_r from the resultant, which acts through $x_r = a$. The corresponding principal deflection for an infinitely small Δx_r is:

$$W_r = -\frac{l}{D\,t}\left[\left(1 - \frac{a}{l}\right)\frac{x_r}{l} - \frac{x_r'}{l}\right] = -\frac{2\,l}{D\,t\,\pi^2}\sum\frac{1}{n^2}\sin\frac{n\,\pi\,a}{l} \qquad (2)$$

This series is more slowly convergent than the one adopted in Appendix 531 and 532 for estimation of the errors due to the omission of series terms. In fact, the principal deflection of (2) does not yield suitable expressions for the second derivative of w_r. This derivative is therefore determined in the usual way by differentiating the deflection w_r caused by a unit load at an arbitrary point of strip s. The principal coefficients in this case are taken from (55.4) in Appendix 55:

$$W_{sn} = \frac{2\,l^3}{\pi^4\,t\,D\,n^4}\sin\frac{n\,\pi\,x_s}{l}$$

Introducing the deflection coefficients $(w_{rm})_{sn}$ corresponding to a principal coefficient $W_{sn} = 1$, the deflection w_r can be written

$$w_r = \frac{2\,l^3}{\pi^4\,t\,D}\sum_n\frac{1}{n^4}\left[\sum_m (w_{rm})_{sn}\sin\frac{m\,\pi\,x_r}{l}\right]\sin\frac{n\,\pi\,x_s}{l} \qquad (3)$$

The second derivative with respect to x_r at $x_r = a$ is:

$$\frac{d^2 w_r}{d x_r^2} = -\frac{2 l}{\pi^2 t D} \sum \frac{1}{n^4} \left[\sum m^2 (w_{rm})_{sn} \sin \frac{m \pi x_r}{l} \right] \sin \frac{n \pi x_s}{l} \quad (4)$$

Altering the order of summation (4) yields the usual series form for the second derivative of a deflection w_r. If terms are neglected in this series the errors can be restricted according to equations in Appendix 531 and 532.

When the unit load is applied on strip r, a more rapidly converging expression is obtained by removing the principal deflection from the series as proposed in 223:

$$\frac{d^2 w_r}{d x_r^2} = -\frac{l}{t} \left[\left(1 - \frac{a}{l}\right) \frac{x_r}{l} - \frac{x_r'}{l} \right] + \frac{2 l}{\pi^2 t D} \sum \left[\frac{1}{n^2} \sin \frac{n \pi a}{l} - \right.$$

$$\left. - \frac{1}{n^4} \sum m^2 (w_{rm})_{sn} \sin \frac{m \pi a}{l} \right] \sin \frac{m \pi x_r}{l} \quad (5)$$

If the unit load is carried by an outside strip, (4) and (5) should be multiplied by 2.

Influence functions for the moments M_y and M_{xy} can be obtained as described for M_x. The twisting moment given in (213. 7) involves first derivatives of the deflections. These derivatives are obtained by differentiating (3) with r replaced by $r+1$, $r-1$. When the unit load is applied on the strip where M_{xy} acts, the convergence may be improved by excluding the slope of the principal deflection from the trigonometric series.

The method will be applied to a plate with Poissons ratio $\nu = 0$, Fig. 234. 1. The angle $\Theta = 45°$. The plate is divided into five strips; $l/t = 3$.

Approximate expressions for s_{rn} and a_{rn} are taken from the diagrams in Appendix 563. The adjusted coefficients computed by considering the corrections ΔW_{rn} and ΔA_{rn} for $n = 1, 2, 3$, Appendix 57, are given in Tab. 234. 1. Three accurate figures are obtained after four successive approximations.

Table 234. 1.

Plate with $\Theta = 45°$ and Poissons ratio $\nu = 0$, Fig. 234. 1. Coefficients s_{rn} and a_{rn} for different values of the principal coefficients S_{rn} and A_{rn}.

Multiplier	$n=1$					$n=2$					$n=3$				
	s_{01}	s_{11}	s_{21}	a_{01}	a_{11}	s_{02}	s_{12}	s_{22}	a_{02}	a_{12}	s_{03}	s_{13}	s_{23}	a_{03}	a_{13}
S_{01}	.232	.053	.025	—	—	—	—	—	—.005	—.027	—.002	.000	.003	—	—
S_{11}	.097	.182	.108	—	—	—	—	—	.024	.001	—.001	—.001	.000	—	—
S_{21}	.017	.049	.151	—	—	—	—	—	—.004	.024	.002	.000	—.003	—	—
A_{01}	—	—	—	.230	.042	—.005	—.031	.002	—	—	—	—	—	—.002	.000
A_{11}	—	—	—	.078	.152	.025	—.004	—.046	—	—	—	—	—	—.001	—.004
S_{02}	—	—	—	—.253	.202	.592	—.032	—.061	—	—	—	—	—	—.024	—.029
S_{12}	—	—	—	—.868	—.166	—.139	.639	—.169	—	—	—	—	—	.058	—.009
S_{22}	—	—	—	—.080	—.273	—.020	—.081	.572	—	—	—	—	—	—.010	.036
A_{02}	—.224	.224	.115	—	—	—	—	—	.576	—.030	—.024	—.024	.006	—	—
A_{12}	—.845	—.059	.474	—	—	—	—	—	—.127	.691	.059	.004	—.081	—	—
S_{03}	—.097	—.104	.060	—	—	—	—	—	—.262	.166	.760	—.106	.008	—	—
S_{13}	.071	—.074	—.036	—	—	—	—	—	—.191	.012	—.226	.766	—.251	—	—
S_{23}	.165	.029	—.094	—	—	—	—	—	.069	—.151	.013	—.128	.739	—	—
A_{03}	—	—	—	—.096	—.096	—.260	.165	—.056	—	—	—	—	—	.761	—.107
A_{13}	—	—	—	.106	—.176	—.184	—.072	.291	—	—	—	—	—	—.229	.753

The influence functions for the bending moment $(M_{x0})_{l/2}$ at the mid-point, P, of a free edge is required. The coefficients $(w_{rm})_{sn}$ are then determined by applying the equation

$$w_{0m} = s_{0m} - a_{0m}$$

and the values of Table 234. 1:

$$(w_{01})_{01} = .231, \quad (w_{01})_{02} = .239, \quad (w_{01})_{03} = -.097$$

$$(w_{03})_{01} = -.002, \quad (w_{03})_{02} = .024, \quad (w_{03})_{03} = .761$$

$$(w_{01})_{11} = .088, \quad (w_{01})_{12} = .857, \quad (w_{01})_{13} = .089$$

$$(w_{03})_{11} = -.001, \quad (w_{03})_{12} = -.059, \quad (w_{03})_{13} = -.228$$

$$(w_{01})_{21} = .009, \quad (w_{01})_{22} = 0, \quad (w_{01})_{23} = .083$$

$$(w_{03})_{21} = .001, \quad (w_{03})_{22} = 0, \quad (w_{03})_{23} = .007$$

$$(w_{01})_{31} = .010, \quad (w_{01})_{32} = -.012, \quad (w_{01})_{33} = -.018$$

$$(w_{03})_{31} = .000, \quad (w_{03})_{32} = -.001, \quad (w_{03})_{33} = .002$$

$$(w_{01})_{41} = .001, \quad (w_{01})_{42} = -.015, \quad (w_{01})_{43} = -.001$$

$$(w_{03})_{41} = .000, \quad (w_{03})_{42} = .000, \quad (w_{03})_{43} = -.001$$

Substitution of these coefficients in (4), (5), (1) yields, after multiplication by 2 (outside strip):

F on strip 0: $(M_{x0})_{l/2} = 3\frac{x_0}{l} - 6\frac{x_0'}{l} - 0.948 \sin\frac{\pi x}{l} +$

$$+ 0.002 \sin\frac{2\pi x}{l} + 0.038 \sin\frac{3\pi x}{l}$$

F on strip 1: $(M_{x0})_{l/2} = 0.117 \sin\frac{\pi x}{l} + 0.105 \sin\frac{2\pi x}{l} +$

$$+ 0.032 \sin\frac{3\pi x}{l}$$

F on strip 2: $(M_{x0})_{l/2} = -0.001 \sin\frac{\pi x}{l}$

F on strip 3: $(M_{x0})_{l/2} = 0.012 \sin \frac{\pi x}{l} - 0.001 \sin \frac{2\pi x}{l}$

F on strip 4: $(M_{x0})_{l/2} = 0.001 \sin \frac{\pi x}{l} - 0.001 \sin \frac{2\pi x}{l}$

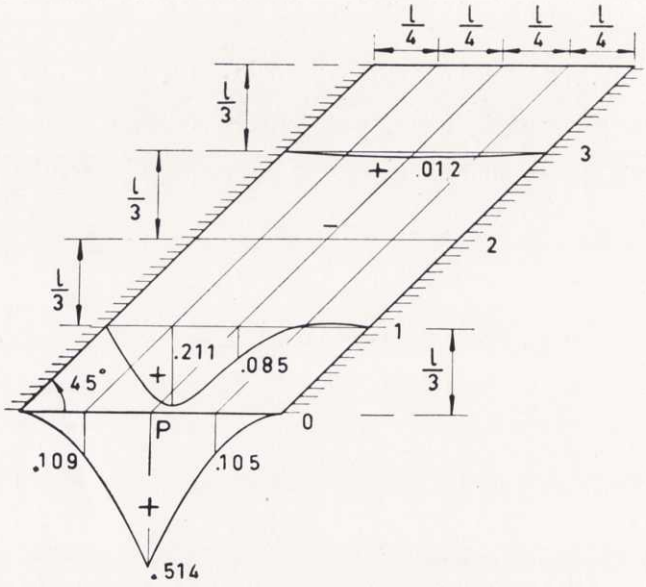

Fig. 234. 1. Plate with $\Theta = 45^\circ$ divided into five strips. Influence lines for bending moment M_{x0} at $x_0 = l/2$.

The coefficients $(w_{0m})_{0n}$ in these equations have been corrected for the width of load $t_0 = l/3$. The influence lines are represented graphically in Fig. 235. 1.

235. The effect of displacements of the supports

If a plate is simply supported along two parallel edges and these are moved parallel to each other, no additional forces are transmitted to the plate. On the other hand, if the supports are twisted relative to each other, the plate will be subjected to reactive forces. The latter case will be examined here.

Consider a plate, Fig. 235. 1, where the supports have been given a small rotation around the median line AB of the plate.

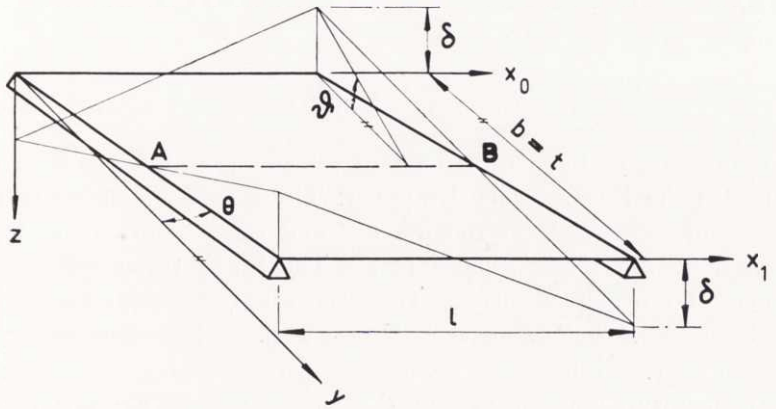

Fig. 235. 1. Plate with supports rotated round the centre line (AB).

The angle of rotation

$$\vartheta = 2\,\delta / b \tag{1}$$

where δ is the displacement of the acute corners. At the obtuse corners the displacement has the same numerical value, but is of opposite sign.

The deflections of the strips cannot be described by pure sine series. Some supplementary terms, w_r, must be added in order to give the right values of the displacements at the supports. These supplements are assumed to be linear functions of the coordinates x_r. All derivatives of w_r of higher order than the first are then zero.

For a plate divided into two strips the deflections of strip 0 are expressed in the form

$$w_0 = \Sigma\, w_{0n} \sin \frac{n\,\pi\, x_0}{l} + w_0 \tag{2}$$

where

$$w_0 = (1 - 2\,x_0 / l)\,\delta$$

For strip 1 the deflection w_1 is written

$$w_1 = \Sigma w_{1n} \sin \frac{n \pi x_1}{l} + \mathrm{w}_1 \tag{3}$$

with

$$\mathrm{w}_1 = -(1 - 2 x_1/l)\, \delta$$

On substituting the expressions in (2) and (3) for w_0 and w_1 in (212.12) the linear terms disappear. The displacement δ has no effect on the series coefficients w_{0n} and w_{1n} when the boundary conditions are those treated in 22. The linear terms affect the slopes of the elastic surface, and accordingly the supplementary coefficients ΔS_{rn}^{**} and ΔA_{rn}^{**} as well. When deriving the boundary conditions for simply supported plates in 231, expressions were determined for the partial second derivatives of w. An additional term corresponding to the functions w_r, $\left(\frac{\partial^2 \mathrm{w}}{\partial x\, \partial y}\right)_0$, must be added to the expression obtained for $\left(\frac{\partial^2 w}{\partial x\, \partial y}\right)_0$,

$$\left(\frac{\partial^2 \mathrm{w}}{\partial x\, \partial y}\right)_0 \approx \frac{1}{t}\left(\frac{d\, \mathrm{w}_1}{d\, x_1} - \frac{d\, \mathrm{w}_0}{d\, x_0}\right) = \frac{4\, \delta}{l\, t}$$

The same increment is obtained for the second derivative at $y = t$.

Substituting the total expression for the derivative $\frac{\partial^2 w}{\partial x\, \partial y}$ in (231.6), the curvatures at the boundaries, ΔK_{00} and ΔK_{0l}, may be obtained:

$$\Delta K_{00} = \frac{2 \pi \operatorname{tg} \Theta}{l t (1 + \nu)} \sum m\, (w_{1m} \cos m \mu - w_{0m}) + \frac{8\, l \operatorname{tg} \Theta}{t (1 + \nu)} \delta$$

$$\Delta K_{0l} = \frac{2 \pi \operatorname{tg} \Theta}{l t (1 + \nu)} \sum m\, (w_{1m} \cos m \mu - w_{0m}) \cos m \mu + \\ + \frac{8\, l \operatorname{tg} \Theta}{t (1 + \nu)} \delta$$

The last term on the right hand side of these equations indicates the effect of the displacements of the supports. It has the same magnitude for ΔK_{00} and ΔK_{0l}.

The supplementary coefficients ΔW_{rn}^{**} are obtained by introducing the above expressions for the curvatures in (232.12):

$$\left.\begin{aligned}
\Delta W_{0n}^{**} &= -\Sigma g_{mn}\,(w_{1m}\cos m\mu - w_{0m})\sin^2\frac{\pi}{2}(m+n) - \\
&\quad - \frac{32\,l\,\delta\,(1-\nu)\,\mathrm{tg}\,\Theta}{\pi^3 t}\;\frac{\lambda_{Nn}\sin^2\dfrac{n\pi}{2}}{n^3} \\
\Delta W_{1n}^{**} &= -\Sigma g_{mn}\,(w_{1m} - w_{0m}\cos m\mu)\sin^2\frac{\pi}{2}(m+n) - \\
&\quad - \frac{32\,l\,\delta\,(1-\nu)\,\mathrm{tg}\,\Theta}{\pi^3 t}\;\frac{\lambda_{Nn}\sin^2\dfrac{n\pi}{2}}{n^3}
\end{aligned}\right\} \qquad (4)$$

The corresponding coefficients ΔS_n^{**} and ΔA_n^{**} are obtained by halving the sum and difference of these expressions. The displacement δ only appears in the coefficients ΔS_n^{**}, and there in the same position as in (4). The terms containing δ do not include any unknown quantities, and in fact form the known part of the principal coefficients. Thus s_{rn} and a_{rn} can be determined in the usual way for the principal coefficients:

$$\left.\begin{aligned}
S_n &= -\frac{32\,l\,\delta\,(1-\nu)\,\mathrm{tg}\;\Theta}{\pi^3 t}\;\frac{\lambda_{Nn}\sin^2\dfrac{n\pi}{2}}{n^3} \\
A_n &= 0
\end{aligned}\right\}$$

The finite curvatures at the supports are computed from (232.18). The bending and twisting moments are obtained by differentiating expressions for the deflections according to (223.9), supplemented by the functions w_r. These functions only affect the twisting moments M_{xy}, for which an increment M_{xy} is obtained:

$$M_{xy} = D\,(1-\nu)\,\frac{\partial^2 w}{\partial x\,\partial y} = -\frac{4\,D}{l\,t}\,(1-\nu)$$

When treating continuous plates and frames, the slopes $\frac{\partial w_r}{\partial x_r}$ at the supports are of interest. They are obtained by differentiating (2) and (3) and substituting $x_r = 0$ and $x_r = l$. The accuracy of the expressions determined in this way can be improved as shown in 241.

Formulas valid for plates divided into three or five strips are derived in a similar way to that described for plates divided into two strips. For details reference may be made to Appendix 54. The final results are given here.

For a plate divided into three strips the usual sine series for the deflections w_0, w_1 and w_2 are supplemented by the functions

$$\left.\begin{aligned} \mathrm{w}_0 &= (1 - 2\,x_0/l)\,\delta \\ \mathrm{w}_1 &= 0 \\ \mathrm{w}_2 &= -(1 - 2\,x_2/l)\,\delta \end{aligned}\right\} \tag{5}$$

As for two strips, the effect of a small displacement of the supports is expressed by certain principal coefficients:

$$\left.\begin{aligned} S_{0n} &= -\frac{16\,l\,\delta\,\mathrm{tg}\,\Theta}{\pi^3\,t}\,\frac{\sin^2\frac{n\pi}{2}}{n^3}\left[(1-\nu)\,\lambda_{Nn} - 2\left(\frac{l}{n\pi t}\right)^2\right] \\ S_{1n} &= -\frac{16\,l\,\delta\,\mathrm{tg}\,\Theta}{\pi^3\,t}\,\frac{\sin^2\frac{n\pi}{2}}{n^3}\left[\frac{\lambda_{Nn}}{(1+\nu\,\mathrm{tg}^2\,\Theta)\cos^2\Theta} + 2\left(\frac{l}{n\pi t}\right)^2\right] \\ A_{0n} &= 0 \end{aligned}\right\} \tag{6}$$

together with the functions w_r.

The curvatures ΔK_{r0} and ΔK_{rl} may be obtained by substituting (54.2) and (54.3) in (232.18) or (232.20).

Division into five strips requires the addition of the following functions to the usual trigonometric series for the deflections:

$$\left.\begin{aligned} w_0 &= (1 - 2\,x_0/l)\,\delta & w_3 &= -\frac{1}{2}(1 - 2\,x_3/l)\,\delta \\ & & w_2 &= 0 \\ w_1 &= \frac{1}{2}(1 - 2\,x_1/l)\,\delta & w_4 &= -(1 - 2\,x_4/l)\,\delta \end{aligned}\right\} \quad (7)$$

The principal coefficients become

$$\left.\begin{aligned} S_{0n} &= -\frac{8\,l\,\delta\,\operatorname{tg}\Theta}{\pi^3\,t}\,\frac{\sin^2\frac{n\pi}{2}}{n^3}\left[(1-\nu)\,\lambda_{Nn} - 2\left(\frac{l}{n\,\pi\,t}\right)^2\right] \\ S_{1n} &= -\frac{8\,l\,\delta\,\operatorname{tg}\Theta}{\pi^3\,t}\,\frac{\sin^2\frac{n\pi}{2}}{n^3}\left[\frac{\lambda_{Nn}}{(1+\nu\,\operatorname{tg}^2\Theta)\cos^2\Theta} + \left(\frac{l}{n\,\pi\,t}\right)^2\right] \\ S_{2n} &= -\frac{8\,l\,\delta\,\operatorname{tg}\Theta}{\pi^3\,t}\,\frac{\sin^2\frac{n\pi}{2}}{n^3}\,\frac{\lambda_{Nn}}{(1+\nu\,\operatorname{tg}^2\Theta)\cos^2\Theta} \\ A_{0n} &= A_{1n} = 0 \end{aligned}\right\} \quad (8)$$

The curvatures ΔK_{r0} and ΔK_{rl} are determined for the supplementary coefficients in (54.5).

24. Continuous plates

241. Slopes at the supports

The treatment of continuous plates requires expressions for the slopes at the supports. A notation and formulas are given for slopes of a plate resting on two parallel supports j ($x_r = 0$) and k ($x_r = l$), Fig. 241.1.

If the plate is simply supported, a transverse load gives rise to a slope, Φ^0_{rj}, of strip r at j. The symbol Φ is used in the following for slopes at the support $x_r = 0$ of the plate under

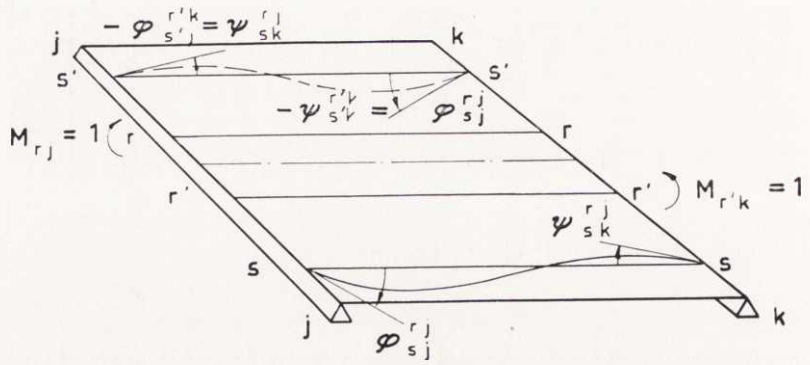

Fig. 241.1. Boundary slopes caused by unit moments $M_{rj} = 1$ and $M_{r'k} = 1$.

consideration. The first subscript indicates the order number of the strip, the second that of the support. The superscript denotes that the slope is valid for a simply supported plate. For $x_r = l$ the slopes are denoted by Ψ combined with subscripts and superscripts as for Φ. Thus the symbol Ψ^0_{rj} indicates the slope of strip r at the support j, $x_r = l$.

A moment $M_{\xi rj} = M_{rj} = 1$ is applied at (j r), the support j of strip r. This unit moment gives rise to the slope ψ^{rj}_{rj} in a simply supported plate, situated to the left of j. A plate to the right of j would have had the slope φ^{rj}_{rj}. The subscripts of φ and ψ indicate the position of the slope, the superscripts that of the moment. The slopes at (s k) corresponding to $M_{rj} = 1$, for instance, are denoted by φ^{rj}_{sk} and ψ^{rj}_{sk}, Fig. 241.1.

The slopes due to transverse loads upon plates with the boundary conditions (232.1) can generally be determined without difficulty from simple expressions by means of (223.7). Differentiating with respect to x_r and putting $x_r = 0$ and $x_r = l$, the slopes at the supports are obtained in the form

$$\left.\begin{aligned} \Phi_{rj} &= \frac{\pi}{l} \sum n\, w_{rn} \\ \Psi_{rk} &= \frac{\pi}{l} \sum n\, w_{rn} \cos n\pi \end{aligned}\right\} \qquad (1)$$

Eqs. (1) yield slowly converging series for slopes corresponding to finite curvatures at the boundaries. The convergence is improved by introducing the loads q_{rj} defined by (232.11). Results obtained in this way should be modified for the parabolic corrections of the curvatures treated in 232. The curvature of strip r is $\left(\frac{d^2 w_r}{d x_r^2}\right)_0$ at j, $x_r = 0$, Fig. 241.2. The second derivative of the

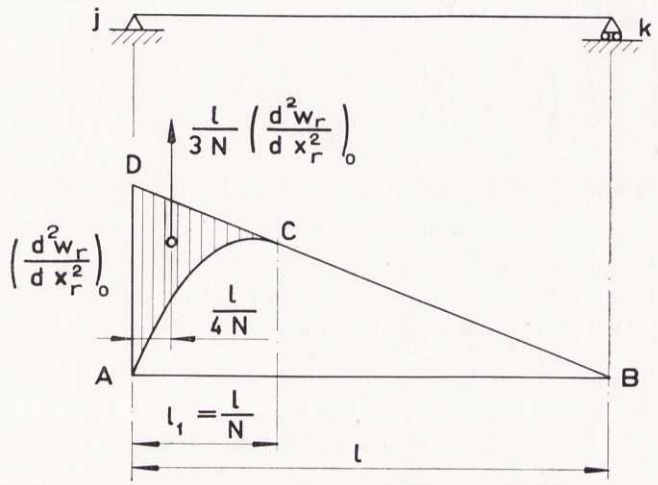

Fig. 241.2. Diagram of strip curvatures due to a boundary moment (line DCB) and to load q_{rj} (curve ACB).

principal deflection is linear and represented by the straight line DB. For the substitute load, which is uniformly distributed between the points $x_r = 0$ and $x_r = l_1 = l/N$, the curvature is represented by the curve ACB. As formerly, N indicates the highest order number appearing in the series for the deflections. The difference between the ordinates of the two diagrams DB and ACB defines a surface, ADC, bounded by straight lines and a parabola. After changing sign it can be treated as a fictitious load, (see TIMOSHENKO—YOUNG), applied to strip r. The corresponding shearing force represents the slope of the deflection curve. Thus for $x_r = 0$ the slope is

$$\Delta \Phi_{rj} = -\frac{l}{3N}\left(1 - \frac{1}{4N}\right)\left(\frac{d^2 w_r}{d x_r^2}\right)_0 = -\frac{l}{3N}\left(1 - \frac{1}{4N}\right)(K_{r0} + \Delta K_{r0}) \quad (2)$$

which is to be added to the slope Φ_{rj} determined from the first of Eqs. (1). An increment to the slope Ψ_{rj} at the support k also emerges, but it is small and can in general be omitted. The boundary curvature in (2) must also include the increment ΔK_{r0} expressed by (232.18).

For a finite curvature $\left(\frac{\partial^2 w_r}{\partial x_r^2}\right)_l$ at k, the increment $\Delta \Psi_{rk}$ of the slope Ψ_{rk} becomes:

$$\Delta \Psi_{rk} = \frac{l}{3N}\left(1 - \frac{1}{4N}\right)\left(\frac{d^2 w_r}{d x_r^2}\right)_l = \frac{l}{3N}\left(1 - \frac{1}{4N}\right)(K_{rl} + \Delta K_{rl}) \quad (3)$$

The slopes φ and ψ are connected with moments $M_\xi = 1$ acting on planes at an angle Θ with the y axis, Fig. 231.1. The boundary curvatures determining the slopes are therefore not obtained simply by multiplying M_ξ by $(-1/D)$. The desired relation is obtained from (231.1). Introducing the unit moment $M_{\xi rj} = M_{rj} = 1$ this equation yields:

$$1 = -D\Big[(\nu \sin^2\Theta + \cos^2\Theta)(K_{r0} + \Delta K_{r0}) -$$

$$-2(1-\nu)\left(\frac{\partial^2 w}{\partial x\, \partial y}\right)_r \sin\Theta\cos\Theta + (\sin^2\Theta +$$

$$+\nu\cos^2\Theta)\left(\frac{\partial^2 w}{\partial y^2}\right)_r\Big]$$

If the deflection is obtained as shown in 232, the corresponding curvature ΔK_{r0} neutralizes terms including $\frac{\partial^2 w}{\partial x\, \partial y}$ and $\frac{\partial^2 w}{\partial y^2}$. This implies that K_{r0} can be computed from the expression

$$K_{r0} = \frac{-1}{D(\nu \sin^2\Theta + \cos^2\Theta)} \quad (4)$$

The slopes due to the action of a unit moment $M_{rj} = 1$ are thus determined in the following way. The finite curvature

K_{r0} at $x_r = 0$, $(r\,j)$ is computed from (4). It defines a principal deflection which can be determined together with its Fourier coefficients from Appendix 55. The series coefficients s_{rn} and a_{rn} are then obtained in the usual way for a simply supported plate. Determining the corresponding coefficients w_{rn}, the slopes φ_{sk}^{rj} and ψ_{sk}^{rj} are found from (1). The increments $\Delta\varphi_{rj}^{rj}$ and $\Delta\psi_{rj}^{rj}$ are computed from (232.18), (2) and (3).

For larger numbers of strips the number of angles φ and ψ corresponding to different positions of M become large. The computations may be shortened by considering the symmetry properties of the plate. If the slopes corresponding to moments acting at one support, j, are determined, the slopes corresponding to moments along the other support, k, are also known. Take e. g. the case when a bending moment $M_{rj} = 1$ acts on the plate shown in Fig. 241.1. The slopes at the supports $(s\,j)$ and $(s\,k)$ of strip s are then φ_{sj}^{rj} and ψ_{sk}^{rj}. Among the other strips the one with the order number r is situated at the same distance from the median line AB of the plate as strip r. In the same way, strip s' is at the same distance from AB as strip s. Assume now that another unit moment $M_{r'k} = 1$ were acting instead of the moment M_{rj}. The corresponding slopes $\varphi_{s'j}^{r'k}$ and $\psi_{s'j}^{r'k}$ are shown in Fig. 241.1. From symmetry the following relations are then obvious:

$$\left.\begin{aligned} \varphi_{s'j}^{r'k} &= -\psi_{sk}^{rj} \\ \psi_{s'k}^{r'k} &= -\varphi_{sj}^{rj} \end{aligned}\right\} \tag{5}$$

The effect of different unit moments is easy to survey if the slopes are tabulated as shown in Table 241.1. The points of application, (rj), of the unit moments are written in the first and last columns. The corresponding slopes are found in the row determined by (rj). The relations (5) have been applied for slopes corresponding to moments at k. Subscripts and superscripts indicating the order number of the supports are omitted.

Table 241. 1

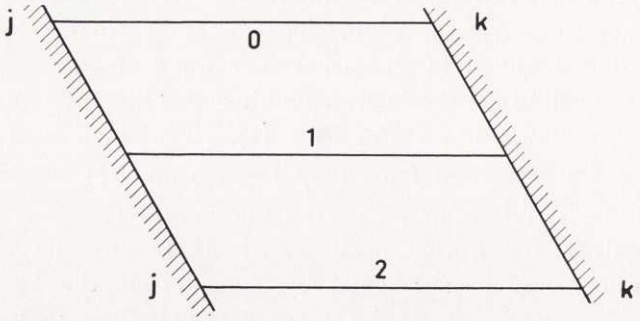

Plate divided into three strips and subjected to unit moments at the supports. Slopes at the end of the strips.

Unit moments acting at	Slopes at						Unit moments acting at
	$0j$	$1j$	$2j$	$0k$	$1k$	$2k$	
$0j$	$\varphi_0^{\,0}$	$\varphi_1^{\,0}$	$\varphi_2^{\,0}$	$\psi_0^{\,0}$	$\psi_1^{\,0}$	$\psi_2^{\,0}$	
	$-\psi_2^{\,2}$	$-\psi_1^{\,2}$	$-\psi_0^{\,2}$	$-\varphi_2^{\,2}$	$-\varphi_1^{\,2}$	$-\varphi_0^{\,2}$	$0k$
$1j$	$\varphi_0^{\,1}$	$\varphi_1^{\,1}$	$\varphi_2^{\,1}$	$\psi_0^{\,1}$	$\psi_1^{\,1}$	$\psi_2^{\,1}$	
	$-\psi_0^{\,1}$	$-\psi_1^{\,1}$	$-\psi_2^{\,1}$	$-\varphi_0^{\,1}$	$-\varphi_1^{\,1}$	$-\varphi_2^{\,1}$	$1k$
$2j$	$\varphi_0^{\,2}$	$\varphi_1^{\,2}$	$\varphi_2^{\,2}$	$\psi_0^{\,2}$	$\psi_1^{\,2}$	$\psi_2^{\,2}$	
	$-\psi_2^{\,0}$	$-\psi_1^{\,0}$	$-\psi_0^{\,0}$	$-\varphi_2^{\,0}$	$-\varphi_1^{\,0}$	$-\varphi_0^{\,0}$	$2k$

242. The moment equations

Two plates I and II are assumed to be stiffly connected along a support j, Fig. 242. 1. They are divided into the same number of strips. External loads produce slopes which must satisfy conditions of continuity at the support j.

The deformations due to the same transverse load can be determined by the methods proposed in 241, provided the plates are simply supported.

However, the slopes Ψ_{rj}^{0} of plate I along j, do not as a rule coincide with those of plate II, Φ_{rj}^{0}. The condition of continuity can be satisfied by introducing boundary moments.

The slope arising from a moment M_{si} at the support i is $M_{si} \cdot \psi_{rj}^{si}$. The moments M_{sj} affect both plates, giving rise to

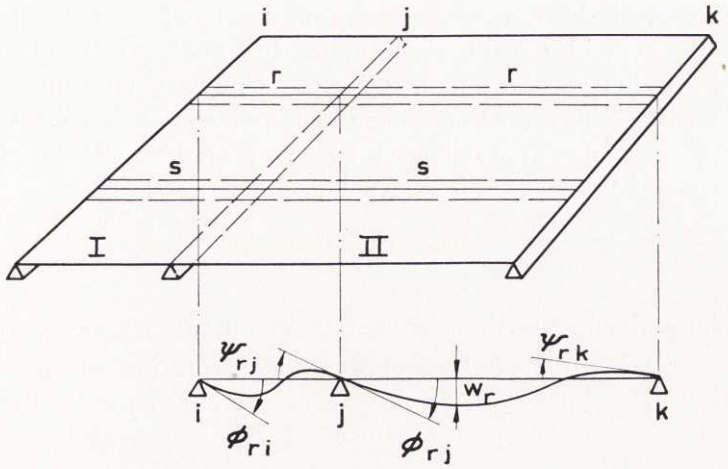

Fig. 242. 1. Boundary slopes of continuous plate.

slopes of magnitude $M_{sj}\,\psi_{rj}^{sj}$ and $M_{si}\,\varphi_{rj}^{si}$. The effect of a moment M_{sk} at the support k becomes $M_{sk}\cdot\varphi_{rj}^{sk}$. If the action of all moments is accounted for, the condition of continuity at $(r\,j)$ becomes

$$\Phi_{rj}-\Psi_{rj}=\Phi_{rj}^{0}-\Psi_{rj}^{0}-\sum_{s}M_{si}\,\psi_{rj}^{si}+\sum_{s}M_{sj}\,(\varphi_{rj}^{sj}-\psi_{rj}^{sj})+$$

$$+\sum_{s}M_{sk}\,\varphi_{rj}^{sk}=0 \tag{1}$$

The equation is simplified by introducing the angular deviations X_{rj} between the strips r of adjacent plates,

$$\Phi_{rj}-\Psi_{rj}=X_{rj} \tag{2}$$

If these quantities are assigned the same subscripts and superscripts as those used for the slopes φ and ψ, substitution in (1) yields:

$$X_{rj}^{0}+\sum_{s}(M_{si}\,\chi_{rj}^{si}+M_{sj}\,\chi_{rj}^{sj}+M_{sk}\,\chi_{rj}^{sk})=0 \tag{3}$$

an equation reminiscent of the equation of three moments for continuous beams. If the relation (3) is written for all the

points $(r\,j)$ at the continuous supports the number of equations available coincides with the number of unknown quantities, and a solution can be obtained for the boundary moments.

When the number of equations is large, the following solution by successive approximation may be preferable. The angular deviations X^0_{rj} due to the external loads,

$$X^0_{rj} = \Phi^0_{rj} - X^0_{rj}$$

are determined, together with the deviations χ^{si}_{rj} due to unit boundary moments. A first approximation for the moments is obtained from (3) by taking into consideration only the transverse loads and the boundary moment M^{I}_{rj} acting at $(r\,j)$, the point for which the condition of continuity is to be established:

$$X^0_{rj} + M^{\mathrm{I}}_{rj}\,\chi^{rj}_{rj} = 0 \tag{4}$$

The moments M^{I}_{rj} being determined, the corresponding angular deviations X_{rj} can be computed from the equations

$$X_{rj} = X^{\mathrm{I}}_{rj} = \Sigma\,(M^{\mathrm{I}}_{si}\,\chi^{si}_{rj} + M^{\mathrm{I}}_{sj}\,\chi^{sj}_{rj} + M_{sk}\,\chi^{sk}_{rj}) \tag{5}$$

The sum of all angular deviations is now put equal to zero by multiplying the moments by a factor, k:

$$k = -\left(\sum_r \sum_j X^0_{rj}\right) / \left(\sum_r \sum_j X_{rj}\right) \tag{6}$$

Corrections $k \cdot \Delta M^{\mathrm{I}}_{rj}$ for the moments $k\,M^{\mathrm{I}}_{rj}$ are obtained by applying (4) with X^0_{rj} replaced by $X^0_{rj} + k\,X^{\mathrm{I}}_{rj}$:

$$k\,\Delta M^{\mathrm{I}}_{rj} = (X^0_{rj} + k\,X^{\mathrm{I}}_{rj}) / \chi^{rj}_{rj} \tag{7}$$

Eq. (5) yields improved values of the angular deviations X_{rj} if M^{I}_{rj} is replaced by $k\ (M^{\mathrm{I}}_{rj} + \Delta M^{\mathrm{I}}_{rj})$. Then a new value of k may be determined from (6), and so on till the unknowns are evaluated with the desired accuracy.

The equations of continuity can be applied to plates for which the flexural rigidity D is only constant between adjacent supports, changing its magnitude abruptly at the edges. In such cases the variability of D should be observed by computing the coefficients w_{rn} and the curvatures K_{r0} and K_{rl} from (241.4).

24. Frames

For frames the conditions of continuity are more complicated than for continuous plates. This is due to the fact that in general plates forming a frame have different oblique angles Θ. The vertical members of the frame in Fig. 25.1, for example,

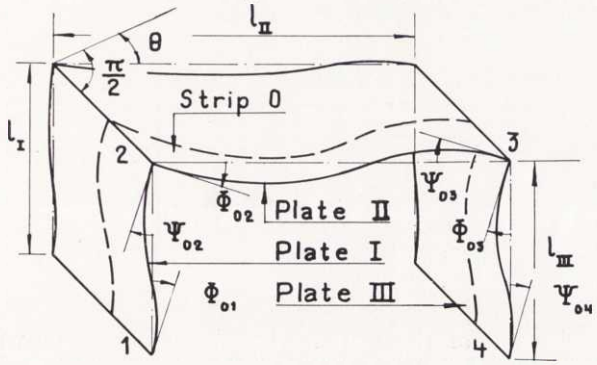

Fig. 25.1. Strip r of plates I, II and III in an oblique frame.

are rectangular plates. The horizontal part may be an oblique plate. The linear joints between the walls I, III and the slab II will be called joints for short.

The joints are first assumed to be fixed. Introducing the same symbols as in 242, the resulting slopes of plate I, Fig. 242.1, at joint 2 can then be written:

$$\Psi_{r2} = \Psi^0_{r2} + \Sigma (M_{s1}\, \psi^{s1}_{r2} + M_{s2}\, \psi^{s2}_{r2}) \tag{1}$$

The slopes Φ_{r2} of the horizontal plate II at the support 2 become:

$$\Phi_{r2} = \Phi^0_{r2} + \Sigma (M_{s2}\, \varphi^{s2}_{r2} + M_{s3}\, \varphi^{s3}_{r2}) \tag{2}$$

The slopes of plate I are valid for deflections in planes perpendicular to the joint 2. The slopes Φ_{r2} of plate II, however, are determined from deflections in planes parallel to the free edges. These slopes are referred to a direction at an angle Θ to planes normal to the joint 2. The slope of plate I in the corresponding direction is Ψ_{r2} times cos Θ. This expression must be equal to Φ^0_{r2} whereupon application of (1) and (2) gives

$$-\Psi^0_{r2}\cos\Theta+\Phi^0_{r2}+\Sigma[-M_{s1}\psi^{s1}_{r2}\cos\Theta+M_{s2}(-\psi^{s2}_{r2}\cos\Theta+\varphi^{s2}_{r2})+$$

$$+M_{s3}\varphi^{s3}_{r2}]=0 \tag{3}$$

Let the following symbols be introduced:

$$\left.\begin{aligned} X^0_{r2} &= -\Psi^0_{r2}\cos\Theta+\Phi^0_{r2}\\ \chi^{s1}_{r2} &= -\psi^{s1}_{r2}\cos\Theta\\ \chi^{s2}_{r2} &= -\psi^{s2}_{r2}\cos\Theta+\varphi^{s2}_{r2}\\ \chi^{s3}_{r2} &= \varphi^{s3}_{r2}\end{aligned}\right\} \tag{4}$$

After substitution of these quantities in (3) the following equation emerges:

$$X^0_{r2}+\Sigma\,(M_{s1}\,\chi^{s1}_{r2}+M_{s2}\,\chi^{s2}_{r2}+M_{s3}\,\chi^{s3}_{r2})=0 \tag{5}$$

coinciding with (242. 3) for continuous plates. Equations of this type can also be established for the joint 3. At the joints 1 and 4 the conditions are the same as those for continuous plates. The solution of the equations for the boundary moments can proceed as described in 242.

If the joints are displaced, the moments are altered, and results obtained by (5) must be modified. Some cases of practical interest are treated in this paper.

To begin with, joints 2 and 3 are assumed to be movable in the horizontal direction while joints 1 and 4 remain fixed. For a given loading, the displacements δ, Fig. 25. 2, are so large

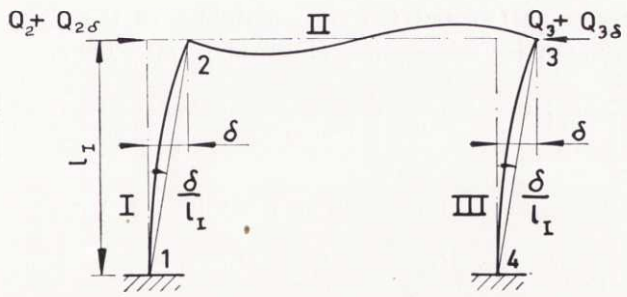

Fig. 25. 2. Slopes and reactions of a frame with horizontal displacement δ of the upper joints (2 and 3).

that the difference between the reactions Q_2 and Q_3 of the plates I and III at fixed joints 2 and 3 is neutralized. The total moments are thus determined by adding the effect of a horizontal displacement to the moments obtained from (5).

The reactions Q_2 and Q_3 can be computed if the moments M_{rj} at 1, 2, 3 and 4 are known. The equilibrium of plate I requires:

$$Q_2 = \frac{t_I}{l_I}\left[\frac{1}{2}(M_{01} - M_{02} + M_{R1} - M_{R2}) + \sum_{1}^{R-1}(M_{r1} - M_{r2})\right] + Q_2^0 \qquad (6)$$

where Q_2^0 is the effect of possible transverse loads on plate I and $R+1$ the number of strips. The reaction Q_3 is obtained in the same way by exchanging subscripts:

$$Q_3 = \frac{t_I}{l_I}\left[\frac{1}{2}(M_{04} - M_{03} + M_{R4} - M_{R3}) + \sum_{1}^{R-1}(M_{r4} - M_{r3})\right] + Q_3^0 \qquad (7)$$

A displacement δ of the joints 2 and 3 of the plates I and II would produce the angular deviations X_{r2}^0 and X_{r3}^0 if the plates were not rigidly connected to plate II,

$$X_{r2}^0 = X_{r4}^0 = -\delta/l_I \qquad X_{r3}^0 = X_{r1}^0 = \delta/l_I$$

The moments at the joints can be computed by inserting angles as known quantities in (5). These moments are denoted by the product $m_{rj} \cdot \delta$, where m_{rj} is the moment corresponding to a unit displacement.

The reactions $Q_{2\delta}$ and $Q_{3\delta}$ corresponding to the displacement δ are obtained by application of (6) and (7). Thus

$$Q_{2\delta} = \frac{t_I}{l_I}\left[\frac{1}{2}(m_{01} - m_{02} + m_{R1} - m_{R2}) + \sum_{1}^{R-1}(m_{r1} - m_{r2})\right]\delta$$

The resulting horizontal reactions must be zero:

$$Q_3 - Q_2 + Q_{3\delta} - Q_{2\delta} = 0$$

Substitution of the expressions for the reactions yields an equation for the displacement δ. After δ has been computed, the total boundary moments are obtained as the sum $M_{rj} + m_{rj}\,\delta$ where M_{rj} are the moments determined for the frame with fixed joints.

Deformations corresponding to a relative horizontal displacement of the joints 1 and 4 of a simple frame are indicated in Fig. 25. 3.

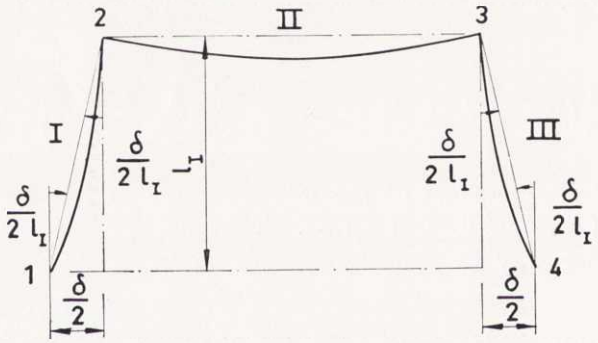

Fig. 25. 3. Slopes due to a change δ of the distance between the supports (1 and 4) of a frame.

If the plates I, II and III were simply supported at the joints the angular deviations at 1 and 4 would be

$$X^0_{r1} = X^0_{r4} = \frac{1}{2}\delta/l_I$$

and at 2 and 3

$$X^0_{r2} = X^0_{r3} = -\frac{1}{2}\delta/l_I$$

They are compensated for by applying boundary moments obtained from equations of type (5).

The joints of a frame can be moved by the kind of displacements treated in 236. Suppose the vertical members of the frame are twisted an angle ϑ relative to each other about the centre line AB of plate II, Fig. 236. 1. For the simply supported plate II, the slopes at joints 2 and 3 can be derived from deflections obtained as shown in 236. The corresponding angular deviations X^0_{r2} and X^0_{r3} emerge from (4). Substituting these into the equations of continuity (5), the resulting equations can be solved for the boundary moments.

Another case implies that the joints 1 and 4 are twisted relative to each other about vertical axes which intersect the respective joints. The known angular deviations are then linearly dependent on the distance y_m from the mid-point of the supports. The angular deviations become for 1 and 4

$$X^0_{r1} = X^0_{r4} = \frac{1}{2}\vartheta\, y_m/l_I$$

where ϑ is the angle of rotation, and for 2 and 3

$$X^0_{r2} = X^0_{r3} = -\frac{1}{2}\vartheta\, y_m/l_I$$

The corresponding boundary moments may be obtained from (5) as in the other cases.

The theory here described also can be extended to frames with several spans. However, this problem is left to future investigations.

3. Experimental part

31. Purpose and planning of the experiments

The theory evolved in this paper is founded upon the differential equation (211.6) for thin plates with small deflections. Exact solutions of this equation yield in general fairly accurate deformations. The introduction of differences and finite trigonometric series causes inaccuracies in the results. Upper bounds are given in 224, 531 and 532 for the effect of some sources of error. However, it has not been possible, for general cases, to deduce exact expressions for the inaccuracy arising from the use of strips of finite width, cf. 226. The boundary conditions for simply supported plates were satisfied in an approximate way, cf. 23. This causes errors which have not been investigated. The difficulties in calculating the errors of approximate theoretical computations make a comparison with experimental data desirable.

In order to do this, model plates of various relative dimensions were tested for different kinds of loading. The models, cut out from plates of ordinary mild steel, were supported along two parallel edges.

First a rectangular plate, Plate I, was tested for a line load acting in the plane of symmetry parallel to the supports. The magnitude of the experimental errors was measured. The influence of irregularities in the plate was observed.

Afterwards three oblique plates, Plates II—IV, were tested. Concentrated loads were placed successively at the centres of the free boundaries and at the centres of the plates. Such loads, combined in different ways, roughly reproduce most cases of practical interest.

In cases where the obliquity Θ of the plate was equal to or greater than 45°, the effect of a force at a free edge at a distance $l/4$ from an obtuse corner was also investigated.

Deflections and strains were measured at various points regularly spaced with respect to the centre of the model plate.

The flexural rigidities, D, of the model plates were computed from (211.3) by inserting numerical values of the thickness h, the modulus of elasticity, E, and Poissons ratio, ν. The deflections and strains were then calculated for the given values of l/t and Θ. The experimental and theoretical values are presented diagrammatically. The results are discussed in 34.

32. Determination of the elastic constants and dimensions of the plates

The moduli of elasticity were determined by observing the resonance frequency of vibrating rods with known dimensions, cut out from the same materials as those used for the plates.

For the lowest of the resonance frequencies, f_b, the following equation connecting f_b with the modulus of elasticity is valid (see TIMOSHENKO, 28):

$$E = 64\,\gamma\, f_b^2\, l^4 / 1.875^2\, g\, d^2 \qquad (1)$$

Here γ = the mass per unit volume,
g = the acceleration due to gravity,
l = the length of the rod
and d = the diameter of the circular section of the rod.

The oscillations were excited magnetically, by means of a solenoid fed from an audio-frequency oscillator. Near resonance the vibrations were audible. The frequency corresponding to the maximum intensity was determined six times, and could be found with good accuracy.

When determining the length l of the rod a certain amount, Δl, should be added to the distance from the free end to the surface of the support. The support was not perfectly rigid and to some extent took part in the vibrations. The increment Δl was taken equal to one third of the diameter d of the rod.

The rectangular plate and one of the oblique plates were made from the same material, denoted by the letter "a". The material of the other plates was given the notation "b". The moduli of elasticity computed from (1) are introduced in Tab. 32.1. The errors included are dominated by the uncertainty of the estimation of Δl. For the bar with the largest sectional area the value $\Delta l = .4\,d$ was obtained by determining and

equating E for different lengths l. Assuming a maximum deviation of $.2\,d$ from the value of l introduced in (1) the maximum error ΔE of the modulus of elasticity becomes

$$\Delta E = .2\,d\,\frac{\partial E}{\partial l} = .8\,d\,E/l \tag{2}$$

For material a, $l = 26.1$ cm and $d = .720$ cm:

$$\Delta E = .8\,\frac{.720}{26.1}\,E = .022\,E$$

Practically the same estimate was obtained for the maximum error of E for material b.

Tab. 32. 1

The modulus of elasticity, E, Poissons ratio, ν, and the flexural rigidity, D, of the model plates.

Plate nr	Material	E kp/cm²	ν	D kpcm
I	a	2.12	.30	1.49
II	b	2.10	.34	1.12
III	a	2.12	.30	1.45
IV	b	2.10	.34	1.82
Multiplier		$.10^6$		$.10^5$

Poisson's ratio was computed from the equation

$$G = E/2\,(1+\nu) \tag{3}$$

where G is the modulus of shear. A rod with circular section of diameter d was clamped at one end and at the other end attached to a mass with the equatorial moment of inertia I_p. When given a slight twist and released the rod performed torsional vibrations of frequency f_t, connected with the modulus of shear by the equation (see TIMOSHENKO, 28)

$$G = 128\,\pi\,f_t^2\,l\,I_p/g\,d^4 \tag{4}$$

Here l denotes the length of the rod. Eq. (4) is only valid when I_p is much larger than the equatorial moment of inertia of the rod. This was the case in the experiments.

The error in ν is chiefly determined by the increment of l, Δl, due to the motion of the support. For $\Delta l = .2\,d$ the corresponding change of Poisson's ratio, $\Delta \nu$, is

$$\Delta \nu = .2\,d \frac{\partial \nu}{\partial d} = 8\,(1+\nu)\frac{d}{l}$$

Substituting the values of l and d for materials a and b an error of 9 % is obtained. The inaccuracy of ν is of small importance as regards the flexural rigidity D, as seen from (211. 3).

Variations in the thickness h of the plate were more important. The thickness was obtained as the mean of measurements at 10 different points. The distribution of these points was chosen to correspond approximately to the deflection curve of a uniformly loaded beam simply supported at the same edges as the plate. The largest variations of h appearad for plate II, where the range (difference between the highest and the lowest values) was 4.2 % of the mean. For plates I, III and IV the range was 2.2, 1.4 and 1.3 %. The errors in the lengths and widths of the plates could be neglected compared to these deviations.

33. Experiments with the model plates

331. General arrangements

During the experiments the plates rested on a frame of cast iron, designed for earlier model tests (see Brink, Svensson, and Thorén), Fig. 331. 1. The reactions of the plates were transferred to the upper, plane surfaces of the frame by two parallel cylinders (*a*), Fig. 331. 2. Forces acting upwards were taken up by two other equidistant cylinders (*b*) from which the reactions were transferred to the frame via covering plates (*c*) and bolts.

The loads were exerted by a hydraulic jack causing compression between the plate and a beam (*d*) connected with the frame.

The magnitude of the loads was determined by an instrument for measurement of compressive forces designed by C. E. Johansson, Eskilstuna. Two spherical bearings, (e_1) and (e_2), were

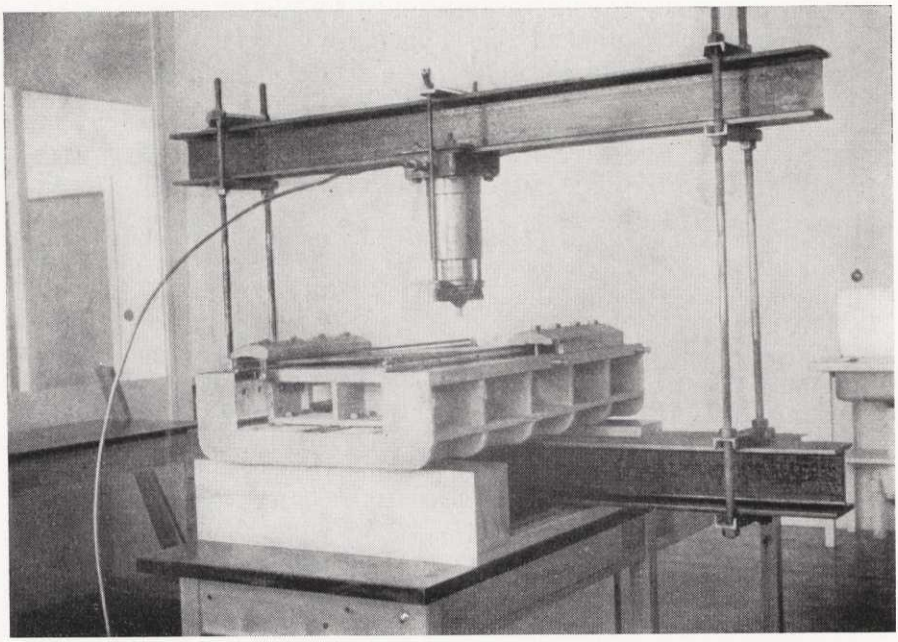

Fig. 331.1. Testing apparatus.

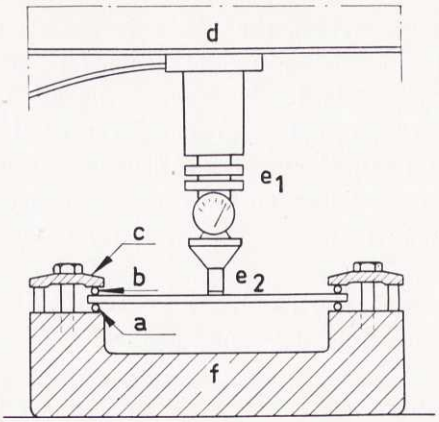

Fig. 331.2. Schematic section of loading apparatus and supporting frame.

inserted above and below the instrument to obtain centric action of forces.

The deflections were determined by dial gauges placed between the model plate and the bottom (f) of the frame. The strains at the surface of the plates were measured by strain gauges connected via a switch-box to a Wheatstone bridge (Philips GM 4571). The strains were read directly in 0/00. Temperature effects were compensated by a gauge with constant strain connected to the bridge.

The effect of strains in the direction perpendicular to that of the tested strains never exceeded 1 % and was therefore neglected.

Before performing the tests the plates were submitted four times to forces 25 % greater than those applied during the tests. No permanent deformations were observed.

332. Plate I (rectangular)

The tests with the rectangular plate were performed in order to obtain an idea of the accuracy which could be expected in the other experiments. The experimental errors could be reduced arbitrarily by repeating the tests. However, the accuracy of the results would not be increased by making the experimental errors smaller than errors originating from inaccuracies of the plates. These, consisting in variability of the thickness h and initial curvatures of the plates could not be disregarded. Their effect upon the results determined the appropriate number of tests for every case of loading.

The plate was subjected to a line load, Fig. 332. 1. The distribution of the force from the jack was accomplished by inserting a system of small beams between the loading apparatus and the plate. The deflections were measured at four points, 1—4, situated symmetrically with respect to the centre of the plate.

These deflections would have been equal for a perfectly homogeneous plate of accurate dimensions and a perfect adjustment of the load.

The dial gauges were read for a small load. The load then was increased by a force between 300 and 500 kp. The four deflections were observed. The plunger of the jack was rotated some 90°. Then the deflections were read once more. The orientation was assumed to influence the magnitude but not the location of the load. Two new orientations of the plunger differing by some 90°, yielded four new pairs of deflections. The load was then reduced to the original amount and the corresponding deflections read. The deflections at a particular point caused by the change of load were obtained by sub-

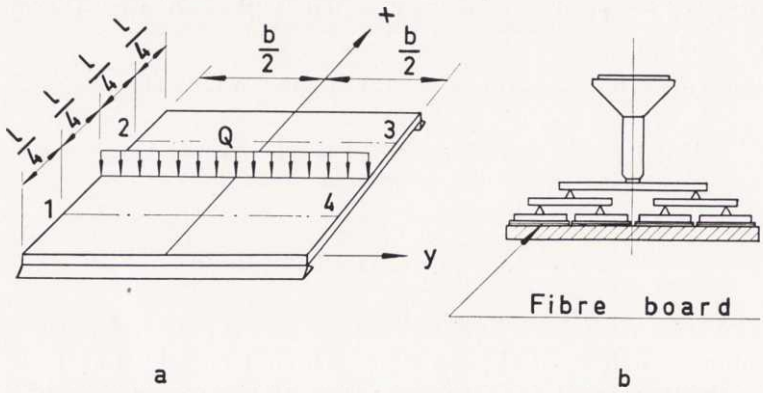

Fig. 332.1. a. Load applied to rectangular plate, Plate I,
b. Arrangement for obtaining line load.

tracting the mean of the two observations made for the original load from the deflections read with the larger load applied.

The test was repeated four times. The results were transformed to a load of 1000 kp by dividing with the observed load, expressed in kp, Tab. 332.1.

An analysis of variance is given in Appendix 581. The analysis shows that the errors of measuring and locating the load are more important than other errors included in an observed deflection. Smaller experimental errors do not, in this case, yield better possibilities of estimating the errors of the theory. The "between points" component in the variance analysis is larger than estimated variances of other error components. Thus the differences between the deflection means at points 1—4 were comparatively large. The constant errors

of the dial gauges being negligible, these differences are chiefly due to inaccuracies of the model plates, the influence of which could not be diminished by improving the measuring methods. On the other hand Figs. 226. 2 and 226. 3 reveal relative differences between exact and approximate theoretical values which are considerably larger than the deviations of the deflection means, at points 1—4 from the grand mean. The plate was therefore sufficiently accurate for the purpose of the experiments, a conclusion which was assumed to apply to other model plates also.

Tab. 332. 1

Plate I carrying a line load $Q = 1000$ kp. Deflections in mm at points 1—4 during four different experiments (tests 1—4) and different orientations of the compression measuring instrument ("Positions 1—4").

Point	Test	Orientation				Mean
		1	2	3	4	
1	1	3.53	3.52	3.49	3.48	
	2	3.52	3.54	3.50	3.54	
	3	3.60	3.57	3.57	3.59	
	4	3.56	3.56	3.47	3.52	3.535
2	1	3.46	3.47	3.44	3.43	
	2	3.51	3.51	3.49	3.53	
	3	3.69	3.63	3.61	3.72	
	4	3.52	3.49	3.44	3.50	3.528
3	1	3.50	3.46	3.43	3.37	
	2	3.46	3.46	3.46	3.45	
	3	3.41	3.39	3.45	3.44	
	4	3.34	3.37	3.32	3.35	3.416
4	1	3.55	3.52	3.49	3.42	
	2	3.50	3.48	3.46	3.47	
	3	3.49	3.45	3.49	3.53	
	4	3.39	3.39	3.33	3.37	3.458

The value of the flexural rigidity of Plate I given in Tab. 32.1 can now be verified. This is possible by applying the theoretic expression for the deflection at points 1—4. The general equations for the deflection w of a plate with curbs along the unsupported edges is (TIMOSHENKO 40):

$$\left.\begin{aligned} & w = z_1 + z_2 \\ & \text{where} \\ & z_2 = \sum \left(B_m \cos h \frac{m\pi y}{l} + C_m \frac{m\pi y}{l} \sin h \frac{m\pi y}{l} \right) \sin \frac{m\pi x}{l} \end{aligned}\right\} \quad (1)$$

Tab. 332.2

Plate I carrying a line load $Q = 1000$ kp. Strains ε_x in 0/00 at points 1—4 during four different experiments (test 1—4).

Point	Test				Mean
	1	2	3	4	
1	.860	.876	.866	.860	.866
2	.851	.867	.860	.840	.856
3	.811	.810	.832	.844	.824
4	.846	.840	.854	.810	.838

Grand mean = .846

The position of the coordinate system is shown in Fig. 332.1. The arbitrary constants B_m and C_m can be determined from the boundary conditions and the type of loading. Putting

$$z_1 = \frac{2\,Q\,l^3}{\pi^4\,b\,D} \sum \frac{1}{m^4} \sin \frac{m\pi}{2} \sin \frac{m\pi x}{l} \quad (2)$$

and the flexural rigidity of the curbs along the unsupported edges equal to zero the following expressions for the constants are obtained:

$$B_m = \frac{2\,Q\,l^3}{b\,D\,\pi^4\,m^4} \sin\frac{m\pi}{2} \frac{\nu(1+\nu)\sin h\,\lambda_m - \nu(1-\nu)\lambda_m \cos h\,\lambda_m}{(3+\nu)(1-\nu)\sin h\,\lambda_m \cos h\,\lambda_m - (1-\nu)^2\lambda_m}$$

$$C_m = \frac{2\,Q\,l^3}{b\,D\,\pi^4\,m^4} \sin\frac{m\pi}{2} \frac{\nu(1-\nu)\sin h\,\lambda_m}{(3+\nu)(1-\nu)\sin h\,\lambda_m \cos h\,\lambda_m - (1-\nu)^2\lambda_m} \qquad (3)$$

where

$$\lambda_m = \frac{1}{2} m\pi\, b/l$$

Substituting in (1) and putting $x = l/4$, $y = -b/2$ the deflection at 1, 2, 3, 4 is obtained:

$$w_{l/4,\,-b/2} = 16.07\,Q\,l^3\,10^{-3}/b\,D \qquad (4)$$

The dimensions of the plate were

$$l = 39.82 \text{ cm}$$

$$b = 19.49 \text{ „}$$

$$h = 9.16 \text{ „}$$

Substitution of the values of l, b, Q and the grand mean $w = .348$ cm in (4) yields the flexural rigidity

$$D = \frac{39.8^3}{.348\,(19.49)}\,16.07 = 1.49 \cdot 10^5$$

This value coincides well with that given in Tab. 32.1. The result does not reveal any effect of initial curvature of the plate.

The flexural rigidity is obtained in a simpler way by applying the methods of part 2 in this paper. If the plate is divided into three strips the width ratio $l/t = 39.82 \cdot 2/12.49 = 4.09$. The principal coefficients are

$$W_{0n} = \frac{Q\,l^3}{\pi^4\,t\,D\,n^4} \sin\frac{n\,\pi}{2} = W_{1n} = W_{2n}$$

Substitution into (222.24) and (222.23) yields:

$$w_0 = \frac{Q\,l^3}{\pi^4\,t\,D}\left(1.123\,\frac{1}{\sqrt{2}} - .014\,\frac{1}{\sqrt{2}}\right) = .0330\,\frac{Q\,l^2}{D}$$

With $w_0 = .348$ cm the flexural rigidity becomes

$$D = .0330 \cdot .348 \cdot 39.82^2\,10^3/.348 = 1.50 \cdot 10^5$$

The points 1, 2, 3, 4 also were investigated with respect to the strains ε_x. These were determined by strain gauges attached to the lower surface of the plate. The observations were made at four different applications of the line load Q. The strains were measured only once for every load as the tests on the deflections had not revealed any effect from the orientation of the jack plunger. The differences between mean strains at different points are considerable, Appendix 582.

The theoretic expression for w given in (1) combined with (2), (3), can be used for determining the strains at the points 1, 2, 3, 4. Differentiating w twice with respect to x and substituting $x = l/4$, $y = .448\,b$ (centre of strain gauge), the strain ε_x is obtained by applying (213.1):

$$\varepsilon_x = \frac{2\,Q\,l}{D\,b\,h}\left\{\frac{1}{8} + \pi^2 \sum n^2\left[B_n \cos h\left(.448\,\frac{b}{l}\right)\pi\,n + \right.\right.$$

$$\left.\left. + .448\,n\,\pi\,\frac{b}{l}\,C_n \sin h\left(.448\,\frac{b}{l}\right)n\,\pi\right] \sin\frac{n\,\pi}{4}\right\}$$

With $Q = 1000$ kp and the dimensions of the plate and the value of D given in Tab. 32.1 the strain becomes

$$\varepsilon_x = .138 \cdot 39.8 \cdot 10^{-2} \cdot .916/1.49 \cdot 19.49 \cdot 2 = .867 \cdot 10^{-3}$$

This falls within the range of the experimental values of Tab. 332.2. An approximate expression for ε_x obtained by differentiating (223.9) is

$$\varepsilon_x = \frac{Q\,l\,h}{2\,D\,t}\left\{\frac{1}{8\,(1-.09)}+\frac{1}{\pi^2}\left(1.123-\frac{1}{1-.09}\right)\frac{1}{\sqrt{2}}+\right.$$

$$\left.+\frac{9}{\pi^2}\left[-.014+\frac{1}{9\,(1-.09)}\right]\frac{1}{\sqrt{2}}\right\} = .853\cdot 10^{-3}$$

333. Plate II ($\Theta = 29°$)

The dimensions of the plate, Fig. 333.1, were:

$l = 33.7$ cm

$b = 30.4$ „

$h = .829$ „

$\Theta = 29.0°$

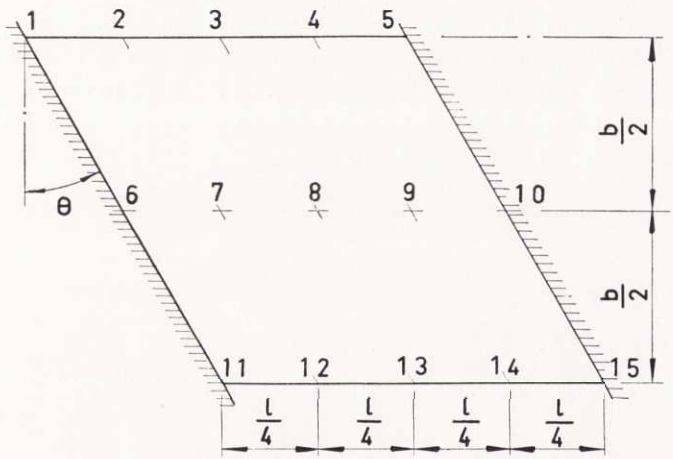

Fig. 333.1. Plate II, dimensions and measuring points.

The plate was loaded at three points, 3, 8, 13, along a line through the centre of the plate and parallel to the supports. The results, transformed to the load $F = 100$ kp, are plotted in Tabs. 333.1 and 333.2. The real loads varied between 500 and 700 kp. The experiments were repeated for every position of the load: for symmetrical loads twice and for unsymmetrical loads once.

The deflections were determined at the points 2, 3, 4, 7, 8, 9, 12, 13, 14. The positions of these points were arranged symmetrically with respect to the centre of the plate. Hence, if the load F were applied at 3 for instance, the deflection at point 2 of a plate of accurate shape should be the same as the deflection at 14 if F were applied at 13. From symmetry, the deflections at 2 and 14 should be equal if F were applied at the centre, 8, of the plate. Using these properties of symmetry, two, six or four values respectively were obtained for every deflection. Such sets of values are grouped horizontally in Tables 333.1 and 333.2.

The accuracy of the mean for every deflection was estimated by computing the confidence limits, $\pm L$, corresponding to a confidence coefficient .95, Appendix 583. If the difference between two means obtained for deflections of the same theoretical value exceeds $2\ L$ it is statistically significant.

The means are shown graphically in Figs. 333.2 and 333.3. The length $2\,L$ is drawn from the x_n-axis along the ordinate of the point concerned. For points x_n where the mean square

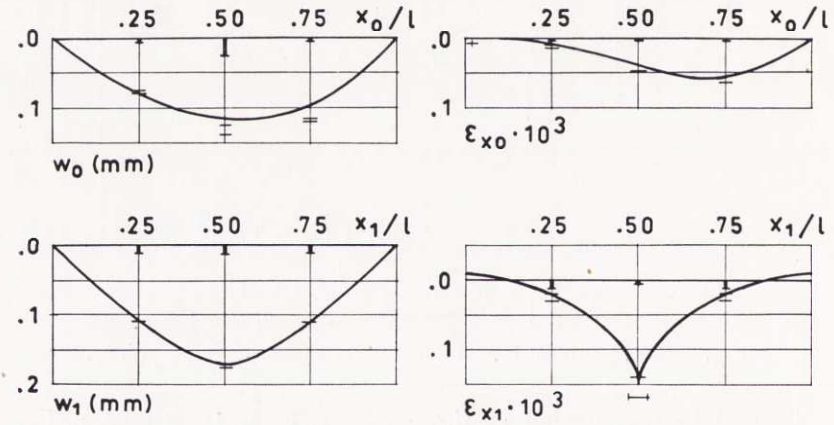

Fig. 333.2. Plate II, concentrated load $F = 100$ kp at the centre. Theoretical curves for outside strip 0 and central strip 1, together with experimental points. Confidence intervals $2\,L$ for the means are indicated by vertical lines from the projections on the x-axis.

a. Deflections w_r, $l/t_0 = 12$

b. Strains ε_x, $l/t_0 = 12$

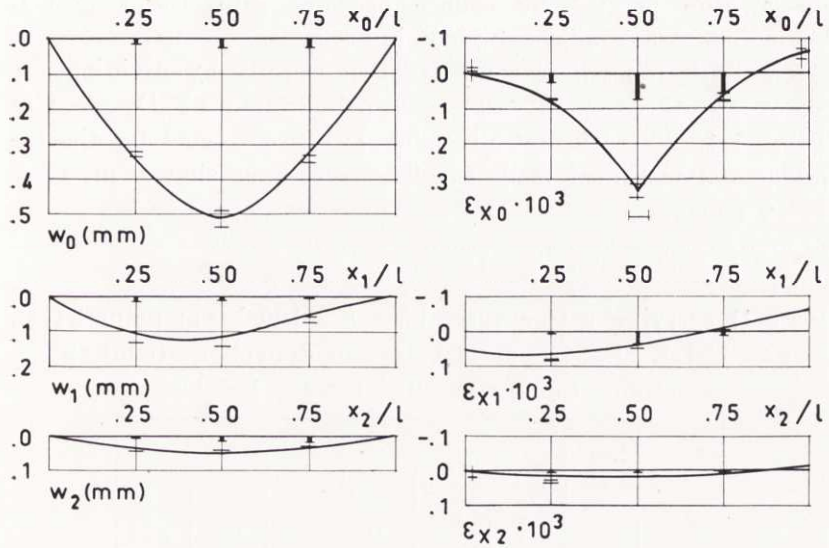

Fig. 333.3. Plate II, concentrated load $F = 100$ kp at centre of a free edge, strip 0. Theoretical curves for strips 0, 1 and 2 together with experimental points. Confidence intervals $2L$ for the means are indicated by vertical lines from the projections on the x-axis.
a. Deflections w_r, $l/t_0 = 2.22$
b. Strains ε_x, $l/t_0 = 6$

Tab. 333.1

Plate II carrying a transverse load $F = 100$ kp at point 8, Fig. 333.1. Experimental values of deflections (mm) and strains (0/00).

Point	w				ε_x			
	Test 1	Test 2	Test 3	Mean	Test 1	Test 2	Test 3	Mean
2	.081	.083	.076	.080	.012	.009	.014	.012
14	.072	.071	.081	.075	.014	.017	.016	.016
3	.137	.138	.139	.138	.049	.049	.048	.049
13	.128	.113	.133	.125	.048	.050	.052	.050
4	.120	.122	.119	.120	.066	.064	.066	.065
12	.116	.115	.114	.115	.065	.065	.067	.066
7	.109	.114	.109	.111	.033	.130	.032	.032
9	.109	.112	.110	.110	.021	.018	.025	.021
8	.177	.177	.172	.175	.141	.143	—	.142

for "within points" by chance becomes zero, the largest L belonging to any adjacent point is used.

The deflections were computed theoretically by dividing the plate into three strips and using the value of D given in Tab. 32.1. The theoretical values were corrected for the experimental width of load, t_0. The result is shown in Figs. 333.2 and 333.3.

Tab. 333.2

Plate II carrying a transverse load $F = 100$ kp at point 3 (13), Fig. 333.1. Experimental values of deflections (mm) and strains (0/00) computed for $F = 100$ kp.

Point	Load at	w			ε_x		
		Test 1	Test 2	Mean	Test 1	Test 2	Mean
2	3	.338	.341	.340	.072	.080	.076
14	13	.327	.323	.325	.072	.074	.072
3	3	.539	.544	.542	.365	.340	.353
13	13	.496	.488	.492	.315	.319	.317
4	3	.353	.359	.356	.071	.085	.078
12	13	.337	.332	.335	.080	—	.080
7	3	.135	.137	.136	.081	.081	.081
9	13	.135	.140	.138	.077	.079	.078
8	3	.141	.144	.143	.052	.045	.049
	13	.143	.140	.142	.029	.038	.034
9	3	.059	.058	.059	−.008	−.005	−.007
7	13	.075	.074	.075	−.001	−.001	−.001
12	3	.038	.039	.039	.033	.032	.033
4	13	.046	.045	.046	.026	.028	.027
13	3	.041	.042	.042	.017	.016	.017
3	13	.046	.052	.049	.015	.014	.015
14	3	.019	.020	.020	.003	.002	.003
2	13	.025	.031	.028	.000	.002	.001

The strains were measured at the same points as the deflections. By using a triple strain gauge at the centre of the plate the strain ε_y in the direction perpendicular to the free edges

could be determined there. The strains in the vicinity of the corners were investigated by strain gauges of a shorter length.

Values of ε_x are given in Tabs. 333. 2 and 333. 3 for different test loadings. In some cases the smaller gauges at the corners of the plate yielded incomplete series of values. These are not included in the tables, though they are used in the graphical representation. The mean strains at every point are shown in diagrams, Figs. 333. 2 and 333. 3. The length $2L$ is drawn from the x_n-axis as described for the deflections.

Strains in the vicinity of concentrated loads vary rapidly with the distance from the load. The measuring length of the gauges therefore affects the results in such regions. A horizontal line below the curves for strains of loaded strips indicates this length.

The curves in Figs. 333. 2b and 333. 3b were obtained theoretically by a division into three strips.

The strains ε_y determined experimentally and theoretically at point 8 are given in Tab. 333. 3

Tab. 333. 3

Plate II carrying a transverse load $F = 100$ kp at points 8 and 3 (13). Experimental and theoretical values of the strains ε_y (0/00) at point 8, Fig. 333. 1

Load at	Test 1	Test 2	Mean	Theoretical value
8	.080	.085	.083	.088
3	−.017	−.015	−.016	−.010
13	−.019	−.018	−.019	

334. Plate III ($\Theta = 45.0°$)

In contrast to the plate treated in 333 plate III was relatively narrow. This appears from Fig. 334.1 and the following data:

$$l = 57.12 \text{ cm}$$

$$b = 19.49$$

$$h = .908$$

$$\Theta = 45.0°$$

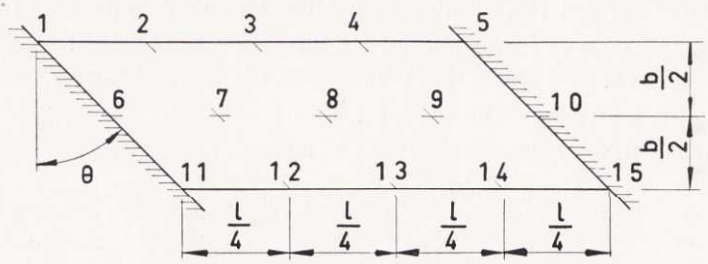

Fig. 334.1. Plate III, dimensions and measuring points.

The deformations were investigated for concentrated loads acting at the centre of the plate and at the centres of the free edges. The angle Θ being large, it was of particular interest to investigate the effect of forces near the corners. For this reason the effect of a force applied at point 4 was also treated.

The variation of the thickness h appeared to be of less importance for plate III than for plate II. The accuracy of the experimental results might therefore be increased by increasing the number of tests. The strain measurements were repeated three times for every position of the load. The experimental results, transformed to be valid for the load $F = 100$ kp, are given in Tabs. 334.1, 334.2 and 334.3. The real values of F varied between 450 and 550 kp.

The standard deviations of the means are computed in the same way as for plate II. They are represented graphically by vertical lines in Figs. 334.2, 334.3 and 334.4. The measuring length of the gauges is indicated in the diagrams of ε_x at the loaded points.

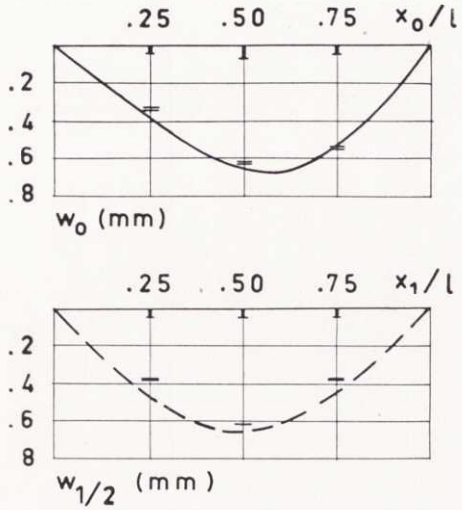

Fig. 334.2. Plate III, concentrated load $F = 100$ kp at the centre. Theoretical deflections for outside strip and centre line, together with experimental points, $l/t_0 = 6$. Confidence intervals 2 L for the means are indicated by vertical lines from the projections on the x-axis.

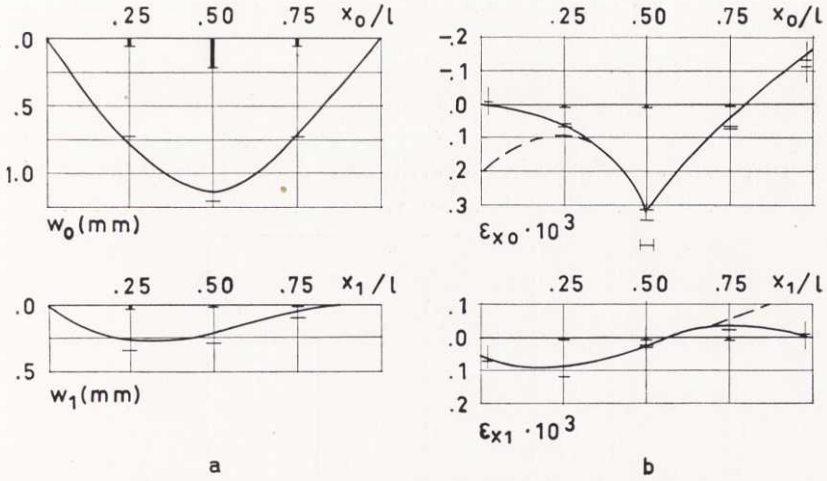

Fig. 334.3. Plate III, concentrated load $F = 100$ kp at the centre of the free edge of strip 0. Theoretical curves for strips 0 and 1 together with experimental points. Confidence intervals 2 L for the means are indicated by vertical lines from the projections on the x-axis.

a. Deflections w_r, $l/t_0 = 10$.

b. Strains ε_x, $l/t_0 = 10$.

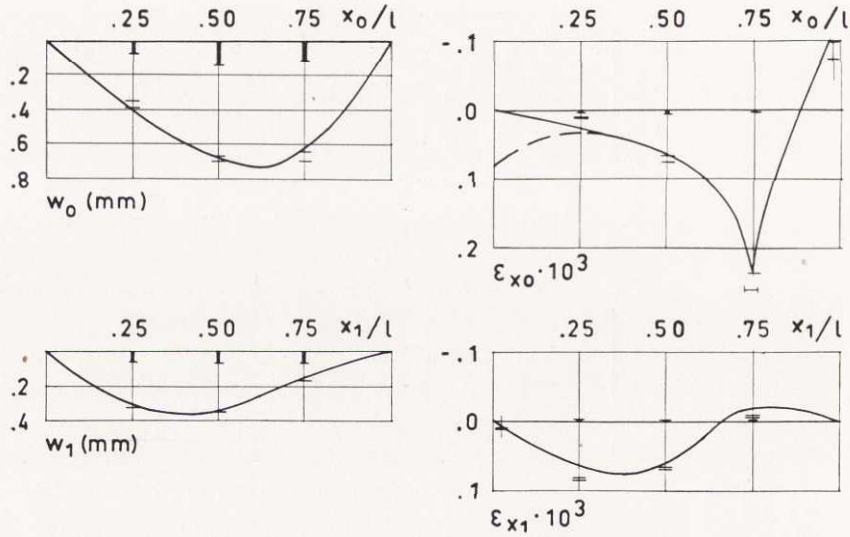

Fig. 334.4. Plate III, concentrated load $F = 100$ kp at $x_0 = 3\,l/4$, strip 0. Theoretical curves for strips 0 and 1 together with experimental points. Confidence intervals $2\,L$ for the means are indicated by vertical lines from the projections on the x-axis.

a. Deflections w_r, $l/t_0 = 10$.

b. Strains ε_x, $l/t_0 = 6$.

Tab. 334.1.

Plate III carrying a transverse load $F = 100$ kp at point 8, Fig. 334.2. Experimental values of deflections (mm).

Point	w		
	Test 1	Test 2	Mean
2	.32	.33	.33
14	.34	.34	.34
3	.61	.62	.62
13	.63	.63	.63
4	.52	.54	.53
12	.55	.55	.55
7	.37	.38	.38
9	.38	.38	.38
8	.61	.62	.62

The width of load t_0 used in theoretical computations of the strains was made $\geqq l/10$. This limit was chosen in order to avoid slowly converging series. In cases when the experimental value of t_0 was smaller then $l/10$ the experimental and theoretical strains describe slightly different loadings. However, this can only cause small deviations in the vicinity of the load.

The theoretical curves in Figs. 334.2, 334.3 and 334.4 have been determined for a division of the plate into two strips. The width ratio then becomes $l/t = 2.93$, smaller than the maximum value 4 proposed for practical computations. An accurate value of the central deflection of the plate is not obtained by using only two strips. However, the deflection $w_{1/2}$ along the centre line parallel with the free edges can be estimated by interpolation. Fig. 334.2 shows the deflections computed by substituting for a load F at the centre two forces $F/2$ acting on strips 0 and 1 at a line through the centre of the plate and perpendicular to the free edges. The deflection $w_{1/2}$ is obtained by taking the mean of w_0 and w_1 for the same values of x_n.

Tab. 334.2

Plate III carrying a transverse load $F = 100$ kp at point 3 (13) Fig. 334.3. Experimental values of deflections (mm) and strains (0/00).

Point	Load at	w			ε_x			
		Test 1	Test 2	Mean	Test 1	Test 2	Test 3	Mean
2	3	.72	.71	.72	.052	.057	.057	.055
14	13	.74	.75	.75	.068	.066	.067	.066
3	3	1.23	1.16	1.20	.293	.321	.327	.314
13	13	1.19	1.21	1 20	.342	.344	.345	.344
4	3	.73	.71	.72	.067	.072	.076	.072
12	13	.75	.75	.75	.062	.061	.061	.061
12	3	.36	.34	.35	1.08	1.20	1.22	1.51
4	13	.35	.34	.35	1.18	1.15	1.17	1.51
13	3	.29	.28	.29	.023	.027	.028	.026
3	13	.29	.29	.29	.019	.019	.021	.020
14	3	.11	.10	.11	−.025	−.027	−.028	−.027
2	13	.11	.11	.11	−.027	−.027	−.024	−.026

Tab. 334. 3

Plate III carrying a transverse load $F = 100$ kp at point 4 (12), Fig. 334. 4. Experimental values of deflections (mm) and strains (0/00).

Point	Load at	w			ε_x			
		Test 1	Test 2	Mean	Test 1	Test 2	Test 3	Mean
2	4	.34	.36	.35	.012	.012	.015	.013
14	12	.38	.39	.39	.009	.008	.009	.009
3	4	.64	.68	.66	.075	.072	.077	.075
13	12	.69	.71	.70	.067	.068	.067	.067
4	4	.62	.65	.64	.236	.235	.236	.236
12	12	.68	.70	.69	.237	.237	.238	.237
12	4	.31	.32	.32	.086	.085	.087	.086
4	12	.31	.31	.31	.080	.081	.081	.081
13	4	.33	.35	.34	.064	.065	.060	.065
3	12	.34	.35	.35	.068	.070	.069	.069
14	4	.16	.17	.17	−.009	−.009	−.007	−.008
2	12	.17	.16	.17	−.005	−.004	−.004	−.004

335. Plate IV

This model plate was an example of an extremely oblique plate. At the angle chosen the width b was bounded by the maximum supporting length obtainable in the frame used in the experiments. The dimensions, were

$$l = 79.58 \text{ cm}$$

$$b = 13.29 \text{ „}$$

$$h = .974 \text{ „}$$

$$\Theta = 59.4^\circ$$

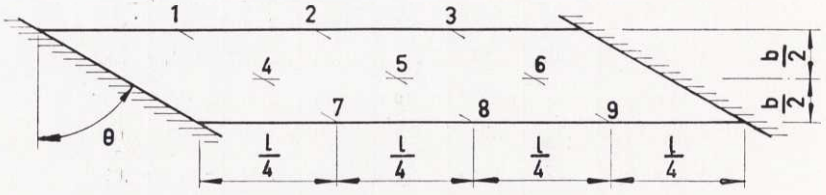

335. 1. Plate IV, dimensions and measuring points.

The flexural rigidity D is stated in Tab. 32.1.

Only deflections were investigated. The positions of the measuring points are shown in Fig. 335.1. The same loading arrangements were studied as those investigated for Plate III. Two tests were performed for every position of the load F. The observations, transformed to be valid for the load 100 kp, are shown in Tabs. 335.1, 335.2 and 335.3. During the experiments F varied between 260 kp and 320 kp. The irregularities of the plate in general had a significant influence upon the deflections.

The theoretical computations were performed by dividing the plate into two strips. The narrowness of the plate yielded a large width ratio ($l/t = 5.99$) even for this simple division. This implies that many terms ought to be included in the deflection series. Nevertheless, terms of higher order than three were neglected in order to find out if this simple method of computation could yield statisfactory results. For all loadings corrections were made to an infinite width ratio l/t_0.

The deflections are shown graphically in Figs. 335.2, 335.3 and 335.4. The experimental values are presented there as for plate III.

Tab. 335.1

Plate IV carrying a transverse load $F = 100$ kp at point 5, Fig. 335.1. Experimental values of deflections (mm).

Point	w		
	Test 1	Test 2	Mean
1	.61	.61	.61
9	.51	.50	.51
2	1.34	1.33	1.34
8	1.23	1.22	1.22
3	1.19	1.17	1.18
7	1.12	1.11	1.12
4	.77	.77	.77
6	.75	.74	.75
5	1.39	1.38	1.39

Tab. 335. 2

Plate IV carrying a transverse load $F = 100$ kp at point 2 (8), Fig. 335. 2. Experimental values of deflections w (mm).

Point	Load at	w		
		Test 1	Test 2	Mean
1	2	1.34	1.37	1.36
9	8	1.18	1.21	1.20
2	2	2.19	2.20	2.20
8	8	2.03	2.09	2.06
3	2	1.31	1.32	1.32
7	8	1.17	1.20	1.19
7	2	.91	.92	.92
3	8	.90	.92	.91
8	2	.49	.48	.49
2	8	.50	.50	.50
9	2	—. 08	— .08	— .08
1	8	—. 01	— .01	— .01

Tab. 335. 3

Plate IV carrying a transverse load $F = 100$ kp at point 3 (7), Fig. 335. 3. Experimental values of deflections w (mm).

Point	Load at	w		
		Test 1	Test 2	Mean
1	3	.59	.60	.60
9	7	.48	.48	.48
2	3	1.19	1.20	1.20
8	7	1.04	1.03	1.03
3	3	1.22	1.23	1.23
7	7	1.10	1.09	1.09
7	3	.76	.77	.77
3	7	.76	.75	.75
8	3	.89	.88	.89
2	7	.91	.89	.90
9	3	.30	.29	.29
1	7	.37	.36	.37

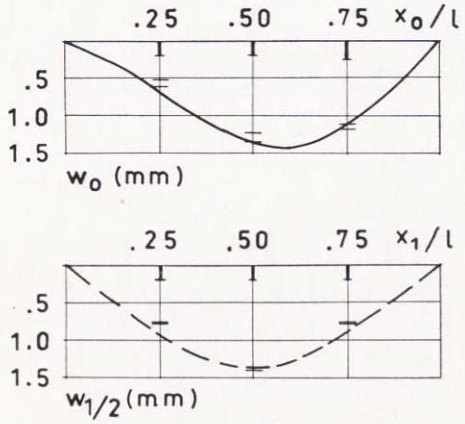

Fig. 335.2. Plate IV, concentrated load $F = 100$ kp at the centre. Theoretical deflections for outside strip and centre line, together with experimental points, $l >> t_0$. Confidence intervals $2L$ for the means are indicated by vertical lines from the projections on the x-axis.

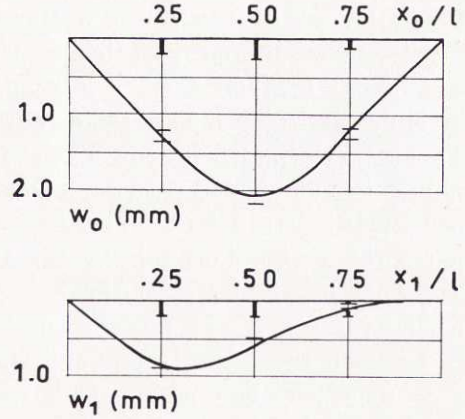

Fig. 335.3. Plate IV, concentrated load $F = 100$ kp at centre of a free edge, strip 0. Theoretical deflections for strips 0 and 1, together with experimental points, $l >> t_0$. Confidence intervals $2L$ for the means are indicated by vertical lines from the projections on the x-axis.

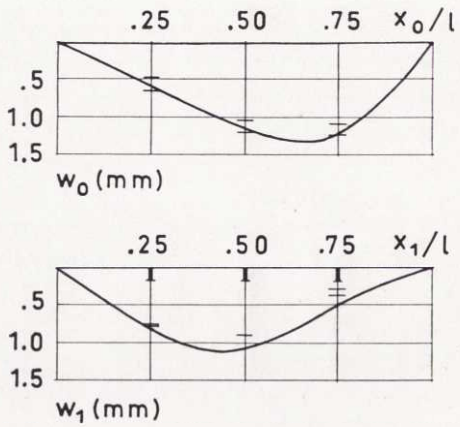

Fig. 335.4. Plate IV, concentrated load $F = 100$ kp at $x_0 = 3\,l/4$, strip 0. Theoretical deflections for strip 0 and 1, together with experimental points, $l \gg t_0$. Confidence intervals $2\,L$ for the means are indicated by vertical lines from the projections on the x-axis.

34. Discussion of the results

The agreement between theoretical and experimental values is in general good. The observations made upon the model plates do not indicate errors in the theoretical results larger than those estimated in Part 2. The upper bounds given there thus include the influence of the finite widths of the strips. The theoretical deflections differed from the corresponding experimental mean value, for a given case of loading, by less than 10 % of the maximum deflection. The same was true for the strains. In all cases investigated a correction for the width of load as proposed in 226 yielded better agreement with the observed data than did uncorrected w_r-functions.

The preliminar series expressions for the curvatures obtained according to 232 yield no strains ε_x at the supports. A correction introducing curvatures K_r at acute corners would cause large disparities between theoretically and experimentally determined strains. As expected, better agreement was obtained by omitting this correction. At obtuse corners large strains were observed in the vicinity of the supports. There, the introduction of finite curvatures in the theoretical expressions for the strains improved the agreement with experiments.

Relatively large deflections have been permitted in the experiments. In the case of plate IV, for instance, the ratio between w_{max} and h attained .75. This value would yield considerable strains in the middle plane of a plate simply supported along all edges. However, the middle surface of a plate on two flexible supports, can assume a conic form yielding large deflections without provoking membrane stresses. For general cases of loading and rigid supports the strains of the middle surface depend upon the difference between the real deflection and the deflection corresponding to some adjacent conic surface. This difference being small compared to the thickness h, the membrane stresses are negligible.

41. Summary

Deflections and moments are approximately determined for thin elastic plates resting on parallel supports. The deflections are assumed to be small compared with the thickness of the plate.

The method employed involves the use of finite differences. A plate is divided into a number of elements, strips $0..r..R$. Inside strips are assigned the width t, outside strips the width $t/2$. The strips are bounded by equidistant planes parallel to the free edges. The deflections, w_r, of the centre lines of the strips are introduced as unknown functions. The derivatives of these functions describe the slopes of the elastic surface in the directions parallel to the free edges. Slopes perpendicular to the free edges are determined from differences between the different deflections w_r.

A system of ordinary linear differential equations is obtained by forming the differential equation of plates, (211.6), for each strip. The deflections are expressed as sine series. Substitution into the differential equations yields linear equations for the series coefficients, w_{rn}. Approximate expressions for these coefficients are given in 222. They include load-dependent factors, the principal coefficients W_{rn}, which are the Fourier coefficients for the principal deflection W_r. W_r is the deflection of strip r considered as a beam of flexural rigidity D, (211.3), and carrying the load q_r. The computations are simplified by introducing new coefficients s_{rn} and a_{rn} according to (222.12), (222.23) or (52.17). Similarly W_{rn} is expressed by the principal coefficients S_{rn} and A_{rn}. General expressions for s_{rn} and a_{rn} are obtained from (222.14), (222.15), (222.24), (222.25), (52.21), (52.22) and diagrams in Appendix 56.

The approximate coefficients s_{rn} and a_{rn} are improved by adding corrections ΔS_{rn} and ΔA_{rn} to the principal coefficients. Values of ΔS_{rn} and ΔA_{rn} are given in Appendix 57. The corrections are valid for simply supported plates.

The series coefficients for the deflections are formed by adding or subtracting s_{rn} and a_{rn}. Deflections and moments are then easily obtained as trigonometric series and polynomials. Since these expressions are simple for uniformly distributed loads and for line loads of arbitrary position the method may conveniently be applied to the design of bridge slabs.

Errors originating from the use of finite differences are compensated for by using factors represented graphically in 226. These increments are obtained by considering a plate of infinite width. The real distribution of load, t_0, perpendicular to the free edges is taken into account.

The slopes of plates subjected to boundary moments can be determined by differentiating the deflections. This makes possible the treatment of continuous plates and frames.

Theoretical estimate of errors indicate that the method can yield sufficiently accurate results for most practical calculations. However, uncertain values are obtained in the vicinity of the corners.

Moments of loads distributed over small areas can not be described conveniently by sine series alone. They are expressed as the sum of the pincipal deflection and trigonometric series. The same method is used for expressing the effect of boundary moments.

Experimental values were determined for four model plates. Both deflections and strains were investigated. One of the model plates was rectangular. For this plate experimental results were compared with teoretical results according to the method described in part 2 and a method known previously. The three oblique plates were treated theoretically according to the former method only. The comparisons showed the expected agreement between experimental and theoretical results. Deflections and strains calculated for unloaded strips differed from the experimental values by less than 10 % of the maximum values for each arrangement of the load. For loaded strips in general no discrepancies were obtained, that is, the theoretical values were situated within the estimated experimental margins of error.

42. Sammanfattning

Elastiska plattors nedböjningar satisfierar en partiell differentialekvation av fjärde ordningen, då vissa allmänna villkor är uppfyllda. För plattor upplagda på parallella stöd är lösningen till denna ekvation ofta mycket komplicerad. Det är möjligt att relativt snabbt erhålla enkla uttryck på deformationerna genom att tillämpa en approximativ metod.

Metoden innebär, att en platta indelas i ett antal strimlor med ordningstalen $0,\ldots, r,\ldots, R$ och begränsade av plan vinkelräta mot plattans medelyta och parallella med de fria kanterna. Inre strimlor har bredden t medan yttre (utefter de fria kanterna belägna) strimlor har bredden $\frac{1}{2}t$. Strimlornas medellinjers nedböjningar, w_r, betraktas som obekanta funktioner. Den ovannämnda, partiella differentialekvationen tecknas för varje strimla, varvid lutningar vinkelrätt mot strimlornas medellinjer approximeras med hjälp av differenser mellan de olika w_r-funktionerna.

På så sätt erhålles ett antal lineära differentialekvationer av fjärde ordningen. I dessa insättes nedböjningarna i form av sinusserier med okända koefficienter, w_{rn}. Differentialekvationerna kan därmed överföras i lineära ekvationssystem, varur seriekoefficienterna löses. Uttrycken på w_{rn} innehåller de "primära koefficienterna" W_{rn} utgörande fourierkoefficienterna för de "primära nedböjningarna", d. v. s. de nedböjningar strimlorna skulle fått under den aktuella belastningen, om de varit fria från varandra och pr breddenhet haft böjstyvheten lika med "plattstyvheten" D.

Beräkningar och formler förenklas, om de primära koefficienterna på lämpligt sätt uppdelas i två komponenter, S_{rn} och A_{rn}, och nedböjningskoefficienterna betraktas som summan av eller skillnaden mellan vissa kvantiteter, s_{rn} och a_{rn}. Dessa kan approximativt uttryckas med enkla formler och, då kontraktionstalet $\nu = 0$, direkt avläsas i diagram. Som oberoende variabler

fungerar därvid vinkeln Θ mellan de fria kanterna och upplagslinjernas normal och kvoten mellan spännvidden l och produkten $n \cdot t$.

De approximativa värdena på nedböjningarnas seriekoefficienter förbättras genom att de primära koefficienterna S_{rn} och A_{rn} ökas med tillskott ΔS_{rn} och ΔA_{rn}, som beror av s_{rn} och a_{rn} och som är beräknade för fritt upplagda plattor.

För praktiska beräkningar erforderliga formler och diagram återfinnes i Bihang 222, 52, 55, 56, 57.

Seriekoefficienterna för strimlornas nedböjningar erhålles som summan eller skillnaden mellan s_{rn} och a_{rn}. Nedböjningar och moment kan därefter tecknas som trigonometriska serier, i vissa fall kombinerade med polynom. Dessa uttryck blir enkla såväl för jämnt fördelade belastningar som för linjelaster med godtycklig placering, varför metoden lämpar sig för beräkning av brobaneplattor.

De fel, som beror på att lutningar vinkelrätt mot de fria kanterna ersatts med differenskvoter, uppskattas genom att jämföra den här introducerade metodens resultat för oändligt breda plattor med exakta värden för samma plattdimension. Denna jämförelse resulterar i diagram, varmed approximativt erhållna nedböjningar och moment för en belastad strimla kan korrigeras vid en viss lastbredd t_0, mätt vinkelrätt mot plattans kanter.

Kontinuerliga plattor behandlas genom att till den fritt upplagda plattans nedböjningar lägga funktioner, som ger från 0 skilda böjmoment på vertikala snitt genom upplagslinjerna, och som möjliggör ett uppfyllande av lutningarnas kontinuitetsvillkor.

Moment av såväl punktlaster som randmoment kan ej med tillräcklig noggrannhet beskrivas med ett fåtal trigonometriska funktioner. Praktiskt användbara värden erhålles emellertid, om serieutvecklingen för strimlornas primära nedböjningar drages från den totala nedböjningens serieutveckling och ersättes med det exakta uttrycket på samma primära nedböjning.

Det är möjligt att finna övre gränser för fel uppkomna genom att endast ett ändligt antal termer medtages i serierna för nedböjningarna. En undersökning av storleken hos dessa fel och fel uppkomna genom bruk av differenskvoter visar, att i allmänhet tillräckligt noggranna resultat uppnås, om förhållandet

l/t väljes mellan 2 och 4 och endast de tre första termerna medtages i nedböjningarnas serieutvecklingar. Då $\Theta > 45°$ måste emellertid ofta l/t ökas och flera termer medräknas. Momenten i närheten av en plattas hörn är svåra att bestämma med mera än överslagsmässig noggrannhet.

Ovan beskrivna metod tillämpades på fyra stålplattor. En av dessa plattor var rektangulär, varför de experimentella värdena på nedböjningar och töjningar kunde jämföras med teoretiska värden beräknade enligt tidigare kända metoder. De tre övriga plattorna var sneda med vinkeln Θ varierande mellan 30° och 60°. Uppmätta värden för olika placering av koncentrerade krafter jämfördes med värden erhållna ur ekvationerna i del 2. För obelastade strimlor iakttagna skillnader understeg samtliga 10 % av maximala värdet vid varje lastställning. För belastade strimlor låg alla avvikelser inom de uppskattade, experimentella felgränserna.

5. Appendix

51. The differential equations for w_0 and w_1

The differential equation for the deflection w_0 of strip 0 is derived in 212:

$$\left[(1-\nu^2)\,t^4\frac{d^4}{d\,x_0^4}-4\,(1-\nu)\,t^2\frac{d^2}{d\,x_0^2}+2\right]w_0+$$

$$+\left[(4-2\,\nu)\,t^2\frac{d^2}{d\,x_0^2}-4\right]w_1+2\,w_2=q_0\,t^4/D \qquad (212.9)$$

This equation is valid for plates divided into more than two strips. If there are only two strips, w_2 describes deflections outside the plate. The function w_2 is determined from the boundary condition $M_y=0$ at $y=t$, Fig. 212.3. Application of (212.8) yields:

$$\frac{1}{t^2}(w_2-2\,w_1+w_0)+\nu\frac{d^2\,w_1}{d\,x_1^2}=0 \qquad (1)$$

On solving this equation for w_2 and substituting in (212.9) the following equation emerges:

$$\left[(1-\nu^2)t^4\frac{d^4}{d\,x_0^4}-4\,(1-\nu)\,t^2\frac{d^2}{d\,x_0^2}\right]w_0+$$

$$+4\,(1-\nu)\,t^2\frac{d^2\,w_1}{d\,x_0^2}=\frac{q_0\,t^4}{D} \qquad (212.12)$$

This equation contains only derivatives of even order. It can be transferred into the differential equation for w_1 by changing subscripts.

The central deflection w_1 of a plate divided into three strips is determined by (212.6) with $r = 1$:

$$w_{-1} + w_3 + \left(2\, t^2 \frac{d^2}{d x_1^2} - 4\right)(w_0 + w_2) +$$

$$+ \left(t^4 \frac{d^4}{d x_1^4} - 4\, t^2 \frac{d^2}{d x_1^2} + 6\right) w_1 = \frac{q_1 t^4}{D} \qquad (2)$$

The deflections w_{-1} and w_3 emerging in this equation can be determined from boundary conditions for M_y. After changing subscripts eq. (1) gives:

$$w_{-1} = -\left(\nu\, t^2 \frac{d^2}{d x_0^2} - 2\right) w_0 - w_1$$

$$w_3 = -w_1 - \left(\nu\, t^2 \frac{d^2}{d x_2^2} - 2\right) w_2$$

Inserting these expressions for w_{-1} and w_3 in (2) the equation for w_1 is obtained in the form

$$\left[(2 - \nu)\, t^2 \frac{d^2}{d x_1^2} - 2\right](w_0 + w_2) +$$

$$+ \left[t^4 \frac{d^4}{d x_1^4} - 4\, t^2 \frac{d^2}{d x_1^2} + 4\right] w_1 = \frac{q_1 t^4}{D}$$

52. The coefficients s_{rn} and a_{rn} for plates divided into three and five strips

The equations for the series coefficients w_{rn} are derived by writing the deflections w_r as trigonometric series

$$\left.\begin{aligned} w_0 &= \Sigma\, w_{0n} \sin (n \pi x_0/l) \\ w_1 &= \Sigma\, w_{1n} \cos n\mu \sin (n \pi x_0/l) - \Sigma\, w_{1n} \sin n\mu \cos (n \pi x_0/l) \\ w_2 &= \Sigma\, w_{2n} \cos 2n\mu \sin (n \pi x_0/l) - \Sigma\, w_{2n} \sin 2n\mu \cos (n \pi x_0/l) \end{aligned}\right\} \qquad (1)$$

These expressions are inserted in the first equation of the system (212.13). Introduction of the abbreviations defined by (222.18), (222.19), (222.20), (222.21) then gives

$$\sum \frac{n^4 \pi^4 t^4}{l^4} \left(\alpha_{1n} w_{0n} - 2 \beta_{1n} w_{1n} + 2 \gamma_n w_{2n} - \frac{q_{0n} t^4}{D} \right) \sin \frac{n \pi x_0}{l} =$$

$$= - \sum \frac{m^4 \pi^4 t^4}{l^4} (2 \beta_{1m} w_{1m} - 4 \gamma_m \cos m \mu w_{2m}) \operatorname{tg} m \mu \cos \frac{m \pi x_0}{l} \quad (2)$$

If w_0, w_1, w_2 are written as functions of x_1,

$$\left.\begin{aligned} w_0 &= \Sigma w_{0n} \cos n \mu \sin (n \pi x_1/l) + \Sigma w_{0n} \sin n \mu \cos (n \pi x_1/l) \\ w_1 &= \Sigma w_{1n} \sin (n \pi x_1/l) \\ w_2 &= \Sigma w_{2n} \cos n \mu \sin (n \pi x_1/l) - \Sigma w_{2n} \sin n \mu \cos (n \pi x_1/l) \end{aligned}\right\} \quad (3)$$

and substituted in the second equation of (212.13), another equation for the coefficients w_{rn} is obtained:

$$\sum \frac{n^4 \pi^4 t^4}{l^4} \left(- \beta_{1n} w_{0n} + \alpha_{2n} w_{1n} - \beta_{1n} w_{2n} - \frac{q_{1n} t^4}{D} \right) \sin \frac{n \pi x_1}{l} =$$

$$= \sum \frac{m^4 \pi^4 t^4}{l^4} \beta_{1m} (w_{0m} - w_{2m}) \operatorname{tg} m \mu \cos \frac{m \pi x_1}{l} \quad (4)$$

A third equation is obtained by interchanging the subscripts 0 and 2 and altering the sign before the cosine series in (2):

$$\sum \frac{n^4 \pi^4 t^4}{l^4} \left(2 \gamma_n w_{0n} - 2 \beta_{1n} w_{1n} + \alpha_{1n} w_{2n} - \frac{q_{2n} t^4}{D} \right) \sin \frac{n \pi x_2}{l} =$$

$$= \sum \frac{m^4 \pi^4 t^4}{l^4} (2 \beta_{1m} w_{1m} - 4 \gamma_m \cos m \mu w_{0m}) \operatorname{tg} m \mu \cos \frac{m \pi x_2}{l} \quad (5)$$

Linear equations for determining the unknown coefficients w_{rn} are formed by multiplying (2), (4) and (5) by $\sin (n \pi x_r/l)$ and integrating between the supports of strip r. After dividing by $n^4 \pi^4 t^4/l^4$, the equations become

$$
\left.
\begin{aligned}
&\alpha_{1n}\, w_{0n} - 2\,\beta_{1n}\, w_{1n} + 2\,\gamma_n\, w_{2n} = \\
&= W_{0n} + \frac{8}{\pi} \sum_{m \neq n} \frac{m^4 \operatorname{tg} m\,\mu}{n^3\,(m^2 - n^2)}\,(\beta_{1m}\, w_{1m} - \\
&- 2\,\gamma_m \cos m\,\mu\, w_{2m}) \sin^2 \frac{\pi}{2}(m+n), \\
&- \beta_{1n}\,(w_{0n} + w_{2n}) + \alpha_{2n}\, w_{1n} = \\
&= W_{1n} - \frac{4}{\pi} \sum_{m \neq n} \frac{m^4 \operatorname{tg} m\,\mu}{n^3\,(m^2 - n^2)}\,\beta_{1m}\,(w_{0m} - \\
&- w_{2m}) \sin^2 \frac{\pi}{2}(m+n), \\
&2\,\gamma_n\, w_{0n} - 2\,\beta_{1n}\, w_{1n} + \alpha_{1n}\, w_{2n} = \\
&= W_{2n} - \frac{8}{\pi} \sum_{m \neq 0} \frac{m^4 \operatorname{tg} m\,\mu}{n^3\,(m^2 - n^2)}\,(\beta_{1m}\, w_{1m} - \\
&- 2\,\gamma_m \cos m\,\mu\, w_{0m}) \sin^2 \frac{\pi}{2}(m+n)
\end{aligned}
\right\} \qquad (6)
$$

This system is modified by forming the sum and difference of the first and the last equations. Introduction of knowns and unknowns expressed by (222.22) and (222.23) yields:

$$
\left.
\begin{aligned}
(\alpha_{1n} + 2\,\gamma_n)\, s_{0n} - 2\,\beta_{1n}\, s_{1n} &= S_{0n} + \Delta\, S_{0n}^{*} \\
-2\,\beta_{1n}\, s_{0n} + \alpha_{2n}\, s_{1n} &= S_{1n} + \Delta\, S_{1n}^{*} \\
(\alpha_{1n} - 2\,\gamma_n)\, a_{0n} &= A_{0n} + \Delta\, A_{0n}^{*}
\end{aligned}
\right\} \qquad (7)
$$

The corrections $\Delta\, S_{rn}^{*}$ and $\Delta\, A_{rn}^{*}$ formed by the series on the right hand side of (6) are given in (227.3).

By solving (6) the coefficients s_{rn} and a_{rn} may be obtained as functions of the principal coefficients and their corrections. If the latter are neglected, (222.24) and (222.25) give the solution.

Applying the equations derived in 212, the following system is obtained for a plate divided into five strips, Fig. 52.1:

$$
\left.
\begin{aligned}
&\left[(1-\nu^2)\,t^4\frac{d^4}{dx_0^4}-4\,(1-\nu)\,t^2\frac{d^2}{dx_0^2}+2\right]w_0+\\
&+\left[(4-2\nu)\,t^2\frac{d^2}{dx_0^2}-4\right]w_1+2\,w_2=\frac{q_0\,t^4}{D}\\
&\left[(2-\nu)\,t^2\frac{d^2}{dx_1^2}-2\right]w_0+\left(t^4\frac{d^4}{dx_0^4}-4\,t^2\frac{d^2}{dx_1^2}+5\right)w_1+\\
&+\left(2\,t^2\frac{d^2}{dx_1^2}-4\right)w_2+w_3=\frac{q_1\,t^4}{D}\\
&w_0+\left(2\,t^2\frac{d^2}{dx_2^2}-4\right)w_1+\left(t^4\frac{d^4}{dx_2^4}-4\,t^2\frac{d^2}{dx_2^2}+6\right)w_2+\\
&+\left(2\,t^2\frac{d^2}{dx_2^2}-4\right)w_3+w_4=\frac{q_2\,t^4}{D}\\
&w_1+\left(2\,t^2\frac{d^2}{dx_3^2}-4\right)w_2+\left(t^4\frac{d^4}{dx_3^4}-4\,t^2\frac{d^2}{dx_3^2}+5\right)w_3+\\
&+\left[(2-\nu)\,t^2\frac{d^2}{dx_3^2}-2\right]w_4=\frac{q_3\,t^4}{D}\\
&2\,w_2+\left[(4-2\nu)\,t^2\frac{d^2}{dx_4^2}-4\right]w_3+\\
&+\left[(1-\nu^2)\,t^4\frac{d^4}{dx_4^4}-4\,(1-\nu)\,t^2\frac{d^2}{dx_4^2}+2\right]w_4=\frac{q_4\,t^4}{D}
\end{aligned}
\right\}\qquad(8)
$$

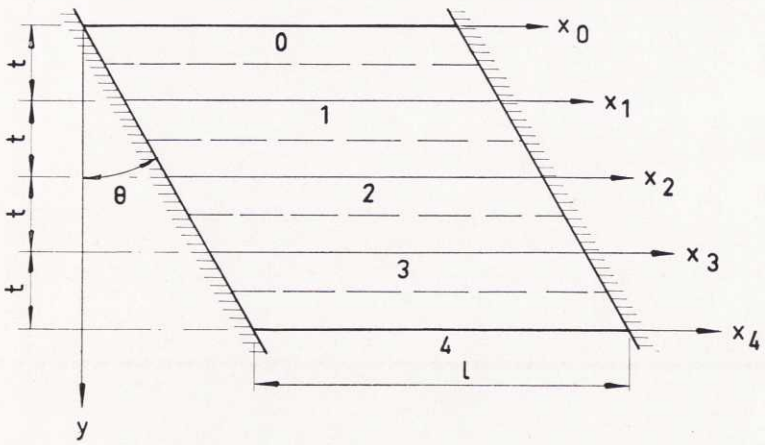

Fig. 52. 1.

The w_r functions are written as sine series. Substitution of these expressions in (8) and introduction of the abbreviations (222.18), (222.20), (222.21), (224.7) and

$$\alpha_{3n} = 1 + 4\,l^2/n^2\,\pi^2\,t^2 + 5\,l^4/n^4\,\pi^4\,t^4 \tag{9}$$

$$\beta_{2n} = (2\,l^2/n^2\,\pi^2\,t^2 + 4\,l^4/n^4\,\pi^4\,t^4)\,\cos\,n\,\mu \tag{10}$$

results in equations

$$\left.\begin{aligned}
&\sum \frac{n^4\,\pi^4\,t^4}{l^4}(\alpha_{1n}\,w_{0n} - 2\,\beta_{1n}\,w_{1n} + 2\,\gamma_n\,w_{2n} - W_{0n})\,\sin\frac{n\,\pi\,x_0}{l} = \\
&= -\sum \frac{m^4\,\pi^4\,t^4}{l^4}(2\,\beta_{1m}\,w_{1m} - 4\,\gamma_m\cos m\,\mu\,w_{2m})\,\mathrm{tg}\,m\,\mu\,\cos\frac{m\,\pi\,x_0}{l}, \\
&\sum \frac{n^4\,\pi^4\,t^4}{l^4}(-\beta_{1n}\,w_{0n} + \alpha_{3n}\,w_{1n} - \beta_{2n}\,w_{2n} + \gamma_n\,w_{3n} - W_{1n})\sin\frac{n\,\pi\,x_1}{l} = \\
&= \sum \frac{m^4\,\pi^4\,t^4}{l^4}(\beta_{1m}\,w_{0m} - \beta_{2m}\,w_{2m} + \\
&+ 2\,\gamma_m\cos m\,\mu\,w_{3m})\,\mathrm{tg}\,m\,\mu\,\cos\frac{m\,\pi\,x_1}{l}, \\
&\sum \frac{n^4\,\pi^4\,t^4}{l^4}[\gamma_n\,(w_{0n} + w_{4n}) - \beta_{2n}\,(w_{1n} + w_{3n}) + \alpha_{1n}\,w_{3n} - \\
&- W_{2n}]\,\sin\frac{n\,\pi\,x_2}{l} = -\sum \frac{m^4\,\pi^4\,t^4}{l^4}[2\,\gamma_m\cos m\,\mu\,(w_{0m} - w_{4m}) - \\
&- \beta_{2m}\,(w_{1m} - w_{3m})]\,\mathrm{tg}\,m\,\mu\,\cos\frac{m\,\pi\,x_2}{l}, \\
&\sum \frac{n^4\,\pi^4\,t^4}{l^4}(\gamma_n\,w_{1n} - \beta_{2n}\,w_{2n} + \alpha_{3n}\,w_{3n} - \beta_{1n}\,w_{4n} - \\
&- W_{3n})\,\sin\frac{n\,\pi\,x_3}{l} = -\sum \frac{m^4\,\pi^4\,t^4}{l^4}(2\,\gamma_m\cos m\,\mu\,w_{1m} - \beta_{2m}\,w_{2m} + \\
&+ \beta_{1m}\,w_{4m})\,\mathrm{tg}\,m\,\mu\,\cos\frac{m\,\pi\,x_3}{l}, \\
&\sum \frac{n^4\,\pi^4\,t^4}{l^4}(2\,\gamma_n\,w_{2n} - 2\,\beta_{1n}\,w_{3n} + \alpha_{1n}\,w_{4n} - W_{4n})\,\sin\frac{n\,\pi\,x_4}{l} = \\
&= -\sum \frac{m^4\,\pi^4\,t^4}{l^4}(4\,\gamma_m\cos m\,\mu\,w_{2m} - 2\,\beta_{1m}\,w_{3m})\,\mathrm{tg}\,m\,\mu\,\cos\frac{m\,\pi\,x_4}{l}
\end{aligned}\right\} \tag{11}$$

These equations are multiplied by $\sin(n\pi x_r/l)$, integrated over the spans of strips r, and divided by $n^4\pi^4 t^4/l^4$. The result is

$$\alpha_{1n} w_{0n} - 2\beta_{1n} w_{1n} + 2\gamma_n w_{2n} = W_{0n} +$$

$$+\frac{8}{\pi}\sum_{m\neq n}\frac{m^4 \operatorname{tg} m\mu}{n^3(m^2-n^2)}(\beta_{1m} w_{1m} - 2\gamma_m \cos m\mu\, w_{2m}) \sin^2\frac{\pi}{2}(m+n) \quad (12)$$

$$-\beta_{1n} w_{0n} + \alpha_{3n} w_{1n} - \beta_{2n} w_{2n} + \gamma_n = W_{1n} -$$

$$-\frac{4}{\pi}\sum_{m\neq n}\frac{m^4 \operatorname{tg} m\mu}{n^3(m^2-n^2)}(\beta_{1m} w_{0m} - \beta_{2m} w_{2m} +$$

$$+ 2\gamma_m \cos m\mu\, w_{3m}) \sin^2\frac{\pi}{2}(m+n) \quad (13)$$

$$\gamma_n(w_{0n} + w_{4n}) - \beta_{2n}(w_{1n} + w_{3n}) + \alpha_{4n} w_{2n} = W_{2n} +$$

$$+\frac{4}{\pi}\sum_{m\neq n}\frac{m^4 \operatorname{tg} m\mu}{n^3(m^2-n^2)}[2\gamma_m \cos m\mu(w_{0m} - w_{4m}) - \beta_{2m}(w_{1m} -$$

$$- w_{3m})] \sin^2\frac{\pi}{2}(m+n) \quad (14)$$

$$\gamma_n w_{1n} - \beta_{2n} w_{2n} + \alpha_{3n} w_{3n} - \beta_{1n} w_{4n} = W_{3n} +$$

$$+\frac{4}{\pi}\sum_{m\neq n}\frac{m^4 \operatorname{tg} m\mu}{n^3(m^2-n^2)}(2\gamma_n \cos m\mu\, w_{1m} - \beta_{2m} w_{2m} +$$

$$+\beta_{1m} w_{4m}) \sin^2\frac{\pi}{2}(m+n) \quad (15)$$

$$2\gamma_n w_{2n} - 2\beta_{1n} w_{3n} + \alpha_{1n} w_{4n} = W_{4n} +$$

$$+\frac{8}{\pi}\sum\frac{m^4 \operatorname{tg} m\mu}{n^3(m^2-n^2)}(2\gamma_m \cos m\mu\, w_{2m} - \beta_{1m} w_{3m}) \sin^2\frac{\pi}{2}(m+n) \quad (16)$$

The coefficients W_{rn} are replaced by S_{rn}, A_{rn}, and w_{rn} by s_{rn}, a_{rn}:

$$\left.\begin{aligned} s_{0n} &= \frac{1}{2}(w_{4n} + w_{0n}) & a_{0n} &= \frac{1}{2}(w_{4n} - w_{0n}) \\ s_{1n} &= \frac{1}{2}(w_{3n} + w_{1n}) & a_{1n} &= \frac{1}{2}(w_{3n} - w_{1n}) \\ s_{2n} &= w_{2n} \end{aligned}\right\} \tag{17}$$

$$\left.\begin{aligned} S_{0n} &= \frac{1}{2}(W_{4n} + W_{0n}) & A_{0n} &= \frac{1}{2}(W_{4n} - W_{0n}) \\ S_{1n} &= \frac{1}{2}(W_{3n} + W_{1n}) & A_{1n} &= \frac{1}{2}(W_{3n} - W_{1n}) \\ S_{2n} &= W_{2n} \end{aligned}\right\} \tag{18}$$

Furthermore (12) is added to (16) and (13) to (15). These sums, together with (14), form a system of three equations:

$$\left.\begin{aligned} \alpha_{1n}\, s_{0n} - 2\,\beta_{1n}\, s_{1n} + 2\,\gamma_n\, s_{2n} &= S_{0n} + \Delta\, S_{0n}^{*} \\ -\beta_{1n}\, s_{0n} + (\alpha_{3n} + \gamma_n)\, s_{1n} - \beta_{2n}\, s_{2n} &= S_{1n} + \Delta\, S_{1n}^{*} \\ 2\,\gamma_n\, s_{0n} - 2\,\beta_{2n}\, s_{1n} + \alpha_{4n}\, s_{2n} &= S_{2n} + \Delta\, S_{2n}^{*} \end{aligned}\right\} \tag{19}$$

Subtracting (12) from (16), and (13) from (15), another system of equations emerges:

$$\left.\begin{aligned} \alpha_{1n}\, a_{0n} - 2\,\beta_{1n}\, a_{1n} &= A_{0n} + \Delta\, A_{0n}^{*} \\ -\beta_{1n}\, a_{0n} + (\alpha_{3n} - \gamma_n)\, a_{1n} &= A_{1n} + \Delta\, A_{1n}^{*} \end{aligned}\right\} \tag{20}$$

The corrections $\Delta\, S_{rn}^{*}$ and $\Delta\, A_{rn}^{*}$ are defined by (227.6).

Neglecting the corrections $\Delta\, S_{rn}^{*}$, the solution of (19) becomes:

$$\left.\begin{aligned} s_{0n} &= \frac{1}{N_s}\{[\alpha_{4n}(\alpha_{3n} + \gamma_n) - 2\,\beta_{2n}^{2}]\, S_{0n} + 2(\alpha_{4n}\,\beta_{1n} - 2\,\gamma_n\,\beta_{2n})\, S_{1n} + \\ &+ [2\,\beta_{1n}\,\beta_{2n} - 2\,\gamma_n(\alpha_{3n} + \gamma_n)]\, S_{2n}\}, \\ s_{1n} &= \frac{1}{N_s}\{(\alpha_{4n}\,\beta_{1n} - 2\,\gamma_n\,\beta_{2n})\, S_{0n} + (\alpha_{1n}\,\alpha_{4n} - 4\,\gamma_n^{2})\, S_{1n} + \\ &+ (\alpha_{1n}\,\beta_{2n} - 2\,\gamma_n\,\beta_{1n})\, S_{2n}\}, \\ s_{2n} &= \frac{1}{N_s}\{[2\,\beta_{1n}\,\beta_{2n} - 2\,\gamma_n(\alpha_{3n} + \gamma_n)]\, S_{0n} + (2\,\alpha_{1n}\,\beta_{2n} - \\ &- 4\,\gamma_n\,\beta_{1n})\, S_{1n} + [\alpha_{1n}(\alpha_{3n} + \gamma_n) - 2\,\beta_{1n}^{2}]\, S_{2n}\} \end{aligned}\right\} \tag{21}$$

where

$$N_s = \begin{vmatrix} \alpha_{1n} & -2\beta_{1n} & 2\gamma_n \\ -\beta_{1n} & \alpha_{3n}+\gamma_n & -\beta_{2n} \\ 2\gamma_n & -2\beta_{2n} & \alpha_{4n} \end{vmatrix}$$

If the corrections ΔA_{rn}^* are neglected the solution of (20) becomes:

$$\left.\begin{aligned} a_{0n} &= \frac{1}{N_a}\left[(\alpha_{3n}-\gamma_n)A_{0n}+2\beta_{1n}A_{1n}\right] \\ a_{1n} &= \frac{1}{N_a}\left[\beta_{1n}A_{0n}+\alpha_{1n}A_{1n}\right] \end{aligned}\right\} \qquad (22)$$

where

$$N_a = \alpha_{1n}(\alpha_{3n}-\gamma_n)-2\beta_{1n}^2$$

53. Errors due to neglected terms in the series for ΔW_{rn}

531. Estimation of errors due to neglected terms in the series for ΔW_{rn}^*

After the introduction of the corrections ΔW_{rn}^* the principal coefficients are no longer independent of the coefficients w_{rn}. The equations derived in 224 therefore determine only some of the errors arising from the neglect of higher order terms. The corrections ΔW_{rn}^* may be rather large, which means that a large number of terms in the series must be chosen.

In practical cases concentrated loads give the largest errors—according to 224. The principal coefficients can then be bounded by

$$|W_{rn}| \leq \frac{1}{m^4}|m^4 W_{rm}|_{max}$$

This bound is approximately valid for the corresponding coefficients w_{rn} also:

$$|w_{rn}| \leq \frac{1}{m^4}|m^4 W_{rm}|_{max}$$

The expressions in 227 for the corrections ΔW_{rn}^* do not exceed the sum

$$\Sigma (d_{mn} + f_{mn}) \mid w_{rm} \mid_{max} \geqq \mid \Delta W_{rn}^* \mid$$

where cos $m\mu$ and sin $m\mu$, included as factors in d_{mn} and f_{mn}, are put equal to one. Applying (227. 5), (227. 7), and (1), this inequality can be written ($m = n$):

$$\mid \Delta W_{rn}^* \mid \leq \frac{16\, l^2}{\pi^3\, n^3\, t^2} \mid m^4\, W_{rm} \mid_{max} \sum_{m \neq n} \left(1 + \frac{3\, l^2}{m^2\, \pi^2\, t^2}\right) \frac{\sin^2 \frac{\pi}{2} (m+n)}{m^2\,(m^2 - n^2)} \quad (2)$$

If only the first N series terms are taken into account, the following quantity is neglected:

$$\Delta \mid \Delta W_{rn}^* \mid <$$

$$< \frac{16\, l^2}{\pi^3\, n^3\, t^2} \left[1 + \frac{3\, l^2}{(N+2)^2 \pi^2 t^2}\right] \mid m^4\, W_{rm} \mid_{max} \sum_{\substack{N+2 \\ m \neq n}}^{\infty} \left| \frac{\sin^2 \frac{\pi}{2} (m+n)}{m^2\,(m^2 - n^2)} \right| \quad (3)$$

If $n \leqq N + 1$, the sum in (3) is bounded above as follows:

$$\sum_{\substack{N+2 \\ m \neq n}}^{\infty} \left| \frac{\sin^2 \frac{\pi}{2} (m+n)}{m^2\,(m^2 - n^2)} \right| < \frac{1}{2} \int_{N+1}^{\infty} \frac{d\, m}{m^4 \left[1 - \left(\frac{n}{N+2}\right)^2\right]} =$$

$$= \frac{1}{6\,(N+1)^3 \left[1 - \left(\frac{n}{N+2}\right)^2\right]}$$

Substitution of this upper limit in (3) yields:

$$\Delta \mid \Delta W_{rn}^* \mid < \frac{8 l^2 \left[(N+2)^2 + \frac{3\, l^2}{\pi^2\, t^2}\right]}{3\, \pi^3\, n^3\, t^2\, (N+1)^3\, [(N+2)^2 - n^2]} \mid m^4\, W_{rm} \mid_{max} \quad (4)$$

These maximum errors differ for different n. The coefficients ΔW_{rn}^* are multiplied by the factor $n^2 \pi^2 / l^2$ in the ex-

pressions (213. 5) for the moments M_x. The maximum errors given in (4) are therefore first multiplied by n^2 before comparison. If the largest of the increment $n^2 \Delta |\Delta W_{rn}^*|$ is that with $n=1$, the first term in the series for the moments includes the largest error. This is then true a fortiori for the first term in the series for the deflections. Multiplication of (4) by n^2 yields:

$$n^2 \Delta |\Delta W_{rn}^*| < \frac{8 l^2 \left[(N+2)^2 + \frac{3 l^2}{\pi^2 t^2} \right]}{3 \pi^3 t^2 n (N+1)^3 [(N+2)^2 - n^2]} |m^4 W_{rm}|_{max}$$

The second derivative with respect to n of this expression is positive for $n \geqq 1$. Hence maximum values can occur only for $n=1$ or $n = n_{max} = N+1$. The absolute maximum is obtained for $n=1$:

$$\Delta |\Delta W_{rn}^*| < \frac{8 l^2 \left[(N+2)^2 + \frac{3 l^2}{\pi^2 t^2} \right]}{3 \pi^3 t^2 (N+1)^4 (N+3)} |m^4 W_{rm}|_{max} \qquad (5)$$

Eq. (5) shows that the errors increase rapidly with rising l/t. For $N=2$ and the largest l/t appearing in the diagrams in Appendix 56, $l/t = 4$, the maximum error becomes

$$\Delta |\Delta W_{rn}^*| < .072 |m^4 W_{rm}|_{max} \qquad (6)$$

Eq. (5) or (6) can be used in estimating the maximum errors at any stage of the determination of w_{rn}. These equations are useful only when the corrections ΔW_{rn}^* decrease by a factor of at least $1/n^4$.

In order to investigate the convergence of the correction terms ΔW_{rn}^*, an upper bound is derived for the general term. According to (2)

$$|\Delta W_{rn}^*| \leqq \frac{B}{n^3} \sum_{\substack{1 \\ m \neq n}}^{\infty} \frac{\sin^2 \frac{\pi}{2} (m+n)}{m^2 (m^2 - n^2)}$$

B is a constant, independent of n.

For uneven numbers, $n > 1$, only even numbers m will occur. The terms with order numbers $m = n-1$ and $m = n+1$ are

treated separately. The rest of the sum is approximated by two integrals:

$$|\Delta W_{rn}^{*}| < \frac{B}{n^3}\left[-\frac{1}{2}\int_{1}^{n-2}\frac{dm}{m^2(m^2-n^2)}+\frac{1}{(n-1)^2(2n-1)}+\right.$$

$$\left.+\frac{1}{(n+1)^2(2n+1)}+\frac{1}{2}\int_{n+2}^{\infty}\frac{dm}{m^2(m^2-n^2)}\right]<$$

$$<\frac{B}{n^3}\left[\frac{4}{n^3}-\frac{1}{2n^2}\int_{2}^{n-2}\left(\frac{1}{m}+\frac{1}{2n}\ln\frac{n-m}{n+m}\right)+\frac{1}{2n^2}\int_{n+2}^{\infty}\left(\frac{1}{m}+\frac{1}{2n}\ln\frac{m-n}{m+n}\right)\right]<$$

$$<\frac{B}{n^4}\left(\frac{C_1}{n^2}+\frac{C_2}{n}+\frac{C_3\ln n}{n^2}\right)<\frac{C_4}{n^4}$$

Where C_i are constants. A similar result is obtained for even n greater than 2, i.e. for odd m.

The corrections of the principal deflections thus decrease more rapidly with n than their coefficients W_{rn}. The condition for the validity of (5) or (6) is therefore satisfied.

532. Estimation of errors in the supplementary coefficients ΔW_{rn}^{**}

In practice only a finite number of the coefficients s_{rn} and a_{rn} is included in the series for the deflections. The supplementary coefficients ΔW_{rn}^{**} then become incorrect. An estimation of the errors due to neglected terms in the series should be made for the coefficients with the greatest absolute values. From (232. 14) and (232. 15) it may be seen that one of the following two inequalities must be valid:

$$\Delta|\Delta W_{rn}^{**}| \leqq \Big|\sum_{N+1}^{\infty} g_{mn}(1+\cos m\mu)\, w_{rm}\Big|_{max} \qquad (1$$

$$\Delta|\Delta W_{rn}^{**}| \leqq 2\Big|\sum_{N+1}^{\infty} h_{mn}\, w_{rm}\Big|_{max}$$

The number N is in practice never less than 2, which corresponds to $m \geqq 4$. Omitting extreme cases for which $\Theta < 60°$, and replacing $\cos m\mu$ and $\sin m\mu$ by their maximum values, the following inequality is obtained from (232. 17).

$$h_{mn} < \frac{1}{2} g_{mn} \left(1 + \frac{l \operatorname{tg} \Theta}{4 \pi t}\right)$$

The fraction $l \operatorname{tg} \Theta / 4 \pi t$ is less than 1 whenever $l/t < 7$. In such a case h_{mn} is smaller than g_{mn}, and (1) will be decisive for the magnitude of the maximum error.

The approximate series coefficients w_{rn} in 228 were assumed to be smaller than the maximum principal coefficient. Replacing w_{rm} in (1) by this upper bound the following error maximum is obtained:

$$\Delta \left| \Delta W_{rn}^{**} \right| \leqq \left| \sum_{N+1}^{\infty} g_{mn} (1 + \cos m\mu)\, w_{rm} \right|_{max} \leqq$$

$$\leqq \frac{16 N_1^2 l^2 \mu}{\pi^5 t^2 n^5} \left(1 - \cos \frac{n\pi}{N_1}\right) \sum m \left| W_{rm} \right|_{max} (1 + \cos m\mu) \sin^2 \frac{\pi}{2} (m+n) \quad (2)$$

N_1 is the maximum order number appearing in any of the deflection series. It determines the lengths l_1 of the loads q_{rj} defined by (232. 11). These loads yield principle deflections with Fourier series converging more rapidly than those for concentrated loads. The latter loads are decisive for the maximum value of W_{rm}:

$$\left| W_{rm} \right| \leqq \frac{1}{m^4} \left| n^4 W_{rn} \right|_{max} \quad (3)$$

Substitution of (3) in (2) yields:

$$\Delta \left| \Delta W_{rn}^{**} \right| \leqq$$

$$\leqq \frac{16 N_1^2 l^2 \mu}{\pi^5 t^2 n^5} \left(1 - \cos \frac{n\pi}{N_1}\right) \left| n^4 W_{rn} \right|_{max} \sum \frac{1 + \cos m\mu}{m^3} \sin^2 \frac{\pi}{2} (m+n) \quad (4)$$

The maximum value of the expression on the right hand side of this inequality emerges for $n = 1$. Replacing the sum in (4) by the maximum value of the $(N+2)$th term and an integral,

$$\sum \frac{1+\cos m\mu}{m^3} \sin^2 \frac{\pi}{2}(m+n) < \frac{2}{(N+2)^3} + \int_{N+3}^{\infty} \frac{dm}{m^3} = \frac{2}{(N+2)^3} + \frac{1}{2(N+2)^2}$$

the upper bound of $\Delta|\Delta W_{rn}^{**}|$ is obtained in the form:

$$\Delta|\Delta W_{rn}^{**}| < \frac{32\, l \operatorname{tg}\Theta}{\pi^4 t}\left(1-\cos\frac{\pi}{N_1}\right)|n^4 W_{rn}|_{max}\left[\frac{1}{(N+2)^3} + \right.$$

$$\left. + \frac{1}{4(N+2)^2}\right] N_1^2 \qquad (5)$$

The number N in (5) must be even since n is odd. When the highest number appearing in any deflection series is $N_1 = 3$, eq. (5) gives, for $N = 2$:

$$\Delta|\Delta W_{rn}^{**}| < .038\, \frac{l \operatorname{tg}\Theta}{t} |n^4 W_{rn}|_{max} \qquad (6)$$

This error maximum increases with growing values of l/t and tg Θ.

Eq. (5) is derived for an unfavourable case. All coefficients w_{rn} of order n have the same numerical value, and signs such that the supplements attain their largest possible values. In reality, these conditions never occur. Actual errors are as a rule considerably smaller than those determined by (5).

When Poisson's ratio $\nu \neq 0$, errors also arise from the use of an incorrect expression for the slope $\frac{\partial w}{\partial y}$ at the corners of the plate. The effect of neglecting the last term in (213.10), as was done by writing (231.7), can be estimated in the following way. If the term formerly omitted is taken to account when forming the second derivative $\left(\frac{\partial^2 w}{\partial x\, \partial y}\right)_0$ at the support $x_0 = 0$ of strip O, the curvature ΔK_{00} determined by (231.6) increases by

$$\Delta^2 K_{00} = \frac{\nu\, t\, \mathrm{tg}\, \Theta}{1+\nu}\left(\frac{d^3 w_0}{d x^3}\right)_0$$

At the other support of the strips an increment

$$\Delta^2 K_{0l} = \frac{\nu\, t\, \mathrm{tg}\, \Theta}{1+\nu}\left(\frac{d^3 w_0}{d x^3}\right)_l$$

is obtained. Substitution of $\Delta^2 K_{00}$ and $\Delta^2 K_{0l}$ for ΔK_{r0} and ΔK_{rl} in (232.12) and multiplication by $1-\nu^2$ yields the following increments, $\Delta^2 W_{0n}^{**}$, of the supplementary coefficients:

$$\Delta^2 W_{0n}^{**} = -\frac{2\,\nu\,(1-\nu)\,t\,l^2\,\lambda_{Nn}}{\pi^3\, n^3}\left[\left(\frac{d^3 w_0}{d\, x_0{}^3}\right) - \left(\frac{d^3 w_0}{d\, x_0{}^3}\right)_l \cos n\pi\right] \mathrm{tg}\, \Theta$$

A similar expression $\Delta^2 W_{Rn}^{**}$ is derived for the other outside strip, R. The corresponding increments for the coefficients $\Delta^2 S_{rn}^{**}$ and $\Delta^2 A_{rn}^{**}$ become:

$$\Delta^2 S_{0n}^{**} = \frac{\nu\,(1-\nu)\,t\,l^2\,\lambda_{Nn}}{\pi^3\, n^3}\left[\left(\frac{d^3 w_R}{d\, x_R{}^3}\right)_0 - \left(\frac{d^3 w_0}{d\, x_0{}^3}\right)_0 + \left(\frac{d^3 w_0}{d\, x_0{}^3}\right)_l \cos n\pi - \right.$$

$$\left. - \left(\frac{d^3 w_R}{d\, x_R{}^3}\right)_l \cos n\pi\right] \mathrm{tg}\, \Theta$$

$$\Delta^2 A_{0n}^{**} = \frac{\nu\,(1-\nu)\,t\,l^2\,\lambda_{Nn}}{\pi^3\, n^3}\left[\left(\frac{d^3 w_R}{d\, x_R{}^3}\right)_0 + \left(\frac{d^3 w_0}{d\, x_0{}^3}\right)_0 - \left(\frac{d^3 w_0}{d\, x_0{}^3}\right)_l \cos n\pi - \right.$$

$$\left. - \left(\frac{d^3 w_R}{d\, x_R{}^3}\right) \cos n\pi\right] \mathrm{tg}\, \Theta$$

The third derivatives appearing here should be computed from (223.9), as the simpler series expressions converge too slowly.

The coefficients $\Delta^2 S_{0n}^{**}$ and $\Delta^2 A_{0n}^{**}$ generally have little effect on the deflections. The largest effect emerges when Θ is large and loads are applied on an outside strip.

54. Principal coefficients due to displacements of the supports

The deflections w_r for a plate divided into three strips may be written

$$w_0 = \Sigma w_{0n} \sin (n \pi x_0/l) + w_0$$

$$w_1 = \Sigma w_{1n} \sin (n \pi x_1/l) + w_1$$

$$w_2 = \Sigma w_{2n} \sin (n \pi x_2/l) + w_2$$

On substituting in (212. 13), terms containing the second and fourth derivatives of w_r vanish. The influence of the w_r functions upon the first equation of (212. 13) is confined to three terms on the left hand side:

$$2 w_0 - 4 w_1 + 2 w_2 = 2 \delta \left(1 - \frac{2 x_0}{l} - 1 + \frac{2 x_2}{l} \right) = - \frac{8 \delta t \operatorname{tg} \Theta}{l}$$

Terms dependent on w_r also appear on the left hand side of the second equation,

$$- 2 w_0 + 4 w_1 - 2 w_2 = \frac{8 t \delta \operatorname{tg} \Theta}{l}$$

and of the third,

$$2 w_0 - 4 w_1 + 2 w_2 = - \frac{8 t \delta \operatorname{tg} \Theta}{l}$$

These quantities are transferred to the right hand side of the equations and treated as uniformly distributed loads. They yield principal coefficients W_{rn}, which can be evaluated by applying (55. 2) in Appendix 55. The coefficients S_{rn} and A_{rn} become

$$\left.\begin{aligned} S_{0n}^{*} &= \frac{32 \delta l^3 \operatorname{tg} \Theta}{\pi^5 t^3} \frac{\sin^2 \frac{n \pi}{2}}{n^5} \\ S_{1n}^{*} &= - \frac{32 \delta l^3 \operatorname{tg} \Theta}{\pi^5 t^3} \frac{\sin^2 \frac{n \pi}{2}}{n^5} \\ A_{0n}^{*} &= 0 \end{aligned}\right\} \qquad (1)$$

That is, the usual series expression for $\frac{\partial^2 w}{\partial x \partial y}$ is supplemented by an increment

$$\frac{\partial^2 w}{\partial x \partial y} = \frac{2\delta}{lt}$$

which is constant for all points of the plate. The moment M_ξ expressed by (231.1) is zero along simple supports. This implies that the increments will cause boundary curvatures:

$$\frac{2(1-\nu)\operatorname{tg}\Theta}{1+\nu\operatorname{tg}^2\Theta}\,\frac{2\delta}{lt}$$

The corresponding principal coefficients W_{1n}^{**} are obtained by applying (232.12):

$$W_{1n}^{**} = -\frac{16(1-\nu)\delta l \operatorname{tg}\Theta}{\pi^3 t(1+\nu\operatorname{tg}^2\Theta)} \cdot \frac{\lambda_{Nn}\sin^2\frac{n\pi}{2}}{n^3} = S_{1n}^{**} \qquad (2)$$

At the supports of strips 0 and 2 the $w_r$functions correspond to curvatures, which, according to (231.6), are

$$\frac{2\operatorname{tg}\Theta}{1+\nu}\,\frac{2\delta}{lt}$$

with the principal coefficients

$$W_{0n}^{**} = -\frac{16(1-\nu)\delta l \operatorname{tg}\Theta}{\pi^3 t}\,\frac{\lambda_{Nn}\sin^2\frac{n\pi}{2}}{n^3} = S_{0n}^{**} \qquad (3)$$

Combining the supplements S_{rn}^{**} according to (2) and (3) with the corrections given in (1), the resulting principal coefficients given in (235.6) are obtained.

For a plate divided into five strips the procedure is analogous. Terms dependent on w_r appear in the system (52.8)

on substituting the expressions for w_r from (223. 7) and (235. 7). These terms can be regarded as originating from uniformly distributed loads, q_r,

$$q_0 = q_4 = -\frac{D}{t^4}\left[4\left(1-\frac{2x_0}{l}\right)-4\left(1-\frac{2x_1}{l}\right)+2\cdot 0\right]\delta = \frac{8\,D\,\delta\ \mathrm{tg}\ \Theta}{l\,t^3}$$

$$q_1 = q_3 = -\frac{D}{t^4}\left[-4\left(1-\frac{2x_0}{l}\right)+5\left(1-\frac{2x_1}{l}\right)-4\cdot 0-\left(1-\frac{2x_3}{l}\right)\right]\delta =$$

$$= -\frac{4\,D\,\delta\ \mathrm{tg}\ \Theta}{l\,t^3}$$

$$q_2 = 0$$

The principal coefficients for these loads are obtained by applying (55. 2):

$$\left.\begin{aligned} S_{0n}^{*} &= \frac{4\,q_1\,l^4}{\pi^5\,D}\,\frac{\sin^2\frac{n\pi}{2}}{n^5} = \frac{32\,l^3\,\delta\ \mathrm{tg}\ \Theta}{\pi^5\,t^3}\,\frac{\sin^2\frac{n\pi}{2}}{n^5} \\ S_{1n}^{*} &= -\frac{16\,l^3\,\delta\ \mathrm{tg}\ \Theta}{\pi^5\,t^3}\,\frac{\sin^2\frac{n\pi}{2}}{n^5} \\ S_{2n}^{*} &= A_{0n}^{*} = A_{1n}^{*} = 0 \end{aligned}\right\} \qquad (4)$$

The functions w_r correspond to a constant increment to the second derivative $\frac{\partial^2 w}{\partial x\,\partial y}$,

$$\frac{\partial^2 w}{\partial x\,\partial y} = \delta/l\,t$$

The corresponding supplementary coefficients are determined as for a plate divided into three strips:

$$\left.\begin{aligned} W_{0n}^{**} = S_{0n}^{**} &= -\frac{8(1-\nu)\,l\,\delta\ \mathrm{tg}\ \Theta}{\pi^3\,t}\,\frac{\lambda_{Nn}\sin^2\dfrac{n\pi}{2}}{n^3} \\ W_{1n}^{**} = S_{1n}^{**} &= -\frac{8(1-\nu)\,l\,\delta\ \mathrm{tg}\ \Theta}{\pi^3\,t\,(1+\nu\,\mathrm{tg}^2\,\Theta)}\,\frac{\lambda_{Nn}\sin^2\dfrac{n\pi}{2}}{n^3} \\ A_{0n}^{**} = A_{1n}^{**} &= 0 \end{aligned}\right\} \qquad (5)$$

Lastly, the resulting principal coefficients given in (235.8) are obtained by adding the coefficients in (4) and (5).

55. Principal deflections and coefficients for some cases of loading

Loading	Principal deflection W_r	Principal coefficient W_{rn}
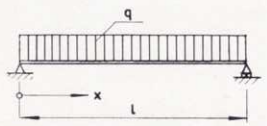	$\frac{q l^4}{24 D}\left[\frac{x}{l}-2\left(\frac{x}{l}\right)^3+\left(\frac{x}{l}\right)^4\right]$ (55.1)	$\frac{4 q l^4}{\pi^5 D}\frac{\sin^2\frac{n\pi}{2}}{n^5}$ (55.2)
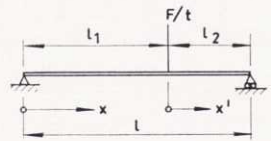	$\frac{F l^3}{6 t D}\left[\frac{l_1 l_2}{l^2}\left(1+\frac{l_2}{l}\right)\frac{x}{l}-\frac{l_2}{l}\left(\frac{x}{l}\right)^3+\left(\frac{x'}{l}\right)^3\right]$ (55.3) $x' = \begin{cases} 0 \text{ for } x > l_1 \\ x-l_1 \text{ „ } x \geqq l_1 \end{cases}$	$\frac{2 F l^3}{\pi^4 t D}\frac{\sin\frac{n\pi l_1}{l}}{n^4}$ (55.4)
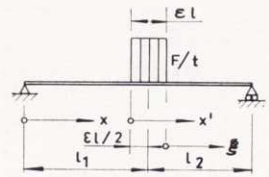	$\frac{F l^3}{6 t D}\left[\frac{l_2}{l}\left(1-\frac{l_2^2}{l^2}-\frac{\varepsilon^2}{4}\right)\frac{x}{l}-\frac{l_2}{l}\left(\frac{x}{l}\right)^3+\frac{1}{4\varepsilon}\left(\frac{x'}{l}\right)^4-\right.$ $\left.-\frac{1}{4\varepsilon}\left(\frac{\xi'}{l}\right)^4\right]$ (55.5) $x' = \begin{cases} 0 \text{ for } x < l_1-\frac{1}{2}\varepsilon l \\ x-l_1+\frac{1}{2}\varepsilon l \text{ „ } x \geqq l_1-\frac{1}{2}\varepsilon l \end{cases}$ $\xi' = \begin{cases} 0 \text{ for } x < l_1+\frac{1}{2}\varepsilon l \\ x-l_1-\frac{1}{2}\varepsilon l \text{ „ } x \geqq l_1+\frac{1}{2}\varepsilon l \end{cases}$	$\frac{4 F l^3}{\pi^5 \varepsilon t}\frac{\sin\frac{n\pi\varepsilon}{2}\sin\frac{n\pi l_1}{l}}{D n^5}$ (55.6)

Loading	Principal deflection W_r	Principal coefficient W_{rn}
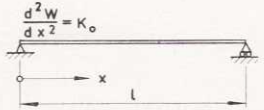	$-\frac{K_0 l^2}{3}\left[\frac{x}{l}-\frac{3}{2}\left(\frac{x}{l}\right)^2+\frac{1}{2}\left(\frac{x}{l}\right)^3\right]$ (55.7)	$-\frac{2 K_0 l^2}{\pi^3 n^3}$ (55.8)
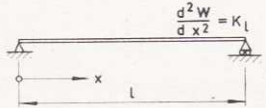	$-\frac{K_l l^2}{6}\left[\frac{x}{l}-\left(\frac{x}{l}\right)^3\right]$ (55.9)	$\frac{2 K_l l^2}{\pi^3 n^3}\cos n\pi$ (55.10)
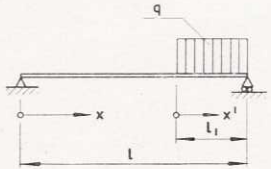	$\frac{q l^4}{24 D}\left[\left(2-\frac{l_1^2}{l^2}\right)\frac{l_1^2}{l^2}\frac{x}{l}-2\frac{l_1^2}{l^2}\left(\frac{x}{l}\right)^3+\left(\frac{x'}{l}\right)^4\right]$ (55.11) $x'=\begin{cases}0 & \text{for } x<l-l_1\\ x-l+l_1 & \text{„ } x\geqq l-l_1\end{cases}$	$-\frac{4q l^4}{\pi^5 n^5 D}\cos n\pi \sin^2\frac{n\pi l_1}{2l}$ (55.12)

56. Diagram of the approximate coefficients s_{rn} and a_{rn}, $r = 0$

561. Division into two strips

The deflections of strips 0, 1 are, Fig. 212.3,

$$\left.\begin{aligned} w_0 &= \Sigma\,(s_n - a_n)\sin(n\,\pi\,x_0/l) \\ w_1 &= \Sigma\,(s_n + a_n)\sin(n\,\pi\,x_1/l) \end{aligned}\right\}$$

where

$$\left.\begin{aligned} s_n &= B_n\,(S_n + \Delta\,S_n) \\ a_n &= C_n\,(A_n + \Delta\,A_n) \end{aligned}\right\} \qquad (1)$$

with

$$S_n = \frac{1}{2}\,(W_{0n} + W_{1n}) \qquad A_n = \frac{1}{2}\,(W_{1n} - W_{0n})$$

The W_{rn} are obtained from 55, the $\Delta\,S_n$ and $\Delta\,A_n$ from 57. Series convergence is improved by applying (223.9). The factors B_n in (1) are given by the curves in Fig. 561.1. The quantities C_n are found by reading the B_n values for the abscissas $\pi - n\mu$.

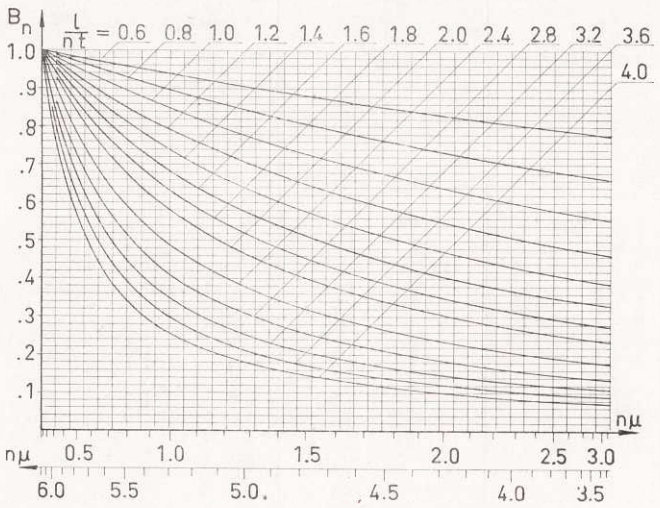

Fig. 561.1. Factor B_n as function of l/nt and $n\mu$ for $.6 \leqq l/nt \leqq 4$.

562. Division into three strips

The deflections of strips 0, 1, 2 are, Fig. 212,4,

$$\left.\begin{aligned} w_0 &= \Sigma\,(s_{0n} - a_{0n}) \sin(n\pi x_0/l) \\ w_1 &= \Sigma\, s_{1n} \sin(n\pi x_1/l) \\ w_2 &= \Sigma\,(s_{0n} + a_{0n}) \sin(n\pi x_2/l) \end{aligned}\right\}$$

where

$$\left.\begin{aligned} s_{0n} &= B_{00n}(S_{0n} + \Delta S_{0n}) + B_{01n}(S_{1n} + \Delta S_{1n}) \\ s_{1n} &= B_{01n}(S_{0n} + \Delta S_{0n}) + B_{11n}(S_{1n} + \Delta S_{1n}) \\ a_{0n} &= C_{0n}(A_{0n} + \Delta A_{0n}) \end{aligned}\right\} \qquad (1)$$

with

$$S_{0n} = \frac{1}{2}(W_{0n} + W_{2n}) \qquad A_{0n} = \frac{1}{2}(W_{2n} - W_{0n})$$

$$S_{1n} = W_{1n}$$

The W_{rn} are obtained from 55, the ΔS_{rn} and ΔA_n from 57. Series convergence is improved by applying (223.8) and (223.9). The factors B_{rsn} and C_{0n} in (1) are given by the curves in Figs. 562.1, 2, 3, 4.

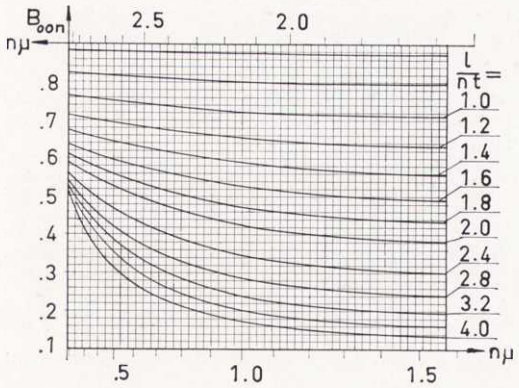

Fig. 562.1 Factor B_{00n} as function of l/nt and $n\mu$ for $.6 \leqq l/nt \leqq 4$.

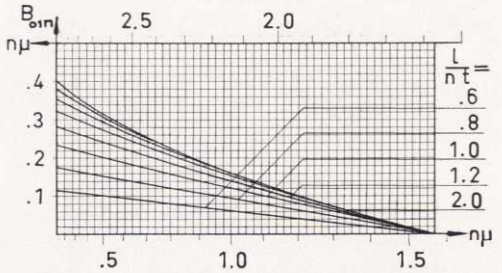

Fig. 562.2. Factor B_{01n} as function of l/t and $n\mu$ for $.6 \leqq l/nt \leqq 2$. The factor is negative for values of $n\mu$ in the second and third quadrant.

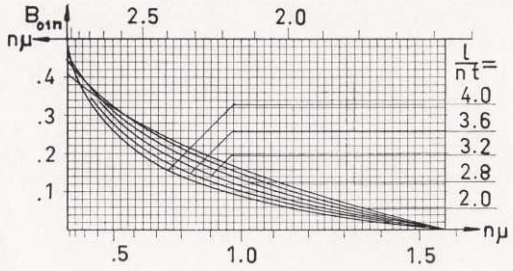

Fig. 562.3. Factor B_{01n} as function of l/nt and $n\mu$ for $2 \leqq l/nt \leqq 4$. The factor is negative for values of $n\mu$ in the second and third quadrant.

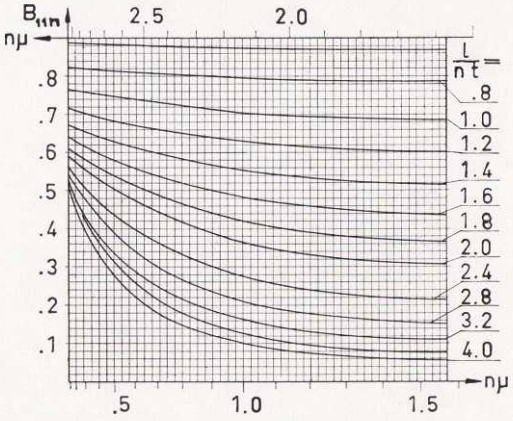

Fig. 562.4. Factor B_{11n} as function of l/nt and $n\mu$ for $.6 \leqq l/nt \leqq 4$.

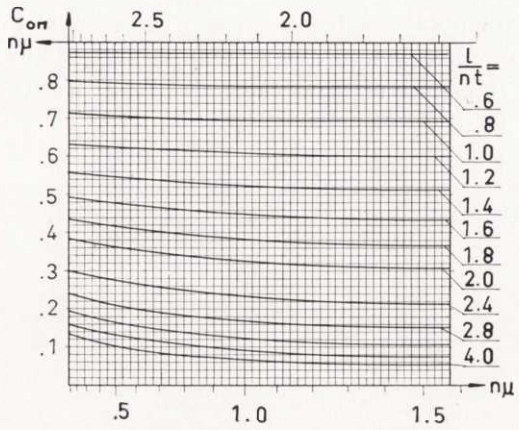

Fig. 562.5. Factor C_{0n} as function of l/nt and $n\mu$ for $.6 \leqq l/nt \leqq 4$.

563. Division into five strips

The deflections of strips 0, 1, 2, 3, 4 are, Fig. 52.1,

$$\left.\begin{aligned} w_0 &= \Sigma (s_{0n} - a_{0n}) \sin (n\pi x_0/l) \\ w_1 &= \Sigma (s_{1n} - a_{1n}) \sin (n\pi x_1/l) \\ w_2 &= \Sigma s_{2n} \sin (n\pi x_2/l) \\ w_3 &= \Sigma (s_{1n} + a_{1n}) \sin (n\pi x_3/l) \\ w_4 &= \Sigma (s_{0n} + a_{0n}) \sin (n\pi x_4/l) \end{aligned}\right\}$$

where

$$\left.\begin{aligned} s_{0n} &= B_{00n}(S_{0n} + \Delta S_{0n}) + B_{01n}(S_{1n} + \Delta S_{1n}) + B_{02n}(S_{2n} + \Delta S_{2n}) \\ s_{1n} &= \frac{1}{2} B_{01n}(S_{0n} + \Delta S_{0n}) + B_{11n}(S_{1n} + \Delta S_{1n}) + \frac{1}{2} B_{21n}(S_{2n} + \Delta S_{2n}) \\ s_{2n} &= B_{02n}(S_{0n} + \Delta S_{0n}) + B_{21n}(S_{1n} + \Delta S_{1n}) + B_{22n}(S_{2n} + \Delta S_{2n}) \\ a_{0n} &= C_{00n}(A_{0n} + \Delta A_{0n}) + C_{01n}(A_{1n} + \Delta A_{1n}) \\ a_{1n} &= \frac{1}{2} C_{01n}(A_{0n} + \Delta A_{0n}) + C_{11n}(A_{1n} + \Delta A_{1n}) \end{aligned}\right\} \quad (1)$$

with

$$S_{0n} = \frac{1}{2}(W_{0n} + W_{4n}) \qquad A_{0n} = \frac{1}{2}(W_{4n} - W_{0n})$$

$$S_{1n} = \frac{1}{2}(W_{1n} + W_{3n}) \qquad A_{1n} = \frac{1}{2}(W_{3n} - W_{1n})$$

$$S_{2n} = W_{2n}$$

The W_{rn} are obtained from 55, the ΔS_{rn} and ΔA_{rn} from 57. Series convergence is improved by applying (223.8) and (223.9). The factors B_{rsn} and C_{rsn} in (1) are given by the curves in Figs. 563.1, 2, 3, 4, 5, 6, 7, 8, 9, 10, 11, 12.

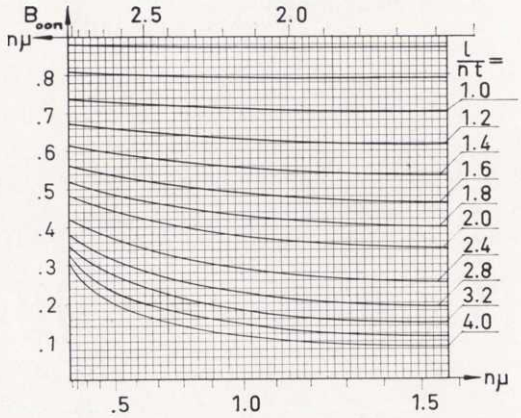

Fig. 563.1. Factor B_{00n} as function of l/nt and $n\mu$ for $.6 \leqq l/nt \leqq 4$.

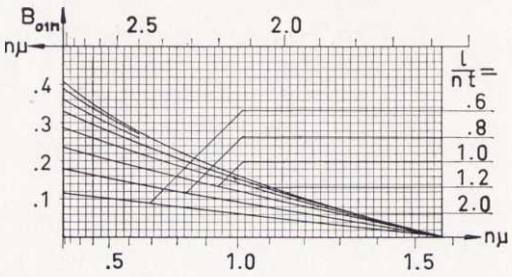

Fig. 563.2. Factor B_{01n} as function of l/nt and $n\mu$ for $.6 \leqq l/nt \leqq 2$. The factor is negative for values of $n\mu$ in the second and third quadrant.

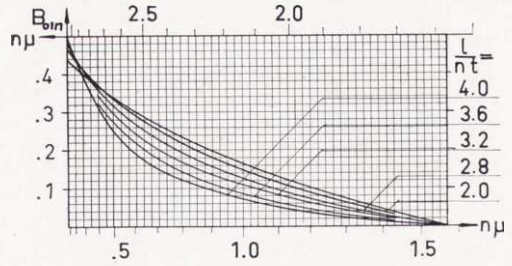

Fig. 563.3. Factor B_{01n} as function of l/nt and $n\mu$ for $2 \leqq l/nt \leqq 4$. The factor is negative for values of $n\mu$ in the second and third quadrant.

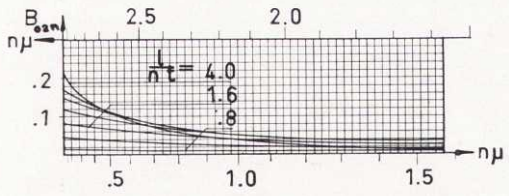

Fig. 563.4. Factor B_{02n} as function of l/nt and $n\mu$ for $.8 \leqq l/nt \leqq 4$.

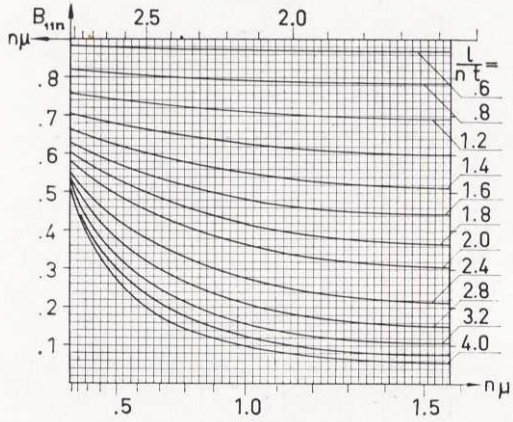

Fig. 563.5. Factor B_{11n} as function of l/nt and $n\mu$ for $.6 \leqq l/nt \leqq 4$.

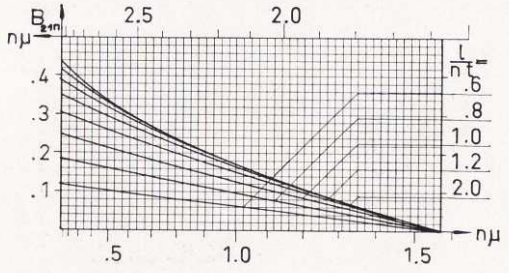

Fig. 563.6. Factor B_{21n} as function of l/nt and $n\mu$ for $.6 \leqq l/nt \leqq 2$. The factor is negative for values of $n\mu$ in the second and third quadrant.

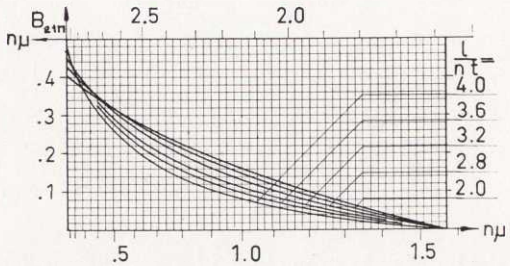

Fig. 563.7. Factor B_{21n} as function of l/nt and $n\mu$ for $2 \leqq l/nt \leqq 4$. The factor is negative for values of $n\mu$ in the second and third quadrant.

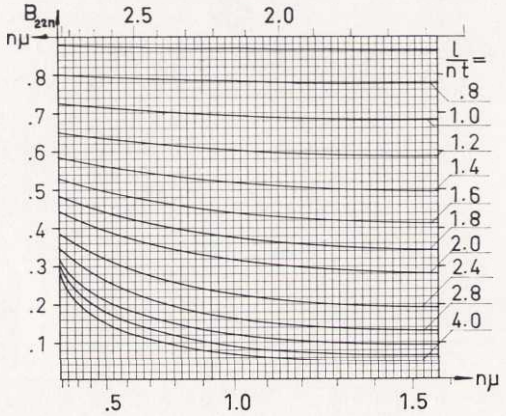

Fig. 563.8. Factor B_{22n} as function of l/nt and $n\mu$ for $.6 \leqq l/nt \leqq 4$.

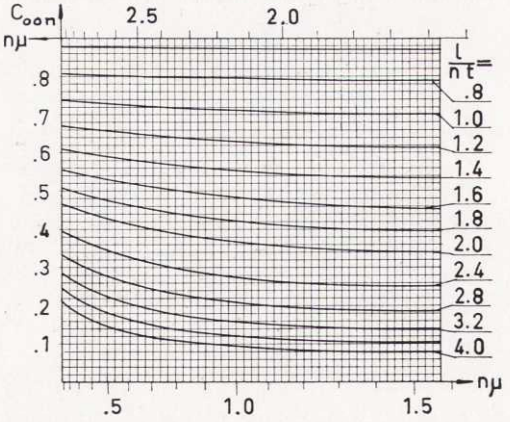

Fig. 563.9. Factor C_{00n} as function of l/nt and $n\mu$ for $.6 \leqq l/nt \leqq 4$.

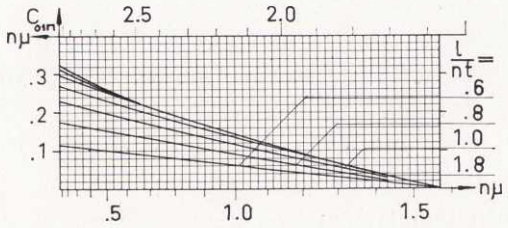

Fig. 563.10. Factor C_{01n} as function of l/nt and $n\mu$ for $.6 \leqq l/nt \leqq 1.8$. The factor is negative for values of $n\mu$ in the second and third quadrant.

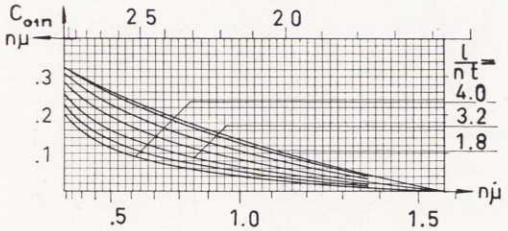

Fig. 563.11. Factor C_{01n} as function of l/nt and $n\mu$ for $1.8 \leqq l/nt \leqq 4$. The factor is negative for values of $n\mu$ in the second and third quadrant.

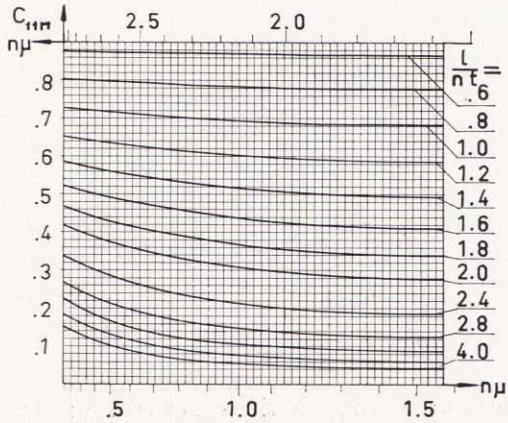

Fig. 563.12. Factor C_{11n} as function of l/nt and $n\mu$ for $.6 \leqq l/nt \leqq 4$.

57. Formulas for the total increments to the principal coefficients for simply supported plates

The total increments are obtained by adding the quantities given in 227 and 232.

Division into two strips:

$$\left.\begin{aligned} \Delta S_n &= \sum [c_{mn} - g_{mn}(1 + \cos\ m\,\mu)]\, a_m \\ \Delta A_n &= \sum [-c_{mn} - g_{mn}(1 - \cos\ m\,\mu)]\, s_m \end{aligned}\right\}$$

Division into three strips:

$$\left.\begin{aligned} \Delta S_{0n} &= -\sum (d_{mn} + g_{mn})\, a_{0m} \\ \Delta S_{1n} &= \sum (e_{mn} - 2\,h_{mn})\, a_{0m} \\ \Delta A_{0n} &= \sum [(d_{mn} - g_{mn})\, s_{0m} + (-e_{mn} + g_{mn} \cos\ m\,\mu)\, s_{1m}] \end{aligned}\right\}$$

Division into five strips:

$$\left.\begin{aligned} \Delta S_{0n} &= \sum [-g_{mn}\, a_{0m} - (e_{mn} - g_{mn} \cos\ m\,\mu)\, a_{1m}] \\ \Delta S_{1n} &= \sum \left[\left(\frac{1}{2} e_{mn} - h_{mn}\right) a_{0m} - \frac{1}{2} d_{mn}\, a_{1m}\right] \\ \Delta S_{2n} &= \sum [-d_{mn}\, a_{0m} + (f_{mn} - 2\,h_{mn})\, a_{1m}] \\ \Delta A_{0n} &= \sum [-g_{mn}\, s_{0m} - (e_{mn} - g_{mn} \cos\ m\,\mu)\, s_{1m} + d_{mn}\, s_{2m}] \\ \Delta A_{1n} &= \sum \left[\left(\frac{1}{2} e_{mn} - h_{mn}\right) s_{0m} + \frac{1}{2} d_{mn}\, s_{1m} - \left(\frac{1}{2} f_{mn} - h_{mn}\right) s_{2m}\right] \end{aligned}\right\}$$

The constants appearing in these series are:

1. $$c_{mn} = \frac{16\, m^2 (1 - \nu)}{\pi^3\, n^3 (m^2 - n^2)} \frac{l^2}{t^2} \sin\ m\,\mu \cdot \sin^2 \frac{\pi}{2} (m + n)$$

m \ n	1	2	3	4	Multiplier
1	0	— .0215	0	— .0005	$\frac{l^2}{t^2}(1-\nu)\sin m\mu$
2	.6880	0	— .0153	0	
3	0	.1161	0	— .0104	
4	.5504	0	.0437	0	

2. $$d_{mn} = \frac{l^2 \cos m\mu}{m^2 \pi^2 t^2 (1-\nu)} c_{mn}$$

m \ n	1	2	3	4	Multiplier
1	0	— .0022	0	— .0001	$\frac{l^4}{t^4}\sin m\mu \cos m\mu$
2	.0174	0	— .0004	0	
3	0	.0013	0	— .0001	
4	.0035	0	.0003	0	

3. $$e_{mn} = \left(1 - \frac{\nu}{2} + \frac{l^2}{m^2 \pi^2 t^2}\right) \frac{c_{mn}}{1-\nu}$$

4. $$f_{mn} = \left(1 + \frac{2 l^2}{m^2 \pi^2 t^2}\right) \frac{c_{mn}}{1-\nu}$$

5. $$g_{mn} = \frac{16 N^2 (1-\nu) l^2}{\pi^5 n^5 t^2} \left(1 - \cos \frac{n\pi}{N}\right) m\mu \sin^2 \frac{\pi}{2}(m+n)$$

where N is the largest order number appearing in the series for the deflections.

When $N = 3$

$g_{12} = .0221 \cdot \mu (1-\nu) l^2/t^2$

$g_{21} = .4706 \cdot$ „

$g_{23} = .0077 \cdot$ „

$g_{32} = .0662 \cdot$ „

6. $$h_{mn} = \frac{g_{mn}}{2(1 + \nu \operatorname{tg}^2 \Theta)} \left(\cos m\mu + \frac{\nu + \operatorname{tg}^2 \Theta}{1-\nu} \frac{\sin m\mu}{m\mu}\right)$$

58. Experimental errors

581. Analysis of variance for deflections of Plate I

In order to estimate the different components of variation a variance analysis was carried out. The following model, which is a special case of a more general model applicable in cases where both random and systematic effects are present (cf. BENNETT and FRANKLIN, sec. 7.63), is assumed to hold approximately:

$$z_{ijk} = a_i + b_{j(i)} + c_k + d_{ik} + e_{ijk},$$

where

z_{ijk} = the observed deflection at the kth point in the ith test with the jth orientation of the instrument,

a_i = the effect, on each point, of the loading error in the ith test,

$b_{j(i)}$ = the effect, on each point, of the error due to the jth orientation in the ith test,

c_k = the difference between the "true" deflection at the kth point, and the average "true" deflection at the four points,

d_{ik} = the effect on the kth point of the location error in the ith test,

e_{ijk} = the residual error.

The a_i, $b_{j(i)}$ and e_{ijk} are assumed to be independent random variables with zero means and variances σ_a^2, σ_b^2 and σ_e^2 respectively. The d_{ik} are assumed to be random variables, independent of a_i, $b_{j(i)}$ and e_{ijk} and satisfying the relation $\sum_{k=1}^{4} d_{ik} = 0$ for each i. The variance σ_d^2 is defined as the average, over the infinite population of tests, of $\sum_{k=1}^{4} d_{ik}^2/3$.

Since the orientation effect only changes the loading and not the location no term for the interaction between orientations and points within tests is needed in the model.

Then the analysis of variance takes the following form[1]:

Source of variation	Degrees of freedom	Sum of squares	Mean square	Average value of mean square
Between tests	3	947.67	315.89	$\sigma_e^2 + 4\,\sigma_b^2 + 16\,\sigma_a^2$
Within tests between orientations	12	360.48	30.04	$\sigma_e^2 + 4\,\sigma_v^2$
Between points	3	1 560.42	520.14	$\sigma_e^2 + 4\,\sigma_d^2 + 16 \sum_{k=1}^{4} c_k^2/3$
Interaction between tests and points	9	946.27	105.14	$\sigma_e^2 + 4\,\sigma_d^2$
Residual	36	144.77	4.02	σ_e^2
Total	63	3 959.61	—	—

582. Analysis of variance for the strains of Plate I

The values of Tab. 332.2 are multiplied by 10^3 before calculating the sums of squares.

Source of variation	Degrees of freedom	Sums of squares	Mean square
Between points	3	4102	1367
Between tests	3	466	155
Residual	9	2034	226
Total	12	6602	550

A comparison of the mean square for "Between points" with the one for "Residual" indicates that the difference between the strains at the different points is statistically significant at the significance level .05.

[1] To determine which terms should be included in the last column of the analysis of variance table take out from Table 7.42 of BENNETT and FRANKLIN the 1st, 2nd, 4th, 7th and last rows, delete all terms containing the letters k and m and the terms containing σ_{ijl}^2 and finally change l into k.

583. Computation of the confidence limits for the means of deflections and strains

The deflection w_m at a point P_m is determined by N tests with the load at the point P_0. Then the deflection $w_{m'}$ at a point $P_{m'}$ is determined by N tests with the load at a point $P_{0'}$, $P_{m'}$ and $P_{0'}$ being situated symmetrically to P_m and P_0 with respect to the centre of the plate. For an accurate model plate w_m should be equal to $w_{m'}$. However, irregularities of the shape and inhomogeneities cause differences between w_m and $w_{m'}$. Observed deflections may be written

$$z_{mn} = w_m + e_{mn}$$

$$z_{m'n} = w_{m'} + e_{m'n},$$

where n denotes the test number in the corresponding series, and e_{mn} and $e_{m'n}$ represent the total errors in the corresponding tests. These errors may be interpreted as independent random variables with means 0 and a common variance σ^2. The latter may be estimated by

$$s^2 = \frac{1}{2(N-1)} \sum_{n=1}^{N} [(z_{mn} - \bar{z}_m)^2 + (z_{m'n} - \bar{z}_{m'})^2]$$

where

$$\bar{z}_m = \frac{1}{N} \sum z_{mn} \quad \text{and} \quad \bar{z}_{m'} = \frac{1}{N} \sum z_{m'n}$$

As an estimate of the average deflection

$$\bar{w}_m = \frac{1}{2} (w_{mn} + w_{m'n})$$

the expression

$$\bar{\bar{z}}_m = \frac{1}{2} (\bar{z}_m + \bar{z}_{m'})$$

is chosen.

The variance of this estimate is $\left(\frac{1}{2}\right)^2$ [(variance of $\bar{z}_m$) + + (variance of $\bar{z}_{m'}$)] $= \frac{1}{4}\left(\frac{1}{N}\sigma^2 + \frac{1}{N}\sigma^2\right) = \frac{1}{2}\sigma^2$. A confidence inter-

val for $\bar{w}_m$ with confidence coefficient .95 is now obtained [1] by subtracting and adding the quantity $L = \frac{s}{\sqrt{n}} t_{2n-2,\ 0.05}$ to the above estimate.

If $\bar{\bar{z}}_m$ differs numerically from the hypothetical value by more than L, the difference is judged as significant (at the 5 % level).

For testing the difference between w_m and $w_{m'}$ the corresponding difference $\bar{z}_m - z_{m'}$ is judged as significant (at the 5 % level) if $\bar{z}_m - \bar{z}_{m'}$ is numerically larger than $2L$.

When studying the effect of loads acting at the centre of the plate, deflections z_{mn} and $z_{m'n}$ are observed in the same test. In this case the z_{mn} and $z_{m'n}$ can be written as in the previous case. However, the e_{mn} and $e_{m'n}$ corresponding to one particular test have some variance components in common. Hence a somewhat different statistical analysis should be used. Each test yields an estimate of $\bar{w}_m$:

$$\dot{z}_{mn} = \frac{1}{2}(z_{mn} + z_{m'n}) = \bar{w}_m + \dot{e}_{mn}$$

where

$$\dot{e}_{mn} = \frac{1}{2}(e_{mn} + e_{m'n})$$

The $\dot{e}_{mn}$ corresponding to a series of N tests may be interpreted as N independent random variables all with mean 0 and a common variance $\dot{\sigma}^2$. N tests yield the estimate

$$\bar{\dot{z}}_m = \frac{1}{N} \sum \dot{z}_{mn} \text{ of } \bar{w}_m$$

and the estimate

$$\dot{s}^2 = \frac{1}{N-1} \sum (\dot{z}_{mn} - \bar{\dot{z}}_m)^2 \text{ of } \dot{\sigma}^2.$$

---

[1] A confidence interval for an unknown parameter Θ, with confidence coefficient $1-p$, is an interval (Θ_1, Θ_2) determined from observed data according to a rule which in repeated applications yields intervals that in 100 $(1-p)$ % of all cases will cover the parameter Θ.

The variance of $\bar{z}$ is $\dot{\sigma}^2/N$. Hence a confidence interval with confidence coefficient .95 for $\bar{w}_m$ is in this case obtained by subtracting and adding the quantity

$\dot{L} = \frac{\dot{s}}{\sqrt{n}} t_{n-1,\,0.05}$ to $\bar{z}$. If $\bar{z}$ differs numerically from the hypothetical value by more than L, the difference is judged as significant (at the 5 % level). To test the difference between w_m and $w_{m'}$ the difference $d_{mn} = z_{mn} - z_{m'n}$ is formed for each test. The average, $\bar{d}_m$, of N such differences is judged as significant if it is numerically larger than the quantity

$$\frac{t_{n-1,\,0.05}}{\sqrt{N}} \sqrt{\frac{1}{N-1} \sum (d_{mn} - \bar{d}_m)^2}$$

References

1. Aitken, A. C., "Determinants and Matrices", 8th ed., N. Y. 1954.
2. Anzelius, A., "Über die elastische Deformation parallellogrammförmige Platten", Bauingenieur, vol. 20, No. 35/36, 1939.
3. Bennet, C. A., and Franklin, N. L., "Statistical Analysis in Chemistry and the Chemical Industry", N. Y. 1954.
4. Bereuter, R., "Theoretische Untersuchungen über die Eigenfrequenz parallellogrammförmiger Platten", Publication No. 3 du Laboratoire de Photoélasticité de l'École polytechnique fédérale, 1946.
5. Bittner, E., "Momententafeln und Einflussflächen für kreuzweise bewehrte Eisenbetonplatten", Wien 1938.
6. Brigatti, C. V., "Applicazione del metodo di H. Marcus al calcolo della piastra parallelogrammica", Ricerche di Ingegneria, vol. 6, No. 2, 1938.
7. Brink, S., Svensson, B., Thorén, S., "Bestämning av nedsänkning hos plattor åverkade av enkelkrafter", unpublished investigation at the Chalmers University of Technology, 1941.
8. Churchill, R., "Fourier Series and Boundary Value Problems", N. Y. 1941.
9. Churchill, R., "Modern Operational Mathematics in Engineering", N. Y. 1944.
10. Davies, O. L., "Statistical Methods in Research and Production", London 1947.
11. Dubas, P., "Calcul numérique des plaques et des parois minces", Publication No. 27 de l'Institut de Statique Appliquée de l'École Polytechnique Fédérale, 1955.
12. Ehasy, F. L., "Structural Skew Plates", Proc. Am. Soc. of Civ. Eng., vol. 71, No. 6, 1945.
13. Favre, H., "Contribution à l'étude des plaques obliques", Schw. Bauzeitung, No. 5/6, 1942.

14. Favre, H., "Le calcul des plaques obliques par la méthode des équations aux différences", Mémoirs Ass. int. des ponts et charpentes, vol. 7, 1943, 1944.
15. Favre, H., "Sur l'introduction des coordonnées cartésiennes obliques dans la Théorie de l'elasticité", Bulletin Technique de la suisse romande, No. 25/26, 1946.
16. Favre, H., Schumann, W., "Étude experimentale de la répartition des moments dans une plaque oblique fléchie en fonction de l'angle formé par les côtés", Bulletin de la Société Française des Mécaniciens, No. 9, 1953.
17. Föppl, A. and L., "Drang und Zwang", Part 1, third ed., 1941.
18. Fuchssteiner, W., "Entwicklungsfunktionen für polygonal begrenzte dünne Platten", Bauingenieur, No. 7, 1953.
19. Girkmann, K., "Flächentragwerke", Wien 1954.
20. Gossard, M. L., Siess, C. P., Newmark, N. M., Goodman, L. E., "Studies of Highway Skew Slab-Bridges with Curbs", Univ. of Ill. Eng. Sta. Bulletin 386, 1950.
21. Graudenz, H., "Beitrag zur Berechnung der Momenten-Einflussfelder schiefwinkliger Platten", Diss. der Techn. Hochschule Hannover, 1948.
22. Herrmann, G., "Theoretische Untersuchungen über die Durchbiegung parallellogrammförmiger Platten unter zentrischer Einzellast", Publication No. 4 du Laboratoire de Photoélasticité de l'École polytechnique fédérale, 1950.
23. Jensen, V. P., "Analysis of Skew Slabs", Univ. of Ill. Eng. Exp. Sta. Bulletin 332, 1941.
24. Jensen, V. P., Allen, J. W., "Studies of Highway Skew Slab-Bridges with Curbs", Univ. of Ill. Eng. Exp. Sta. Bulletin 369, 1947.
25. Johansson, C. E., AB, Mikrokatorkraftmätare 585, Broschyr 8: 787.
26. Koepcke, W., "Umfangsgelagerte Rechteckplatten mit drehbaren und eingespannten Rändern", Diss. der Techn. Hochschule Berlin 1940.
27. Krettner, J., "Zur Theorie und Anwendung der schiefen Platte", Ingenieur-Archiv, vol. 21, No. 2, 1953.
28. Krettner, J., "Beitrag zur Berechnung schiefwinkliger Platten", Ingenieur-Archiv, vol. 22, No. 1, 1954.

29. Lardy, P., "Die strenge Lösung des Problems der schiefen Platten", Schw. Bauzeitung, No. 9, 1949.
30. Marcus, H., "Die Theorie elastischer Gewebe", second ed., Berlin 1932.
31. Nadai, A., "Elastische Platten", Berlin 1925.
32. Newmark, N. M., "Note on Calculation of Influence Surfaces in Plates by Use of Difference Equations", Journal of Applied Mechanics, vol. 8, No. 2, 1944.
33. Nielsen, N. J., "Bestemmelse af spændingen i Plader", København 1920.
34. Nielsen, N. J., "Skævvinklede Plader", Ingeniørvidenskabelige skrifter, No. 3, København 1944.
35. Ohlig, "Zwei- und vierseitig aufgelagerte Rechteckplatten unter Einzelkraftbelastung", Ingenieur-Archiv, Vol. 16, 1947.
36. Olsen, H., Reinitzhuber, F., "Die zweiseitig gelagerte Platte", Part 1, second ed., Berlin 1950, Part 2., Berlin 1951.
37. Pletta, D. H., Frederick, D., "Model Analysis of a Skewed Rigid Frame Bridge and Slab", AVI Journal, Nov. 1954, Proc. vol. 51.
38. Pucher, A., "Die Einflussfelder elastischer Platten", Wien 1951.
39. Ritz, W., "Über eine neue Methode zur Lösung gewisser Variationsprobleme der mathematischen Physik", Journal für reine und angewandte Mathematik, vol. 135, pp. 1—61, 1909.
40. Rongved, P., "Über das Randwertproblem schiefwinkliger Platten", Diss. der Techn. Hochschule Berlin 1945.
41. Rüsch, H., "Fahrbahnplatten von Strassenbrücken", Deutscher Ausschuss für Stahlbeton, No. 106, 1952.
42. Sawada, M., "Approximate Deflection of Plates, Loaded Uniformly and Clamped at Boundaries, in Oblique Coordinates", Soc. Mech. Engrs, Japan Journal. vol. 37, No. 210, 1934.
43. Schultz-Grunow, F., "Greensche Funktionen für elastische Platten", Zeitschrift für Angewandte Mathematik und Mechanik, vol. 33, No. 7, 1953.
44. Timoshenko, S., "Vibration Problems in Engineering", N. Y. 1928.

45. Timoshenko, S., "Theory of Plates and Shells", N. Y. 1940.
46. Timoshenko, S., "Strength of Materials", Part 1, N. Y. 1951.
47. Timoshenko, S., "Theory of Elasticity", Second ed., p. 95, N. Y. 1951.
48. Timoshenko, S., Young, D. H., "Theory of Structures", N. Y. 1945.
49. Vogt, H., "Die Berechnung schiefwinkliger Platten und plattenartiger Brückensysteme", Diss. der Techn. Hochschule Hannover 1940.
50. Vogt, H., "Die Berechnung schiefwinkliger Platten und plattenartiger Brückensysteme", Beton und Eisen, vol. 39, No. 17, 1940.
51. Vogt, H., "Theoretische und experimentelle Untersuchungen an schiefwinkligen Plattenbrücken", Beton- und Stahlbetonbau, vol. 48, No. 12, 1953.
52. Vogt, H., "Die statische Behandlung schiefwinkliger Brücken", Beton, No. 8, 1955.
53. Westergaard, H. M., "Computation of Stresses in Bridge Slabs Due to Wheel Loads", Public Roads, vol. 11, No. 1, 1930.
54. Woinowsky-Krieger, S., "Der Spannungszustand in dicken elastischen Platten", Ingenieur-Archiv, vol. IV, No. 3, 4, 1933.
55. Zurmühl, R., "Matrizen. Eine Darstellung für Ingenieure", Berlin 1950.
56. Ödman, S., "Studies of Boundary Value Problems", Part III, Svenska Forskningsinstitutet för Cement och Betong vid Kungl. Tekniska Högskolan i Stockholm, Handlingar No. 25, 1955.

Pris kr 20:—

UPPSALA 1956
APPELBERGS BOKTRYCKERI AB